University of Alberta

Increasing the selective toxicity of doxorubicin for solid tumors via improved drug bioavailability and ligand-mediated targeting

by

Kimberley Marie Laginha

A thesis submitted to the Faculty of Graduate Studies and Research in partial fulfillment of the requirements for the degree of Master of Science

Department of Pharmacology

Edmonton, Alberta
Spring 2006

Your file Votre référence
ISBN: 0-494-13837-8
Our file Notre référence
ISBN: 0-494-13837-8

Abstract

Conventional cancer chemotherapy lacks specificity for malignant cells, resulting in dose-limiting side effects, sub-optimal dosing and poor patient qualitiy of life. Entrapment of doxorubicin in long-circulating (Stealth®) liposomes (Doxil®) has led to an increase in the selective toxicity of the encapsulated drug. This thesis explores methods to further increase the selective toxicity of liposomal anticancer drugs. These include: the development of a method to measure bioavailable (released, biologically active) drug in solid tumors; the manipulation of bioavailable drug levels by altering drug release rates; attempts to increase bioavailable drug levels in tumor cells via ligand-mediated targeting of liposomal drug to tumor-specific antigens; and development of methods to increase the apparent receptor density on cancer cells that will result in an increase in the amount of drug delivered to tumor cells. This thesis will help in the design of more effective liposomal drugs with improved therapeutic effects and fewer side effects

Acknowledgments

First and foremost I would like to thank my supervisor Dr. Terry Allen for giving me the chance to work in her laboratory and for her guidance and support throughout my graduate training. I would especially like to thank her for help in preparing manuscripts, presentations and especially this thesis.

I would also like to thank my supervisory committee, Dr. Andrew Shaw and Dr. Elena Posse de Chaves for their help and guidance with this project, and I would also like to thank the graduate supervisors in the Department of Pharmacology during my time as a graduate student, Dr. Wendy Gati and Dr. Susan Dunn.

I would like to thank everyone I have worked with in the Allen laboratory during my graduate studies who made going to work an enjoyable experience. I would especially like to thank Elaine Moase and Heather Vandertol-Vanier who always made the lab run smoothly and lended me a hand whenever I needed it. I would also like to thank my fellow graduate and summer students who worked in the Allen laboratory during my time, Wilson Cheng, Jennifer Hare, Puja Sapra, Gregory Charrois, Sylvia Verwoert, Davis Mumbengegwi, Stacy Hall, and Jessie Dhillon.

Most importantly I would like to thank my husband Lucas Duerksen, and my sister Antonia, and both my parents for always being there and helping me whenever I needed it. You guys are the best and nobody could ask for a better family.

Table of Contents

List of Tables

List of Figures

List of Abbreviations

Ab	antibody
AIDS	human acquired immunodeficiency syndrome
Anti-CD19	monoclonal antibody IgG_{2a}, against the B cell antigen, CD19
Anti-CD20	monoclonal antibody IgG_1, against the B
cell	antigen, CD20
Anti-HER2/*neu*	monoclonal antibody IgG_1 against the HER2/*neu* oncogene
ASC	aqueous counting scintillant
AUC	area under the time versus concentration curve
BD	biodistribution
Chol	cholesterol
CL	plasma clearance
C_{max}	maximal tissue drug concentration
d	days
D5W	dextrose, 5% in sterile water
DMSO	dimethyl sulphoxide
DNase 1	deoxyribonuclease 1
DOPC	dioleoylphosphatidylcholine

DOPC-PLD	dioleoylphosphatidylcholine PEGylated liposomal DXR
DXR	doxorubicin
DXR-SL	DXR-loaded Stealth® liposomes
DXR-SIL[anti-CD19]	DXR-loaded Stealth® immunoliposomes, targeted via anti-CD19
DXR-SIL[anti-CD20]	DXR-loaded Stealth® immunoliposomes, targeted via anti-CD20
EPR	enhanced permeability and retention
FBS	fetal bovine serum
h	hour
^{3}H-CHE	^{3}H-cholesteryl hexadecylether
HBS	HEPES-buffered saline
HEPES	4-(2-hydroxyethyl)-1-piperazineethanesulfonic acid
HSPC	fully hydrogenated soy phosphatidylcholine
IC_{50}	concentration required for 50% inhibition of cell growth
IgG	immunoglobulin
i.v.	intravenous
KS	Kaposi's sarcoma

kg	kilogram
LTTs	ligand-targeted therapeutics
LUV	large unilamellar vesicles
mAb	monoclonal antibody
Mal-PEG-DSPE	maleimide-derivatized polyethylene glycol (MW 2000) covalently coupled to distearoylphosphatidylethanolamine
mPEG-DSPE	methoxypolyethyleneglycol (M_r 2000) covaltently coupled to distearoylphosphatidylethanolamine
MEM	minimal essential medium
μm	micrometer
mM	millimolar
μg	microgram
μmol	micromole
min	minute
MPS	mononuclear phagocyte system
MRT	mean residence time
MTT	3-[4,5-dimethylthiazole-2-yl]-2,5-diphenyltetrazolium bromide
MLV	multilamellar vesicles
MW	molecular weight

NHL	non-Hodgkin's lymphoma
nm	nanometers
NLB	nuclear lysis buffer
p	probability constant
PBS	phosphate buffered saline, pH 7.4
PEG	polyethylene glycol
PK	pharmacokinetics
PL	phospholipids
pmoles	picomoles
PFV	programmable fusogenic vesicle
RES	reticuloendothelial system
scFv	single chain antibody fragment of the variable region
SCID	severe compromised immunodeficient
S.D.	standard deviation
SL	sterically stabilized Stealth® liposomes
SUV	small unilamellar vesicles
$t_{1/2}$	half-life
t_m	phase-transition temperature
VCR	vincristine
v/v	volume/volume
Vd	volume of distribution

w/v	weight/volume
w/w	weight/weight

CHAPTER 1

Introduction, hypothesis, and objectives

1.1. Introduction

Despite the clinical approval of several liposomal anticancer drug formulations, relatively little is known about the rate and extent of drug bioavailability following liposomal delivery to tumor sites. This is an important research topic because drugs that are encapsulated in liposomes assume the pharmacokinetics (PK) and biodistribution (BD) of the carrier (1-5) and are not bioavailable, i.e., have no biological activity, until they are released from liposomes. To date, selection of lipid formulations for liposomes has been largely empirical. Numerous studies have looked at total liposomal drug accumulation at malignant sites (6-13), but no one has quantitatively assessed the amount of biologically active drug at these sites.

The objective of this project is to assess the levels of total tumor drug (encapsulated drug + released drug) in solid tumors as a function of time and also to measure the levels of bioavailable drug, i.e., released drug, in tumors. A further objective is to correlate levels of bioavailable drug in tumors with therapeutic activity for the same drug formulations. By developing methods that can measure the rate, extent and amount of drug released from liposomes at various sites in the body, we will be able to improve the therapeutic outcome of cancer chemotherapy and decrease its dose-limiting toxicities such as myelosuppression and cardiotoxicity.

1.2. Cancer

Cancer is a worldwide problem. In Canada alone, it is estimated that there will be 149,000 new cases and 69,500 deaths from cancer in 2005 (14). Approximately 40% of Canadians will be diagnosed with cancer, and 1 out of every 4 Canadians will die from it. The economic impact of cancer is staggering. In 1998 the total cost of cancer to Canada was estimated to be $14.2 billion dollars. Of this, $11.8 billion dollars was for indirect costs such as death and loss of work.

Breast cancer, in particular, is a major concern for Canadian women. It is estimated that 1 in every 9 women will be diagnosed with this disease, and 1 in every 27 women will die from it (14). Currently, the primary treatment for breast cancer is surgery followed by radiation therapy, chemotherapy, hormone therapy or a combination of all three.

A recently approved breast cancer therapy in Canada is Herceptin® (anti-HER2/*neu* monoclonal antibody). Herceptin® was initially approved as a monotherapy and more recently was approved for the treatment of advanced breast cancer in combination with chemotherapy (15). Herceptin® therapy has been shown to increase overall survival of breast cancer patients and decrease metastatic spread of the disease (16-18).

Another recently approved drug for metastatic breast cancer in Canada is Caelyx® (Stealth® liposomal DXR, *vide infra*) (19). Doxorubicin (DXR, Fig. 1.1) is an anthracycline antibiotic anticancer agent that is one of the most commonly

used of the chemotherapy drugs (20). DXR has several cytotoxic mechanisms of action, including inhibition of topoisomerase II in the nucleus (20, 21).

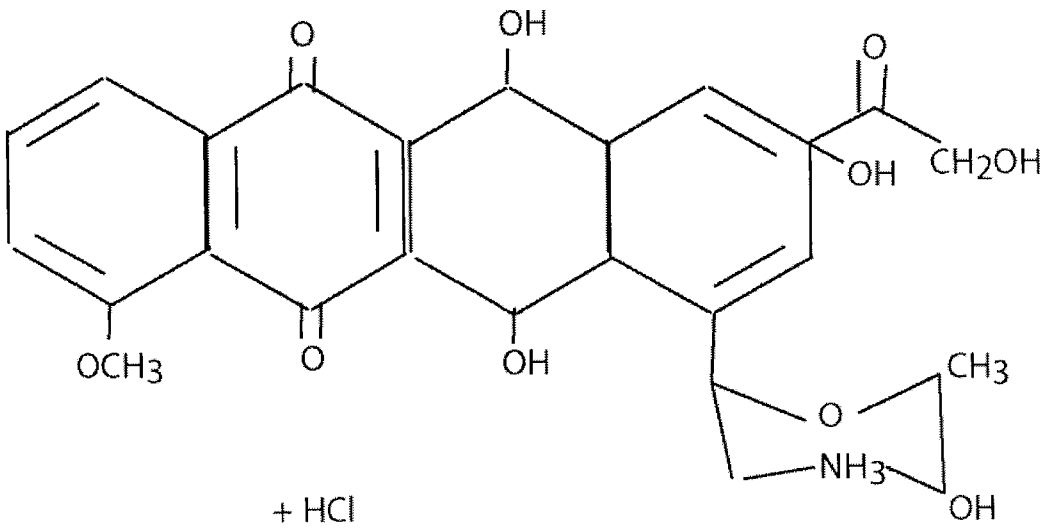

Figure 1.1. Chemical structure of doxorubicin.

1.3. What is a Liposome?

Liposomes are bilayer vesicles composed of amphipathic phospholipids that have hydrophilic head groups and hydrophobic fatty acyl chains. In an aqueous environment, phospholipids self-associate to form lipid bilayers that enclose an aqueous compartment. Cholesterol is often added to phospholipid mixtures for its bilayer stabilizing properties. Liposomes were first described 40 years ago by Dr. Alex Bangham (22) and were extensively studied as models of biological membranes (23). Hydration of phospholipid mixtures in buffer solution results in the formation of multi-lamellar vesicles of approximately 200 to 4000 nm in diameter. In this thesis, we employed a commonly used technique to obtain small (~100 nm) homogenous unilamellar vesicles. This method uses moderate pressure ($\leq$ 300 psi) to extrude lipid mixtures through polycarbonate filters with pore sizes ranging from 0.4-0.08 μm (24).

1.4. Liposomal drug delivery systems

After the discovery of liposomes, their potential as drug delivery systems was soon identified. As early as 1971, enzymes were being entrapped successfully in the aqueous interior of liposomes (25), and soon liposomes were identified as potential carriers for cancer chemotherapy drugs since they were able to alter the PK and BD of their entrapped drugs (26). After a number of technological advances, liposomes are now the leading nano-scale drug delivery system.

The first generation of liposomes, often called 'conventional' or 'classical' liposomes, was composed of unmodified ("naked") phospholipid bilayers; "naked" because no proteins, glycolipids, or other polysaccharides that are present on the exterior of the plasma membrane of all eukaryotic cells are present at the liposome surface. A significant portion of a parenterally administered dose of classical liposomes is rapidly cleared by the mononuclear phagocyte system (MPS), also called the reticuloendothelial system (RES), principally into Kupffer cells of the liver and fixed macrophages of the spleen. This is because opsonins (plasma proteins that adsorbed onto the "naked" surface of liposomes) mark them for destruction by the MPS. Rapid uptake into the MPS is the cause of the saturable, non-linear, dose-dependent (Michaelis-Menten) PK that is seen for classical liposomes (27).

A classical liposomal formulation of doxorubicin, Myocet®, is currently approved in Europe for the treatment of metastatic breast cancer in combination with cyclophosphamide (28). These liposomes, despite having a significant portion of the drug cleared by the MPS, have reduced the dose-limiting cardiotoxicity and maintained the antitumor efficacy that is seen with conventional doxorubicin therapy.

One of the goals of cancer chemotherapy, and drug delivery systems in particular, is to selectively target therapeutic agents to the disease site. Entrapping cytotoxic drugs in classical liposomal formulations that are cleared by the MPS within a few minutes after administration limits the distribution of entrapped drug

to tumors and may result in damage to the liver and spleen. It takes from 24 to 48 h or longer for liposomes to distribute to solid tumors in murine models of cancer (7, 29). In order to increase distribution of liposomal drugs to tumors, a means of increasing the circulation times of liposomes had to be found. The most successful approach to date for increasing the circulation times of liposomes was to graft a polymer coating to the surface of the liposomes, e.g., polyethylene glycol (PEG) (30-32). The PEG coating attracts a layer of water around the liposomes, preventing opsonisation with plasma proteins, which in turn significantly increases the circulation half-life ($t_{1/2}$) of these liposomes compared to classical liposomes (3, 27, 33, 34).

When liposomes have diameters in approximately the 60 to 120 nm range and circulation half-lives of several hours, their distribution to solid tumors is increased (called "passive targeting") through the enhanced permeability and retention (EPR) effect (35). The EPR effect takes advantage of the relatively large gaps (~200-600 nm) between cells of the newly established endothelium (36). These gaps are large enough to allow extravasation of liposomes into the interstitial space of tumors (36, 37). In addition, tumors have impaired lymphatic drainage and elevated oncotic pressure. This is thought to prevent liposomes from leaving the tumor once they have localized there (38). Sustained release liposomal anticancer drug formulations that have extravasated into the tumor interstitial space will release their drug at a rate that is dependent on the liposome composition, bathing the surrounding tumor cells in cytotoxic drugs (13). A

PEGylated liposomal formulation of doxorubicin (Caelyx®/Doxil®), with reduced dose-limiting toxicity, prolonged circulation and enhanced tumor accumulation, has been clinically approved for treatment in AIDS-related Kaposi's sarcoma, refractory ovarian cancer, and metastatic breast cancer (39-43).

1.5. Methods of Liposome Preparation

While more large scale clinical preparations of liposomes are made by French Press extrusion, the thin film hydration method, followed by extrusion under pressure through polycarbonate filters is a common method of small scale liposome production in research laboratories (24). In this procedure, homogenous lipid mixtures are made in an organic solvent, which is then evaporated to form a thin film. The dried lipid film is then hydrated at a temperature above the most abundant phospholipid's solid-to-liquid crystalline phase transition temperature (T_m). Upon hydration, the lipids self-assemble into large multilamellar vesicles (MLV). These vesicles are composed of multiple concentric bilayers of phospholipids separated by aqueous compartments (Figure 1.2). MLV are heterogeneous in diameter (200-4000 nm) and their trapped volume is relatively small, since much of the interior volume is taken up by multiple phospholipid bilayers (44). Ultrasonication of MLVs or passaging them through a French press at high pressures, produces small unilamellar vesicles (SUV) that are relatively homogenous in size (20-70 nm in diameter) (44). One of the limitations of SUVs is that the trapped volume is relatively small. This restricts the amount of drug

that can be encapsulated inside, which can be problematic for low potency drugs since large amounts of lipid would have to be administered in order to reach therapeutic drug concentrations The most commonly used liposomes are large unilamellar vesicles (LUV), 80-200 nm in diameter. They are most often formed from MLVs by repeated extrusion using moderate pressure (< 500 psi) through polycarbonate filters of defined pore size. LUVs have large trapped volumes relative to their lipid content and can encapsulate more drug per unit weight of lipids than either SUVs or MLVs. The diameter of LUVs can be controlled to some extent by the choice of the pore size for the polycarbonate membranes (80, 100, 200, etc.), Repeated sequential extrusion through membranes of decreasing pore sizes produces a homogeneous liposome mixture of approximately 80-120 nm in diameter. Solvent injection and reverse-phase evaporation can also produce LUVs, and are good methods for large-scale production of liposomes (44-46). In the experiments used in this thesis, we extruded liposomes through polycarbonate filters.

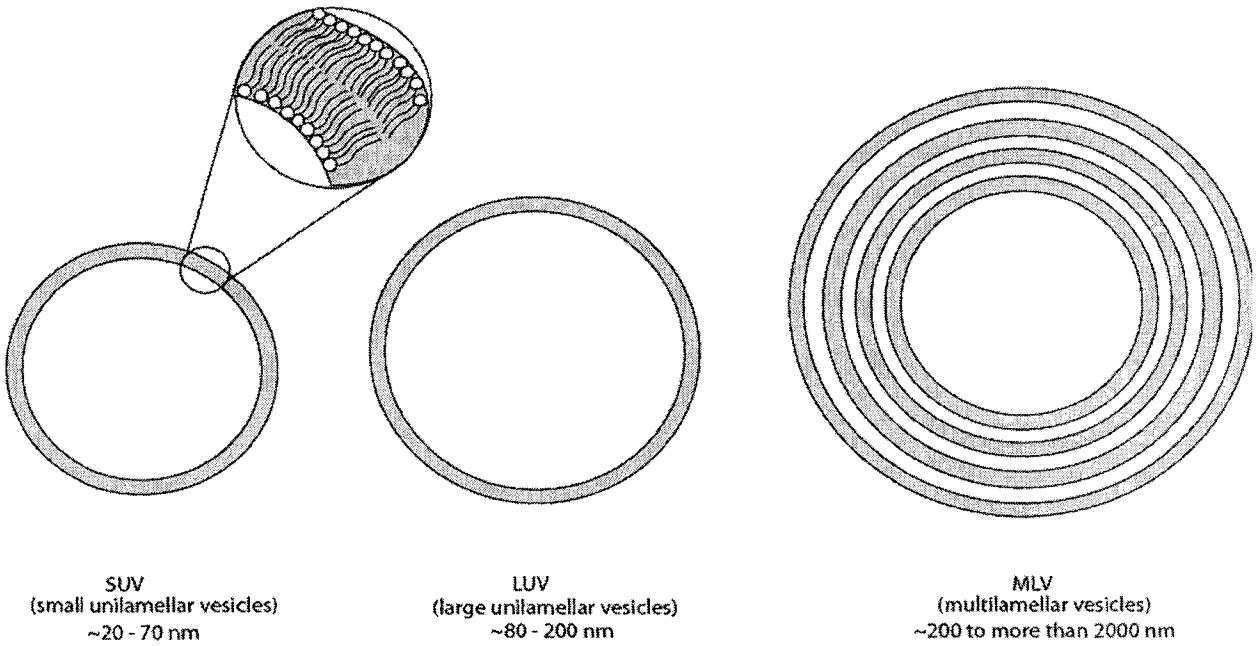

Figure 1.2. Classification of liposomes based on size and lamellarity.

1.6. Drug Loading

There are various ways to entrap drugs in the aqueous interior of liposomes. The choice of method often depends on the properties of the drug being loaded. Hydrophilic drugs like cisplatin or cytosine arabinoside can be passively loaded into liposomes (47, 48) but this results in poor loading efficiency. Drugs such as DXR that have poor water solubility have been entrapped in the aqueous interior of liposomes via a remote-loading method that is applicable to weak acids and weak bases and relies on the ability of the liposomes to retain a proton gradient across their membrane (49).

In this thesis DXR is remote-loaded into the aqueous interior of liposomes as follows. Stable loading of the amphipathic weak base DXR is achieved generating an ammonium sulphate gradient across the liposome membrane, where the concentration of ammonium sulphate is greater inside the liposomes than in the medium surrounding the liposomes (50, 51). Efflux of ammonia out of the liposomes increases the interior proton concentration. At higher pHs outside the liposomes, DXR is in the uncharged state and readily diffuses down its concentration gradient across the lipid bilayer; once inside the acidic pH enviroment in the liposome aqueous interior, it becomes protonated and cannot cross back to the liposome exterior (Figure 1.3.). Protonated DXR in the liposome interior forms a precipitate with SO_4^{2-} ions, allowing the diffusion of more DXR into the liposomes. Remote loading by this method results in $\geq$95% encapsulation efficiency with a ratio of PL to DXR of 1:0.2.

Doxorubicin can also be loaded into liposomes by utilizing a pH gradient (acid inside) or Mn^{2+} complexation (52). Loading DXR into liposomes using a pH gradient is similar to remote loading using an ammonium sulphate gradient. This technique utilizes a citrate gradient to trap DXR in its protonated form inside liposomes (53, 54). Similarly, DXR can also be trapped inside liposomes when it forms a complex with Mn^{2+} (55). Remote loading has also been used for the weak base vincristine, which is even less water-soluble than DXR (56), but the retention of the drug in the liposomes is not high. An ionophore-loading technique at high drug to lipid ratios results in improved drug retention for vincristine and other vinca alkaloids in liposomes (57, 58).

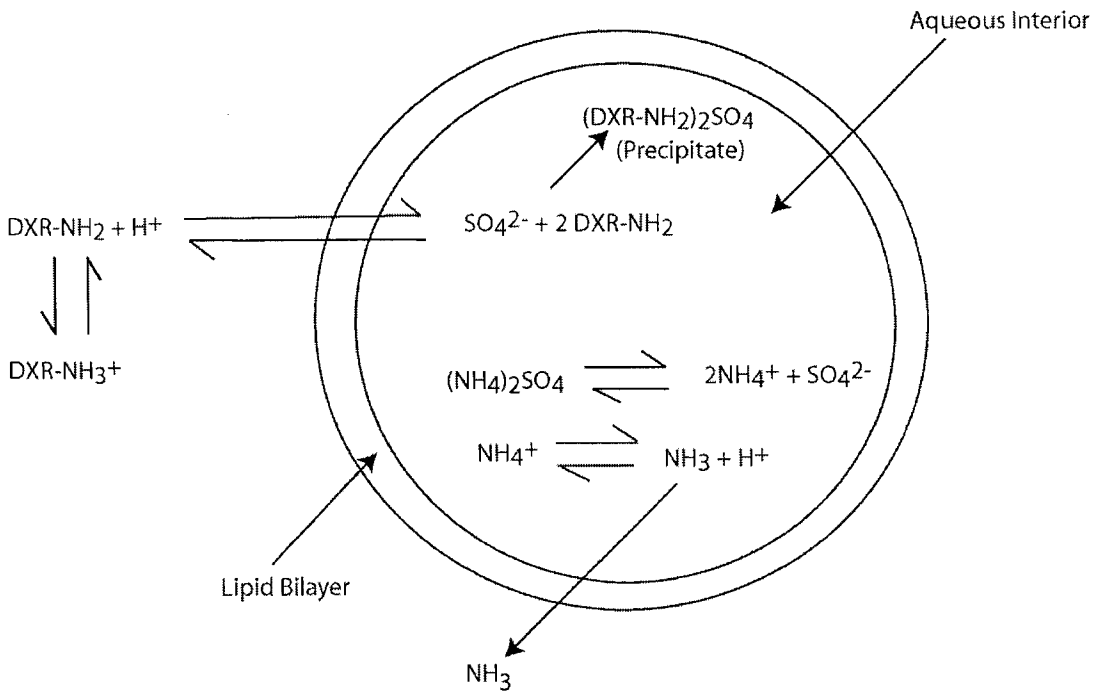

Figure 1.3. Remote-loading of doxorubicin using an ammonium sulphate gradient. The production of hydrogen cations, resulting from the diffusion of ammonia out of the liposomes, creates a pH gradient across the liposomal bilayer. Uncharged DXR outside the liposomes diffuses down its concentration gradient into the liposome interior where it reacts with sulphate anions to form a precipitate. Precipitation of DXR inside the liposome reduces its apparent concentration inside the liposomes allowing more DXR to diffuse into the liposomes and precipitate. Adapted from (51).

1.7. Targeted liposomal drug delivery systems

Another approach to increase the drug payload being delivered to cancerous cells is to selectively target drugs to diseased sites. This is an important goal since the side effects of chemotherapy are often so severe that sub-optimal dosing and/or discontinuation of therapy are common. One approach that is being extensively studied is targeting cancer cells with monoclonal antibodies (mAb) or other ligands specific for cell surface receptors or antigens (59). This is a viable approach in cancer since many cancer cells uniquely express or overexpress antigens or receptors compared to normal cells.

Kohler and Milstein first developed methods to make mAbs from mouse cell lines over thirty years ago (60). In more recent times, humanized or chimeric mAbs have had extremely high success in the clinic, with clinical approval ratings between 18-29% (61). Currently, there are over 150 mAb products in company-sponsored studies worldwide. Small long-circualting liposomes have a natural ability to passively target tumors via the EPR effect, so an obvious extension of this observation is to "actively" target liposomes by coupling ligands or mAbs to their surface. Table 1.1 is a partial list of ligands and mAbs that have been attached to liposomes. Already, some ligand-targeted liposomes are showing potential for clinical develoment, e.g., liposomes targeted via folate, NGR, anti-HER2/*neu* and anti-CD19. The latter two are related to this thesis.

Table 1.1. Ligands or antibodies that have been coupled to liposomes.

Targeting Agent	Target	Reference
Non-antibody		
APRG	Angiogenic blood vessels	(62)
RGD	Cellular adhesion molecules ($\alpha v\beta 3$-integrin	(63)
NGR	Aminopeptidase N (CD13)	(64)
Folate	Folate receptor	(65)
Transferrin	Transferrin receptor	(66)
Hyaluronan	Hyaluronon receptor, CD44	(67)
Antibody		
Anti-CEA	Carcinoembryonic antigen	(68)
Anti-EGFR	Endothelial growth factor receptor	(69)
Anti-HER2/*neu*	HER2/*neu* receptor	(70)
Anti-CD19	CD19, B-cell receptor	(71)
Anti-GD_2	Disialoganglioside expressed on tumors of neuroectodermal origin	(72)
Anti-CD20	CD20, B-cell receptor	(73)
Anti-CD22 (scFv)	CD22, B-cell receptor	(74)
Anti-MUC1	Aberrantly glycosolated epithelial mucin	(75)
Anti-34	CD34, T-cell antigen	(76)
Anti-2C5	Tumor-cell bound nucleosome	(77)
F5 (scFv)	HER2/*neu* receptor	(78)

The therapeutic efficacy of anti-HER2/*neu*-targeted liposomes has been compared in numerous models of breast cancer that exhibit high overexpression of HER2/*neu*. The targeted liposomes have an advantage over non-targeted PEGylated liposomes in these models (70, 79-81). Targeting to the HER2/*neu* receptor does not increase the total amount of drug or liposomes delivered to tumors, but it influences the distribution profile of the liposomes within tumors (81). Using colloidal-gold labeled liposomes, Park et al. showed that targeted liposomes had efficient intracellular delivery in the target cells whereas non-targeted liposomes accumulated in the stroma or within macrophages of tumors. The therapeutic effects were mediated by the complete package of targeting agent, liposome and drug and not to the targeting agent or the free drug alone. Recently, this group has developed a single-chain fragment of the variable region (scFv) that was derived from anti-HER2/*neu* (78, 82, 83). Indeed, numerous antibodies are actively being transformed to scFvs because these small fragments lack the Fc (constant) region of Abs, which is the main region involved in generating an immune response and clearing the Abs from circulation. The scFv derived from anti-HER2/*neu*, F5, was selected for the high rate of receptor-mediated endocytosis that is triggered when it is bound to the HER2/*neu* receptor. DXR-loaded liposomes targeted with F5 are scheduled to undergo clinical trials in the United States in the future.

A targeted liposomal drug delivery system that has been extensively studied in our laboratory is anti-CD19- or anti-CD20-targeted liposomal doxorubicin

(DXR) or liposomal vincristine (VCR). These systems have produced promising preclinical data in which it was demonstrated in a xenograft B-cell lymphoma model (Namalwa cells) that treatment with targeted liposomes resulted in significant increases in murine life span compared to mice treated with non-targeted liposomes (84, 85). Recently, a non-targeted VCR-loaded liposomal formulation was in clinical trials for aggressive non-Hodgkin's lymphoma (NHL) (86). In 2004, this liposomal formulation was denied accelerated approval by the US Food and Drug Administration, so it is currently undergoing randomized clinical trials in non-Hodgkin's lymphoma and acute lymphoblastic leukemia. With the clinical approval of a DXR formulation and the possible clinical approval of a VCR formulation, antibody-targeted DXR- or VCR-containing liposomes are also candidates for clinical development.

1.8. Formation of antibody-targeted liposomes

Antibodies can be coupled to the surface of liposomes by a variety of methods (87). Antibodies were first coupled directly to phospholipid head groups on the surface of PEGylated liposomes, but the PEG-DSPE groups were found to sterically hinder the binding of the antibodies to their target cells (88). It has been shown that coupling antibodies to the terminus of PEG-DSPE prevents steric hinderance of antibody binding (89-91). Several heterobifunctional derivatives of PEG-DSPE have been developed specifically for coupling antibodies to liposomes, including PEG derivatized with hydrazide or maleimide (71, 80, 92).

In a different approach, which has a number of advantages over direct coupling to the liposome surface, ligands are coupled to PEG micelles and the PEG-ligand construct is post-inserted into liposomes (93, 94).

In this thesis we coupled antibodies to liposomes using the Mal-PEG-DSPE coupling lipid. This method involves thiolating free antibodies with 2-iminothiolane (Traut's reagent). This converts amine groups of lysine residues on the antibodies to free sulfhydryl (-SH) groups which then react with terminal maleimide groups on the liposomes. Coupling antibodies to liposomes via this method results in random orientation of the antibodies because many lysine residues on the antibodies are thiolated. In some cases, the Fc portion of the antibodies may be exposed which would increase clearance of the targeted liposomes from plasma via Fc receptor-mediated mechanisms (94).

1.9. Bioavailability of drug in tumors

The liposome bilayer serves as a protective barrier between the entrapped drug and its environment. Also, as long as the drug remains encapsulated in the liposomes, it assumes the PK and BD of the liposomal carrier. Entrappment in liposomes prevents the drug from being metabolized and degraded, but also prevents its therapeutic effects. Release of the encapsulated drug from liposomal drug delivery systems is required for the drug to have biological activity, i.e., for the drug to be bioavailable.

Both circulation half-life and the rate of drug release are important parameters in determining the therapeutic activity of liposomal drugs. It takes

from 24 to 48 h or longer for liposomes to localize to solid tumors via the EPR effect, so long circulation half-lives are necessary to achieve good tumor uptake of liposomal drugs (12). If the drug is released too slowly from liposomes after the carrier localizes to tumors, the therapeutic efficacy may be attenuated. This is seen with the liposomal cisplatin formulation SPI-077. Although pharmacokinetic studies revealed prolonged circulation times and enhanced tumor uptake of the SPI-077 compared to conventional cisplatin, the therapeutic efficacy was similar to conventional cisplatin in a number of mouse tumor models (48). In vitro release experiments showed that very little cisplatin was released from SPI-077, explaining its poor therapeutic efficacy. In Phase I/II clinical trials, this liposomal formulation did not result in improved antitumor effects over conventional treatment (95). In the case of SPI-077, since drug release was very slow, levels of bioavailable drug in tumor likely did not reach the minimum therapeutic drug concentration.

Drug release can also be too rapid. Rapid release of drug from liposomes hardly changes the PK and PD of the associated drug and does not alter the therapeutic effects away from those seen with free drugs (96). When liposome composition was manipulated to achieve a variety of drug release rates for liposomal DXR, the drug could be changed from a minimally effective drug, to a toxic drug to a drug with good efficacy against murine breast cancer tumors (13).

Liposome composition, as well as the physical properties of the drug itself, governs the rate of release of drugs from liposomes. Drug release rates from

liposomes can be manipulated to some degree. When liposomes are injected *in vivo*, lipids from the carrier can be exchanged or transferred to high-density plasma lipoproteins, hence destabilizing the liposomal bilayer (97). Altering the composition of liposome bilayers can confer stability or fluidity. When long-chain fully saturated lipids, such as hydrogenated soy phosphatidylcholine (HSPC), are the major constituent of liposomes, they have rigid bilayers and, except for very hydrophobic drugs, tend, in the presence of plasma, to have higher levels of drug retention than liposomes with fluid bilayers. In contrast, if short-chain or unsaturated lipids are the major bilayer constituent, the bilayer is fluid, and drug release rates in the presence of plasma tend to be more rapid than for liposomes with rigid bilayers.

The importance of the relationship between drug release rate and therapeutic activity, and its unpredictability, can be illustrated with two different liposomal formulations: liposomal mitoxantrone and liposomal DXR. The therapeutic activity of a more rapid release (fluid) liposomal formulation of mitoxantrone was compared that of a rigid formulation (98). Despite the fact that the rigid liposomal formulation had a greater area under the concentration vs. time curve (AUC) for tumor, the liposomal formulation with a more rapid release rate had improved therapeutic activity in both a colon carcinoma model (LS1180) and a squamous cell carcinoma model (A431). In contrast, when a slow release (rigid) liposomal formulation of DXR was compared to a more rapid release (fluid) formulation in a

breast cancer model, the more rigid formulation had greater tumor drug AUC and also greater therapeutic activity (13).

Clearly, the relationship between the rate and levels of drug bioavailability from liposomal carriers at the disease site and their therapeutic efficacy is complex. Depending on the properties of the encapsulated drug and the type of tumor, results may be very different. Even though total levels of liposomal drug can be much higher in tumors than a similar dose of free drug, this may not result in substantially more bioavailable drug uptake by tumor cells or in the drug becoming bioavailable at an inappropriate rate. Thus, there has been interest in increasing the amount of bioavailable drug delivered to tumors, at an optimal rate, through the use of drug carriers.

There is considerable recent interest in the design of liposomes where the release of drug into, or in the vinicity of, the target cell can be triggered by an external stimulus, so-called "triggered release" liposomes. Strategies such as pH-sensitive liposomes, fusogenic liposomes and thermosensitive liposomes are being investigated (52, 99-105). Antibody-targeted pH-sensitive liposomes are designed to destabilize in the acid environment of endosomes of lysosomes following the receptor-mediated internalization into tumor cells (102, 106, 107). Rapid destabilization of the liposome in the lysosomal apparatus is thought to enhance the cytoplasmic delivery of released drug relative to liposomes that do no undergo triggered release.

Another approach to increasing the payload of bioavailable drug delivered to target cells is the use of programmable fusogenic vesicles (PFVs) (99). These liposomes contain a cationic lipid and a stabilizing PEG-lipid derivative that can exchange out of the liposomes at a rate that is dependent on the acyl-chain length of its lipid anchor. Loss of the PEG from the surface leads to exposure of the cationic lipid at the liposome surface, which promotes non-specific binding and internalization into cells and/or release of their contents due to membrane destabilization. As an example of this approach, mitoxantrone-loaded PFVs showed enhanced antitumor activity in both a murine leukemia model (L1210) and a human colon carcinoma model (LS180) (99).

Thermosensitive liposomes have lipid compositions that undergo a phase transition at a temperature that is within the range that is clinically attainable in local hyperthermia (41-42 °C). When this temperature is reached, the liposomes become fluid, allowing the encapsulated drug to be released and become bioavailable at the tumor site. Using this approach, liposome extravasation and accumulation in tumors will also increase since local hyperthermia has been shown to increase tumor blood flow and vascular permeability (108). However, the clinical application of thermosensitive liposomes is limited to those cases where treatment of local tumor will either be curative or will improve patient quality of life, since thermosensitive liposomes are not designed to treat tumor metastases.

All of these studies attempt to develop liposomal formulations that can increase the amount of bioavailable drug at the tumor site and/or optimize the timing of the delivery of bioavailable drug. However, none of these studies have differentiated between encapsulated (non-bioavailable) and released (bioavailable) drug. In order to develop improved liposomal carriers, it is necessary to develop methodologies that can distinguish between bioavailable and non-bioavailable drug in the tumor, and can measure the drug levels of each with respect to time.

1.10. Rationale and Hypothesis

The subject of this thesis is how to meaure levels of bioavailable drug in solid tumors and the implications of these measurements for the therapeutic effect of liposomes. When drugs are encapsulated in liposomes they are not bioavailable; the drug is not therapeutically active because it is physically separated from its site of action by the liposome bilayer. The classical definition of bioavailable drug is a "...measurement of the rate and extent of therapeutically active drug that reaches the systemic circulation and is available at the site of action" (109). In cancer chemotherapy we are primarily interested in the amount of "bioavailable" drug that reaches tumors. We know an increased amount of total drug reaches solid tumors when PEGylated liposomal DXR, i.e., Doxil®/Caelyx®, is administered compared to free DXR. Even though there may be more liposomal drug in tumors, this does not necessarily translate into increased levels of bioavailable drug if the drug is not released from the liposomes. Since

Doxil®/Caelyx® has better therapeutic activity in some highly vascularized cancers such as KS, we assume more bioavailable drug is reaching the tumor cells (110). For other cancers, such as breast cancer, Caelyx® is a clinically approved therapy not because of increased therapeutic efficacy, but because of diminished dose-limiting toxicities, such as cardiotoxicity and myelosuppression. Currently, when we manipulate the rate and extent of drug release from liposomes, we do not have a good understanding of how this affects the amount of bioavailable drug in tumors; this makes it difficult to optimize liposomal formulations, other than empirically. Therefore, developing methods to measure bioavailable drug in tumors is an important aim of this thesis.

A further question deals with how ligand-mediated targeting of liposomal drugs to tumors affects the levels of bioavailable in tumors. It has been established in some tumor models, but not in others, that targeting liposomes to cell surface receptors on cancer cells results in improvements in the therapeutic efficacy compared to non-targeted liposomes. Successful results with targeted liposomes have been achieved with DXR-loaded liposomes targeted with anti-HER2/*neu* in a HER2/*neu* overexpressing breast cancer model compared to non-targeted liposomes, as long as the level of over-expression of HER2/*neu* on the target cells remain high (81). This finding was despite the observation that the total drug uptake into tumor did not increase for the targeted formulations relative to a non-targeted formulations. Therefore, the increased therapeutic activity could be a result of an increase in the levels of bioavailable drug delivered to tumor cells

or the rate at which it is delivered. Hence, another aim of this thesis is to compare levels of bioavailable drug in tumors for targeted vs. non-targeted liposomes.

The therapeutic activity of targeted-liposomal drug delivery is correlated with the density of the targeted receptor on the tumor cells (80). Since it is impossible to increase the receptor density on target cells, an effective means to overcome this limitation may be to target to two or more receptors expressed on cancer cells. This also may lead to an increased amount of bioavailable drug delivered to tumor cells. This thesis contributes to this area of research by developing and testing a method to quantitate two different antibodies coupled to the surface of liposomes.

There are some unique features of doxorubicin that make it an excellent candidate for studying the release of drug from liposomes in tumors, namely its fluorescence and its rapid localization to the nucleus after uptake into cells. Doxorubicin and its metabolites have unique fluorescent properties that enable both the drug and its major metabolites to be detected fluorometrically (111, 112).

1.11. Choice of Animal Model and Drug

A murine model of mammary carcinoma (4T1) was used to evaluate the bioavailability of DXR in tumors after delivery with a rigid liposomal formulation of DXR, a leaky liposomal formulation of DXR, or free DXR. This tumor model, which was derived from a spontaneously arising tumor from a BALB/cfC_3H mouse (113), is a thioguanine-resistant cell line that metastasizes to the lungs and

liver (114). This model was chosen because it has a ≥99% tumor take rate when implanted in mammary fatpads, is sensitive to DXR and grows well in BALB/c mice (75). For targeting studies against the HER2/*neu* receptor, the human breast cancer cell line BT-474 M3C5 was used. This cell line was isolated from an invasive ductal carcinoma of the breast (115). The M3C5 variant, a gift from ALZA Corporation, has been passaged through NCr nude mice three times to improve its tumorigenic profile in athymic nude mice; it expresses 1×10^6 HER2/*neu* receptors per cell and has an immunohistochemistry (IHC) rating of 3^+ (81). This model was chosen because it has been established that receptor density plays a role in the therapeutic activity of targeted liposomal therapy (80), and the high receptor density on this cell line is characteristic of what is seen in women that are eligible for Herceptin® therapy (116, 117).

For experiments comparing the effects of targeting liposomes with two mAbs directed to two different cell surface receptors, the human Burkitt's lymphoma cell line, Namalwa, was used. This cell line is positive for the CD19 and CD22 internalizing surface antigens and the CD20 non-internalizing surface antigen (84, 118-120).

Namalwa cells grow readily in severely compromised immunodeficient (SCID) mice. Anti-CD19 can be produced in large quantities from hybridoma cells in the Allen lab and anti-CD20 (Rituxan®) can be purchased commercially. Furthermore, CD19 and CD20 are expressed on greater than 90% of B-cell

lymphomas (121), and targeting liposomes to these antigens has already been shown in our laboratory to be therapeutically advantageous (73, 84, 122).

DXR has several attractive properties for the development of a bioavailability assay. It has intrinsic fluorescence and it binds strongly to nuclear DNA; therefore the nucleus acts as a sink for bioavailable drug. Measurement of nuclear DXR levels provides a good indicator of the relative amount of drug being released from liposomes, since liposomal DXR cannot reach the nucleus (123, 124). In this thesis we developed methodology to measure nuclear DXR in murine breast cancer tumors and examined levels of bioavailable drug as a function of time and liposome composition.

We hypothesize that a greater understanding of the rate and extent of drug release from liposomal carriers at malignant sites can provide insights into how liposomal drug therapy can be optimized. The observation of correlations between the bioavailability of liposomal drugs at cancerous sites and their therapeutic activity will help in the rational design of future drug carriers.

1.12. Thesis Outline

The studies presented in this thesis explore differences in the bioavailability of drug in murine breast cancer tumors after delivery of various formulations of non-targeted or targeted liposomal DXR compared to free DXR. In addition, the effects on cell association and cytotoxicity of increasing the apparent receptor

density on tumor cells by targeting liposomes via two different mAbs to two different cell surface antigens were evaluated.

Chapters 2 and 2A explore the difference in bioavailability of drug in murine breast cancer tumors when mice are treated with free DXR, a leaky liposomal DXR formulation, or two different dose levels of a slow release formulation of liposomal DXR. Methods were developed for isolating nuclei from tumor cells and for accurately quantitating DXR extracted from tumors and tumor cell nuclei by DXR fluorescence. Controls for tumor processing procedures were developed in order to confirm that DXR did not significantly redistribute from liposomes to tumor nuclei during processing and that processing did not rupture the bilayer of liposomes. We also compared the therapeutic activities of various liposomal DXR formulations in this model to the bioavailability results.

It has been hypothesized that targeted liposomal therapy would deliver a larger drug payload to cancerous cells than non-targeted liposomal therapy and that this would result in greater therapeutic activity. To date, numerous studies have shown that ligand-targeted liposomal drug delivery has greater therapeutic efficacy than passively-targeted delivery when liposomes either have good access to the target cells or are targeted against a highly overexpressed internalizing antigen such as HER2/*neu*. In Chapter 3 we directly compare the amount of bioavailable drug in tumors of BT-474-tumor bearing mice when they were injected with free DXR, untargeted liposomal DXR, or an anti-HER2/*neu* scFv (F5)-targeted liposomal DXR formulation.

In Chapter 4, the effect of targeting B lymphoma cells with liposomes via two different antibodies, anti-CD19 and anti-CD20, was compared to results obtained for targeting liposomes via a single antibody. We hypothesized that liposomes targeted via antibodies against two or more receptor populations would increase the apparent receptor density on target cells, resulting in improved therapeutic effects due to greater levels of bioavailable drug being delivered to the target cells. *In vitro* cytotoxicity experiments and *in vitro* cell association experiments were performed with dual-targeted liposomes using the human B-cell lymphoma cell line, Namalwa.

Lastly, chapter 5 summarizes the findings of this thesis work. Conclusions are made and ideas for future directions of this work are discussed.

CHAPTER 2*

Determination of Doxorubicin levels in whole tumor and tumor nuclei in murine breast cancer tumors.

Laginha, K., Verwoert, S., Charrois, G. J. R., and Allen, T. M. Clin. Cancer Res., *11*: 6944-6949, 2005

* All experimental work completed in this Chapter was performed by K. Laginha

2.1. Abstract

Purpose: Pharmacokinetic studies on liposomal drugs have previously measured total drug levels in tumors, which include non-bioavailable drug. However, drugs must be released from liposomes to have activity. We have developed a method for measuring levels of bioavailable (released) doxorubicin (DXR) in vivo in tumors that will allow therapeutic activity to be correlated with bioavailable drug levels.

Experimental Design: Mice orthotopically implanted with mammary carcinoma (4T1) were injected intravenously (i.v.) 10 d after implantation with free DXR or formulations of liposomal DXR with different drug release rates. Tumors were excised at various times after injection, and total tumor DXR levels were determined by acidified isopropanol extraction of whole tumor homogenates. Bioavailable DXR levels were determined by extraction of DXR from isolated tumor nuclei.

Results: Free DXR had high levels of bioavailability in tumor tissue; 95% of the total DXR in tumors was bound to nuclear DNA by 24 h after injection. Administration of Doxil®, a slow release liposomal formulation of DXR, gave an area under the time vs. concentration curve (AUC) for total DXR 7 d after injection that was 87-fold higher than that obtained for free DXR, and 49% of the liposomal DXR was bioavailable. For liposomes with a more rapid DXR release rate, by 7 d after injection the $AUC_{0\text{-}7\ d}$ for total DXR was only 14-fold higher than that for free DXR, and only 27% of liposomal DXR was bioavailable.

Conclusions: This technique allows correlations to be made between drug bioavailability and therapeutic activity and will help in the rational design of drug carriers.

2.2. Introduction

Long-circulating PEGylated liposomal formulations of doxorubicin (DXR), Doxil®, have been shown to result in increased accumulation of drug in solid tumors and reduced dose-limiting toxicities, such as myelosuppression and cardiotoxicity. This is due to alterations in the pharmacokinetics (PK) and biodistribution (BD) of the encapsulated drug (2, 4, 5). Doxil® is currently approved for use in AIDS-related Kaposi's sarcoma, refractory ovarian cancer, and metastatic breast cancer (19, 40-43).

Doxorubicin-loaded liposomes have enhanced efficacy in some solid tumors compared to free DXR because they passively target solid tumors through the enhanced permeability and retention (EPR) effect (35, 125), resulting in increased drug payloads delivered to tumors. The EPR effect is a result of defective vascular endothelial linings of growing tumors, resulting in gaps in the endothelium up to approximately 800 nm in diameter, which are large enough to permit the extravasation of liposomes with diameters in the range of 100 nm (126). In addition, growing tumors have defective lymphatic drainage, which contributes to the extended residence time of extravasated liposomes in the interstitial space of the tumor. Liposomes residing in the interstitial space gradually release their entrapped drug, exerting anti-tumor effects.

Many studies have measured total drug levels in solid tumors following administration of liposomal drugs (6-11). These studies do not distinguish between entrapped (non-bioavailable) drug and released (bioavailable) drug in the tumor. However, only released drug has biological activity, and the therapeutic effects of liposomal drugs will, we propose, be correlated with the levels of bioavailable drug in tumor as a function of time, not the levels of total drug in the tumor. Therefore, knowledge of the levels of bioavailable drug in tumor tissue and the rate of bioavailability will help in the design of improved liposomal formulations of anticancer drugs.

An important site of cytotoxic action of the anticancer drug DXR is the nucleus, where DXR intercalates into DNA, forming DNA adducts and inhibiting topoisomerase II (21). When free DXR reaches the tumor site, DXR that is released from liposomes within the tumor interstitial space is capable of diffusing widely within the tumor. Doxorubicin can diffuse into surrounding cells, become membrane or protein-associated, or diffuse into subcellular compartments such as mitochondria and nuclei. Confocal studies show that a large proportion of DXR that diffuses into the cell accumulates in the cell nucleus (71), where it binds strongly to nuclear DNA. Nuclear DNA functions as a sink for the drug, including drug initially present in other sub-cellular organelles (123, 124). Therefore, we hypothesize that measurement of DXR bound to nuclear DNA will provide a good estimate of levels of bioavailable DXR in tumor tissue *in vivo*. Levels of DXR in total tumor and tumor nuclei were measured in mice orthotopically implanted with

4T1 murine mammary carcinoma. Tumor-bearing mice were injected intravenously (i.v.) with either free DXR, Doxil® (slow drug release), or with a faster drug release formulation with a fluid bilayer composed of unsaturated dioleoylphosphatidylcholine (DOPC) and cholesterol. Total tumor DXR and nuclear DXR were determined as a function of time after injection.

2.3. Materials and Methods

2.3.1. Chemicals and reagents

Doxorubicin hydrochloride (DXR), Doxil® (PEGylated liposomal DXR (PLD), also called Stealth® liposomal DXR and Caelyx®) and methoxypolyethyleneglycol (M_r 2000)-distearoylphosphatidylethanolamine ($mPEG_{2000}$-DSPE) were provided by ALZA Corporation (Mountain View, CA). Cholesterol (CHOL) and dioleoylphosphatidylcholine (DOPC) were from Avanti Polar Lipids (Alabaster, AL). Minimal essential medium (MEM), deoxyribonuclease 1 (DNase 1) and digitonin were from Sigma-Aldrich (St. Louis, MO). Fetal bovine serum (FBS), penicillin, streptomycin, and L-glutamine were from Invitrogen (Burlington, ON, Canada). Sephadex-G50 and Sepharose CL-4B were from Amersham-Pharmacia Biotech (Baie d'Urfe, PQ). Halothane was from MTC Pharmaceuticals (Cambridge, ON). The DNeasy® Tissue Kit was from Qiagen (Mississauga, ON). Sterile, pyrogen-free saline was from Baxter (Toronto, ON). Dextrose United States Pharmacopeia (USP) (D5W), 5% w/v in water was from Baxter Corp. (Mississauga, ON). Chol-[1,2-^{3}H-(*N*)]hexadecyl

ether ([^{3}H]CHE, 1.48-2.22 TBq/mmol) was from PerkinElmer Life Sciences (Woodbridge, ON). All other chemicals were of the highest grade possible.

2.3.2. Animals, cell line, and tumor implantation

Female BALB/c mice (6-8 weeks) were purchased from Health Sciences Laboratory Animal Services, University of Alberta. Mice were housed under standard conditions and had access to food and water ad libitum. All animal protocols were approved by the Health Sciences Animal Policy and Welfare Committee, University of Alberta, and animals were treated in accordance with the Guide to the Care and Use of Experimental Animals set forth by the Canadian Council on Animal Care.

The 4T1 mouse mammary carcinoma cell line is a metastatic, thioguanine-resistant cell line, donated by Dr. Fred Miller (Barbara Ann Karmanlos Cancer Institute, Detroit, MI). The cell line was maintained in MEM supplemented with 10% FBS, penicillin (100 units/mL), streptomycin (100 μg/mL), and L-glutamine (0.292 mg/mL) at 37°C in a humidified incubator with a 5% CO_2 atmosphere (114). Cells were released from their substrate by rinsing with phosphate-buffered saline containing EDTA (PBS-EDTA; 0.54 mM EDTA, 137 mM NaCl, 3 mM KCl, 8 mM Na_2HPO_4, 1.5 mM KH_2PO_4, pH 7.4), followed by trypsin-EDTA (0.05% trypsin in 137 mM NaCl, 5.4 mM KCl, 7 mM $NaHCO_3$, 0.34 mM EDTA). Cells were kept in exponential growth.

Tumors were orthotopically implanted in female BALB/c mice as previously described (75). Briefly, a small incision was made in the lower right abdominal

region of anaesthetized mice, and 1 x 10^5 4T1 cells, in full media, were injected into the right #4 mammary fat pad. A surgical wound clip was used to close the incision and was removed 7 d later.

2.3.3. Preparation of liposomes

Doxil® was used as obtained from the manufacturer. Liposomes with faster release DXR rates were composed of DOPC:CHOL:$mPEG_{2000}$-DSPE at a 2:1:0.1 molar ratio (DOPC-PLD). For these liposomes, [^{3}H]CHE was added as a non-exchangeable, non-metabolized lipid tracer. A lipid mixture of chloroform stocks was prepared, and dried to form a thin film using a rotovaporator; this was then placed in a vacuum overnight. DXR was remote-loaded into liposomes using the ammonium sulphate gradient method previously described (51). The resulting liposomes contained 0.2:1 (w/w) drug/lipid ratios, and the diameter of liposomes was determined to be 100 ± 20 nm, using a Brookhaven BI-90 particle sizer (Brookhaven Instruments, Holtsville, NY). DXR concentrations were determined in methanol extracts of DXR-loaded liposomes from the absorption of the drug at 480 nm compared to a standard curve; phospholipid concentrations were determined by counting the [^{3}H]CHE on a Beckman LS-6800 scintillation counter.

The *in vitro* half-life values for release of DXR from either Doxil® or from DOPC-PLD were previously determined in 50% (v/v) adult bovine plasma in FBS, pH 7.4, to be approximately 118 h and 12 h, respectively (13).

2.3.4. Measurement of DXR

To determine if the tumor homogenization process disrupted liposomes, resulting in premature DXR release, Doxil® or DOPC-PLD in nuclear lysis buffer (NLB, 0.25 M Sucrose, 5 mM TrisHCl, 1 mM $MgSO_4$, 1 mM $CaCl_2$ pH 7.6) was homogenized in an ice-cooled Potter-S® homogenizer. After each homogenization stroke, aliquots of liposomal DXR were taken. Doxorubicin fluorescence (λ_{ex}= 470 nm; λ_{em}= 590 nm) was measured before and after the addition of 10% (v/v) Triton X-100, which lyses the liposomes and releases 100% of the entrapped DXR. Total tumor DXR and DXR in tumor nuclei were quantified using a method similar to Mayer et al. (29). At various times after injection, 10% w/v tumor homogenates from mice receiving free DXR, Doxil® or DOPC-PLD were prepared in NLB. Samples of the homogenate (200 μL) were placed in 2 mL microcentrifuge tubes, and 100 μL of 10% (v/v) Triton X-100, 200 μL of water, and 1500 μL of acidified isopropanol (0.75 N HCl) were added. The tubes were vortexed to ensure complete mixing, and DXR was extracted overnight at –20°C. The next day, the microcentrifuge tubes were warmed to room temperature, vortexed for 5 min., centrifuged at 15,000 X g for 20 min., and stored at –80°C until analysis. Doxorubicin was quantified fluorometrically (λ_{ex}: 470 nm, λ_{em}: 590 nm). To correct for nonspecific background fluorescence, the samples were compared to a standard curve made from the fluorescence emission of known amounts of DXR added to acidified isopropanol extracts of homogenized tumor tissue from untreated mice. The data are the mean ± standard deviation (SD) of

triplicate aliquots from tumor homogenates from 3 to 5 individual mice, expressed as microequivalents of DXR/g tissue since this assay does not discriminate between DXR and fluorescent DXR metabolites, if any.

Tumor cell nuclei were isolated from total tumor homogenates by differential centrifugation through a 1.3 M sucrose gradient at 1000 X g for 10 min. The efficiency of the nuclear DXR extraction was first compared by 2 different methods: an acidified isopropanol extraction, described above; and a DNase 1 digestion method, previously described (127). Since the extraction efficiency of the acidified isopropanol method was superior to that of the DNase I method, all further nuclear DXR accumulation assessments were performed using the acidified isopropanol extraction method.

In addition, the effect of tumor homogenization on liposome redistribution was investigated. Doxil® or DOPC-PLD in concentrations comparable to what was observed in tumors were homogenized together with tumors in NLB. After homogenization, total tumor DXR and nuclei-associated DXR were determined by the methods described above.

2.3.5. *In vivo* tumor bioavailability experiments

BALB/c mice were orthotopically implanted with 4T1 tumor cells, and 10 d after implantation, the mice were given i.v. injections via the lateral tail vein (200 μL) with 9 mg/kg of DXR either as free DXR, Doxil®, or DOPC-PLD. To see if the method scaled with dose, some mice received 16 mg/kg DXR from Doxil®. Control mice were injected with 200 μL sterile saline. Mice (n = 3-5 per time

point) were euthanized, and tumors were excised at various time points up to 7 d after injection or until DXR levels were below detectable levels (0.005 μequivalents DXR/ml). Total and nuclear DXR in 4T1 tumors were determined via the acidified isopropanol extraction method. The % bioavailability of DXR in tumor tissue was determined from the AUC of nuclear drug relative to the AUC of drug in whole tumors over the time-course of the experiment.

2.3.6. Statistics

The pharmacokinetic parameters, tumor $AUC_{0\text{-}24\,h}$ (free DXR) or tumor $AUC_{0\text{-}7d}$ (liposomal DXR), maximum drug concentration (C_{max}), and time to maximum concentration (T_{max}) were calculated for total and nuclear DXR using WinNonlin 4.1 software (Pharsight Corporation, Mountain View, CA). Statistical differences between groups were determined by analysis of variance (ANOVA) with a Tukey-Kramer post-test using GraphPad InStat Version 3.01 (GraphPad Software, Inc., San Diego, CA).

2.4. Results and Discussion

In determining the amount of bioavailable drug in tumors, it is important that the liposomal formulations do not release their entrapped drug prematurely during the homogenization procedure. The prematurely-released drug could diffuse rapidly to nuclei in the homogenate, thus artificially increasing the amount of tumor bioavailable drug. Drug release from liposomes can be measured by the DXR dequenching assay. When DXR is entrapped at high concentrations in liposomes, its fluorescence signal is quenched, and release of the drug increases

the fluorescence signal (128). For example, addition of 10% Triton X-100 (v/v) to our liposomal DXR samples, mimicking 100% drug release, caused the relative fluorescence signal to increase by approximately 10-fold (data not shown). However, up to 10 strokes of the Potter-S® homogenizer caused no increase in the fluorescence signal, so we conclude that no DXR was released from either Doxil® or DOPC-PLD during homogenization. The effect of homogenization of tumor in the presence of liposomal drug was also investigated. If the presence of tumor tissue during homogenization affects the release of drug and its redistribute to the nucleus, this could also result in an artifactual increase in the amount of bioavailable drug in tumor. Both liposomal DXR formulations used during in vivo experiments were tested with 10 strokes of the Potter-S® homogenizer in the presence of tumor and it was determined that between 3-10% of liposomal drug distributes to the nucleus during this procedure (data not shown).

The extraction efficiency for DXR using the acidified isopropanol extraction method for both total tumor and tumor cell nuclei was >90%; this is consistent with previous findings by us and others that >90% of DXR can be extracted by this method (13, 129). There was a linear relationship between the amount of DXR added to control samples and the amount of DXR recovered from either total tumor homogenates or tumor nuclei purified from the homogenates (data not shown). We used nuclear DXR accumulation as an indicator of bioavailable liposomal drug because the nucleus acts like a "sink" for doxorubicin. Once DXR leaks out of liposomes in the interstitial space of solid tumors, the drug rapidly

diffuses into cells and can traffic to cell nuclei, where it intercalates with DNA, rendering the drug immobile. The nucleus is not the only site of action of DXR, e.g., subcellular organelles such as mitochondria are important sites of drug toxicity (130, 131), but it is the only site that functions as a sink for the drug. Hence, nuclear DXR, we postulates, provides a reasonable first approximation to bioavailable DXR in cells.

Figure 2.1A presents total DXR levels in mouse mammary tumors and DXR levels in tumor nuclei after treatment of the mice with 9 mg/kg of free DXR. As expected, total DXR levels in tumors increased quickly, then dropped rapidly and fell to below-detectable levels by 48 h after injection. The free drug was rapidly bioavailable; the tumor $AUC_{0\text{-}24\ h}$ for nuclear drug was 95% of that of the $AUC_{0\text{-}24\ h}$ of total drug (Table 2.1). The maximum total DXR concentration in tumor (C_{max}) was 8 μequivalents DXR/g tumor and occurred at 30 min after administration. Nuclear DXR levels did not reach C_{max} (3 μequivalents DXR/g tumor) until 4 h after injection. Concentrations of DXR that were determined in these experiments were close to the detectable limits of the drug, so quantification of both total and nuclear DXR resulted in large standard deviations.

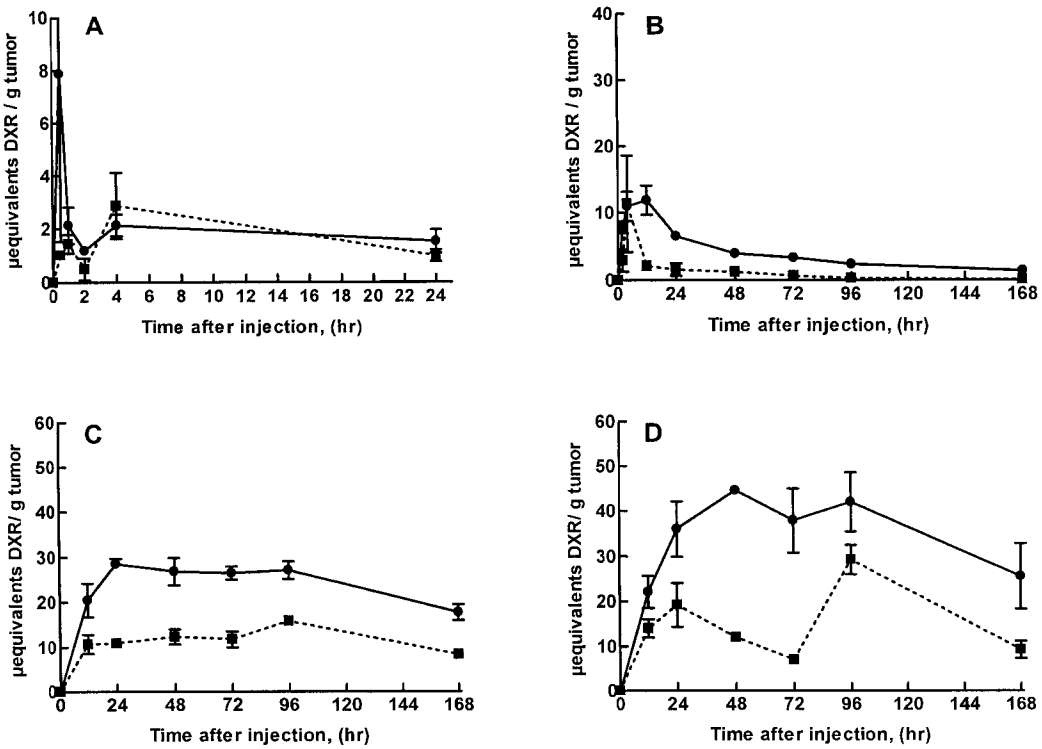

Figure 2.1. DXR concentrations in 4T1 tumors in mice receiving free DXR, DOPC-PLD , or Doxil®. Female BALB/c mice were orthotopically implanted with 4T1 murine mammary carcinoma and were injected 10 d after implantation (time zero) with either free DXR at a dose of 9 mg/kg, DOPC-PLD at a dose of 9 mg/kg, or Doxil® at a dose of 9 or 16 mg/kg. Total (solid line) and nuclear (dashed line) DXR levels were determined following acidified isopropanol extraction. Data represent mean ± SD of triplicate aliquots from 3 to 5 mice per time point. *A.* Free DXR, 9 mg/kg; *B.* DOPC-PLD, 9 mg/kg. *C.* Doxil®, 9 mg/kg; *D.* Doxil®, 16 mg/kg.

Figure 2.1C and 2.1D show levels of total tumor DXR and DXR levels in tumor nuclei for Doxil® at doses of 9 and 16 mg/kg. At a dose of 9 mg/kg, this liposomal formulation of DXR had a very different tumor distribution profile than free DXR, with significantly higher tumor $AUC_{0\text{-}7\ d}$ for total DXR levels (87-fold higher) and nuclear DXR levels (45-fold higher) in the tumors ($p < 0.001$) compared to free DXR (Table 2.1). The $AUC_{0\text{-}7\ d}$ appeared to scale with dose, with the tumor AUC in mice receiving 16 mg/kg being 1.5-fold higher than that in mice receiving 9 mg/kg. Total DXR levels in tumor for either Doxil® dose reached C_{max} much later than free DXR (24-48 h after injection vs. 0.5 h). These differences reflect the different mechanism of accumulation of liposomal vs. free drugs in tumor tissue, both of which are distributed to tumors via the blood stream. Liposomes, however, are particles of approximately 100 nm in diameter, and must extravasate through gaps between the endothelial cells in the permeable blood vessels within solid tumors to accumulate in the interstitial space of tumors (126). This is a slow process. Therefore, the delay in time to C_{max} and the slow rate of clearance reflect the time that it takes for liposomal drugs to extravasate into tumor tissue by the EPR effect (125). These data are similar to the delayed time to C_{max} and prolonged residency times for liposomal drugs that have been observed in other tumor models (12, 132). Nuclear accumulation of liposomal DXR also showed a different profile than free DXR (Figure 2.1C vs 2.1A). For doses of either 9 or 16 mg/kg, C_{max} for nuclear accumulation of DXR in murine mammary tumors occurred at 2 to 3 d after treatment versus 4 h for free DXR. This reflects

the slow rate of release of DXR from the carrier, which must occur before the drug can traffic to the nucleus. During the 7 d time course of these experiments, 40 to 50% of the liposomal drug was bioavailable (Table 2.1).

Table 2.1. Comparison of tumor pharmacokinetics of free DXR vs. liposomal formulations of DXR. Tumor levels of total DXR and nuclear DXR were determined in mice bearing orthotopic 4T1 mammary carcinomas, following administration of 9 mg/kg DXR as Doxil®, DOPC-PLD, or free DXR. Some mice also received 16 mg/kg of Doxil®. Area under the time versus concentration curves are AUC0-24 h for free DXR and AUC0- 7d for liposomal DXR formulations. All parameters were determined using WinNonLin software.

Formulation	Doxil® (16 mg/kg)		Doxil® (9 mg/kg)		DOPC-PLD (9 mg/kg)		Free DXR (9 mg/kg)	
	Total	Nuclear	Total	Nuclear	Total	Nuclear	Total	Nuclear
AUC (μeq h/g tumor)	5918	2444	3988	1970	641	172	45.8	43.3
% Bioavailable	41.3%		49.4%		26.8%		95.1%	
C_{max} (μeq DXR/g tumor)	48.8	25	28.6	15.9	11.9	11.4	7.9	2.9
T_{max} (hr)	48	96	24	96	12	4	0.5	4
$t_{1/2}$ (hr)	135	ND	151	ND	78	ND	25	ND
MRT (hr)	81	ND	81	ND	52	ND	10	ND
Clearance (g/hr/kg)	1.5	ND	1.1	ND	11.3	ND	89	ND

ND=no value determinable by the PK program

AUC =area under the curve, C_{max} = maximum drug concentration, DOPC-PLD = dioleoylphosphatidylcholine:CHOL:$mPEG_{2000}$-DSPE, DXR = doxorubicin, MRT = mean residence time, $t_{1/2}$ = half-life, T_{max} = time to maximum drug concentration, μeq = μequivelent

Liposomes with more rapid release rates than Doxil® have pharmacokinetic (PK) profiles in tumor that are intermediate between Doxil® and free DXR (Figure 2.1B vs. Figures 2.1A and 2.1C). DOPC-PLD liposomes have a more fluid bilayer due to the presence of the unsaturated fatty acyl chains in DOPC. This leads to more rapid rates of drug release from DOPC-PLD than from Doxil®, which contains long-chain saturated fatty acyl chains. Using dual-labeled liposomes (radiolabelled DXR and radiolabelled lipid), the half-life for release of DXR from liposomes *in vivo* has recently been reported to be 1.9 h for DOPC-PLD vs. 315 h for Doxil® (133). In clinical trials, it has been show that less than 10% of the encapsulated DXR is released from Doxil® by 24 h after i.v. administration (134). However, since DOPC-PLD has a substantially greater rate of drug release, a considerable portion of the drug will be released before much tumor accumulation occurs. In other word, drug from DOPC-PLD will reach tumors as a combination of residual DXR still entrapped in liposomes and free DXR that has been released from liposomes into the blood compartment and has redistributed to tissues including tumor tissue.

The levels of total DXR from DOPC-PLD in tumors were only 14-fold higher than those from free DXR, vs. 87-fold higher for Doxil®. The C_{max} for total tumor DXR from DOPC-PLD occurred 12 h after injection, i.e., between the 0.5 h for free DXR and the 24 to 48 h for Doxil®. The tumor $AUC_{0\text{-}7\ d}$ of total drug for DOPC-PLD was over 6-fold lower than that seen for Doxil® at the same dose, and the $AUC_{0\text{-}7\ d}$ of bioavailable drug, i.e., bound to nuclei, was over 11-fold lower.

When drug-depleted liposomes accumulate in the tumor, only limited amounts of the drug are available for release, cellular uptake, and trafficking to the nuclei. Nuclear DXR concentrations reached maximum levels by 4 h post-injection, similar to free DXR and much more rapidly than Doxil®. This suggests that a considerable amount of the drug was reaching tumor nuclei as released drug. Doxorubicin bioavailability from the DOPC-PLD formulation was 26.8%, and there was 4-fold more bioavailable DXR delivered to tumors than for free DXR (Table 2.1). Nuclear levels of drug were at or below measurable limits for many of the later time points, possibly resulting in an underestimate of the amount of bioavailable drug. Also provided in Table 2.1 are the $t_{1/2}$ for DXR in tumor tissue, mean residence time (MRT), and tumor clearance of DXR, which reflect a similar rank order as those seen for other PK parameters.

Our results for bioavailable drug levels in tumor tissue for the two liposomal formulations correlate well with the pharmacokinetics and therapeutic effects for the same formulations in the same animal model, reported recently by our group (13). In this PK study, we reported that the plasma half-life for DXR was 18.2 h when the slow release formulation was administered to tumor-bearing mice, and the plasma $AUC_{0-\infty}$ was 3020 μg ·h/ml. In contrast, the plasma half-life for DXR in DOPC-PLD was only 2.1 h, and the plasma $AUC_{0-\infty}$ was 430 μg ·h/ml. The plasma $AUC_{0-\infty}$ for the lipid component of the liposomes was very similar for the two formulations (10,600 for DSPC vs. 12,700 ug·h/ml for DOPC), indicating that drug-depleted liposomes were circulating in plasma (13). In distribution

experiments using fast versus slow release liposomal DXR, DXR in the slow release liposomes (similar formulation to Doxil®) accumulated to a significantly higher extent in 4T1 tumors compared to liposomes with fast release rate (DOPC-PLD) (12). In therapeutic experiments, the slow release formulation had superior therapeutic activity to the fast release formulation (13), which correlates with the observations on DXR bioavailability in tumor tissue report in the paper.

Currently, several strategies to optimize liposomal drug delivery are being evaluated by us and others, and a bioavailability assay for DXR in tumor tissue will be useful in designing optimal formulations. One approach is to use targeting moieties against malignancies that uniquely express or over-express cell surface antigens. Targeting drug-loaded liposomes with monoclonal antibodies such as anti-HER2 or anti-CD19, for example, has resulted in improved efficacy in vivo in murine xenograft models over non-targeted liposomes or free drug (122, 135). We have begun studies to examine how targeting internalizing or non-internalizing epitopes at the surface of cancer cells affects the rate and extent of bioavailability of the entrapped drugs. Another strategy is to design triggered release formulations of liposomes that release their contents in a burst when triggered by temperature or pH after the liposomes have localized to tumors (101, 136). Bioavailable measurements will also be useful in the design of these types of formulations.

The fluorescent properties of DXR and its interchelation into DNA made it relatively easy to make bioavailability measurements for this drug in tumor tissue.

For other drugs, more complex techniques may be required. For example, it has been hypothesized that lack of bioavailability of liposomal cisplatin may account for the relatively poor clinical results found for liposomal formulations of cisplatin (137). Recently, the release of active platinum from liposomes was determined in murine melanoma tumors by the use of microdialysis probes and atomic absorption spectrophotometry (138). Although more total liposomal cisplatin distributed to tumors than free cisplatin in this study, less Pt was released into the tumor extracellular fluid, suggesting that tumor bioavailability of active Pt was sub-optimal. In an alternative approach, liposome drug concentrations and levels of released drugs were measured by MRI using liposomes loaded with DXR and $Mn(SO_4)$ and measuring the relaxivity T(1) of Mn^{++}. When the drug is inside the liposomes T(1) was relatively unaffected; release of the drug from a flank fibrosarcoma tumor, mediated by hyperthermia, resulted in a significant shortening of T(1) (139).

The ability to quantitate bioavailable drug at the site of drug action may assist in developing new anticancer drug carriers, such as the ones mentioned above, that may have improved therapeutic effects and reduced side effects compared to conventional drug treatments. We believe the results presented in this paper are a good first approximation of the rate and extent of bioavailable drug in tumor tissues for liposomal carriers; refinement of the methodology may be necessary to achieve definitive results. For example, studies on the rate and extent of tumor tissue bioavailability of liposomal DXR, done in combination with

apoptotic assays, can provide valuable information on the minimum concentrations of bioavailable DXR required for cell kill and on the exposure times needed for driving the cells into apoptosis.

CHAPTER 2A (Addendum to Chapter 2)

Therapeutic activity of various doxorubicin formulations in murine breast cancer

2A.1. Rationale

In chapter 2 we determined the rate and extent of bioavailable DXR in 4T1 tumors after DXR delivery with different DXR formulations. We concluded that a greater amount of bioavailable drug in 4T1 tumors would lead to increased therapeutic activity in the 4T1 murine mammary carcinoma model. We referred to a paper published in our laboratory by Charrois et al., which described a therapeutic study in the same model with similar liposomal formulations, but at a different drug dosage and lacking data on the therapeutic effects of Doxil® (13). In order to more accurately assess the impact of the rate and extent of bioavailable DXR in 4T1 tumors on therapeutic activity, we completed a therapeutic study evaluating the therapeutic activity of the exact dosage and formulations that were used in Chapter 2.

2A.2. Materials and Methods

BALB/c mice were orthotopically implanted with 4T1 tumor cells as described in the previous chapter. Four days after tumor implantation, groups of 7 mice were given i.v. injections via the tail vein (200 μL) with either 9 mg/kg free DXR, 9 mg/kg DOPC-PLD, or 9 and 16 mg/kg Doxil®. Control mice received 200 μL of sterile D5W. The mice were injected 4 d after tumor implantation instead of 10 d after implantation, as in the bioavailability experiments, because the 4T1 tumors grow very rapidly. Tumor size was measured using calipers at various times after treatment and tumor volume was calculated using the formula: v = 0.4ab2 were a and b are perpendicular diameters and a>b.

2A.3. Results and Discussion

The results of the tumor growth delay experiment are presented in Figure 2A.1. Mice in the 16 mg/kg Doxil® group were euthanized on day 12 due to severe weight loss. These toxicities did not occur in the previous bioavailability experiments, likely because the final group in those experiments were euthanized 7 d after drug injection. The rank order of tumor growth delay for mice treated with 9 mg/kg DXR in various formulations was Doxil® had greater effects than DOPC-PLD, which in turn had greater effects than free DXR. Treatment with free DXR resulted in minimal tumor growth delay. These results are consistent with what we expected to find based on the tumor bioavailability data in Chapter 2. In those studies, mice treated with free DXR had the least amount of drug in the tumors and tumor nuclei, and this resulted in no delay in tumor growth compared to control mice. In addition, mice injected with the fast drug release formulation, DOPC-PLD, had significantly more total tumor drug and nuclear levels of drug compared to free DXR but drug levels were significantly less than what was seen for mice treated with 9 mg/kg of Doxil®.

We hypothesized that the ability to quantitate total and bioavailable drug at the site of drug action, will aid in the design of new drug carriers or help to optimize currently available drug carriers. We conclude that our measurements with DXR provide a good first approximation of the therapeutic activity.

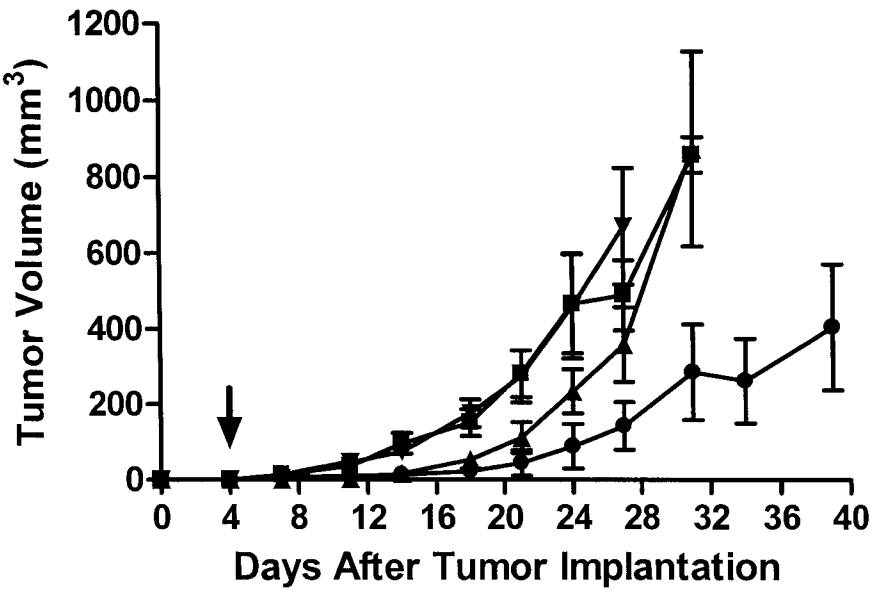

Figure 2A.1. Therapeutic activity of different formulations of DXR against 4T1 murine mammary carcinoma. BALB/c mice were orthotopically implanted with the 4T1 murine mammary carcinoma. Four days after tumor implantation (arrow), mice were treated with 9 mg/kg free DXR (▼), 9 mg/kg DOPC-PLD (▲), 9 mg/kg Doxil® (●), 16 mg/kg Doxil® (♦) or D5W control (■).

CHAPTER 3

Doxorubicin levels in tumors after targeted or non-targeted liposomal drug delivery in a human breast cancer model

3.1 Abstract

Purpose: An increase in therapeutic activity has been reported when doxorubicin (DXR)-loaded liposomes are targeted via anti-HER2/*neu* compared to non-targeted liposomal DXR in mice bearing tumors with high levels of overexpression of HER2/*neu*. We have attempted to quantitate the amount of total and bioavailable drug in tumors that overexpress HER2/*neu* when exposed to targeted and non-targeted formulations of DXR and free drug.

Experimental Design: Cell association and *in vitro* cytotoxocity of anti-HER2/*neu*-targeted liposomes, Doxil® and free DXR were determined in the BT-474 ATCC human breast cancer cell line. Total and bioavailable drug levels were determined in NCr nude mice bearing 200-300 mm^3 BT-474 M3C5 tumors as a function of time after administration of 9 mg/kg free DXR, Doxil®, and anti-HER2/*neu* scFv-targeted Doxil®. Total tumor DXR and tumor cell nuclei levels of DXR were determined for excised tumors at various times after injection (140).

Results: Anti-HER2/*neu*-targeted liposomes associated with BT-474 ATCC cells to a significantly greater extent than non-targeted liposomes and, when DXR-loaded, were more cytotoxic than non-targeted liposomes. Administration of anti-HER2/*neu*-targeted liposomal DXR to tumor-bearing mice resulted in 1.8 fold higher total tumor DXR levels over 7 d after injection compared to Doxil®. For targeted liposomes, 26% of the drug was bioavailable compared to 46% for Doxil®. There was no significant difference in maximum nuclear levels of DXR after administration of free DXR, F5-Doxil®, and Doxil®

Conclusions: More total drug was delivered to tumors using F5-Doxil® compared to Doxil® but the amount of DXR associated with tumor nuclei over the 7 d time-course was the same.

3.2 Introduction

Since the clinical approval of the liposomal formulation of doxorubicin (DXR), Doxil®, only two more anticancer liposomal drug formulations have been approved for clinical use, DaunoXome® (daunorubicin) and Myocet® (doxorubicin)(141-143). All of the approved liposomal anticancer drugs alter the pharmacokinetics (PK) or biodistribution (BD) of the encapsulated drug (27, 144, 145). This results in decreased dose-limiting side effects and may or may not increase therapeutic efficacy over conventional chemotherapy in the cancers for which they are clinically approved.

One approach that is being rigorously explored in order to increase the therapeutic efficacy of liposomal formulations is to target liposomes with ligands or antibodies that bind to receptors or proteins that are uniquely expressed or overexpressed on cancer cells. Liposomes such as Doxil® increase drug accumulation in solid tumors because they passively target solid tumors through the enhanced permeability and retention (EPR) effect (35, 125). This is a result of the "leaky vasculature" and impaired lymphatic drainage of growing solid tumors. The rate at which drug entrapped in extravasated liposomes becomes bioavailable is dependent on the rate of drug leakage from the liposomes. One method that has been proposed to increase the amount of bioavailable drug in tumors is to

selectively target the liposomes to cancer cells. If liposomes are targeted with an internalizing antibody or ligand that binds to a cell surface receptor expressed on the cancer cells, the whole drug package will be internalized and more drug will accumulate inside the tumor cells. This is postulated to lead to an increase in therapeutic activity.

Numerous cancers uniquely express or overexpress cell surface receptors (146). In particular, 25-30% of human breast cancers overexpress the cell surface receptor HER2/*neu*. Overexpression of this receptor is characteristic of an aggressive form of breast cancer that has a very poor prognosis (147, 148). In 1998, a monoclonal antibody (mAb), Herceptin® (anti-HER2/*neu*) was clinically approved for treatment of breast cancers that have high levels of overexpression of the HER2/*neu* receptor. It has recently been shown in a clinical trial that adjuvant treatment with Herceptin® plus chemotherapy in operable disease improved therapeutic outcomes compared to chemotherapy treatment alone (149).

In mice, treatment with DXR-loaded liposomes targeted to the HER2/*neu* receptor resulted in improved therapeutic efficacy in HER2/*neu* overexpressing murine models of breast cancer compared to non-targeted liposomal therapy (80, 81, 150). Investigators speculated that the improved therapeutic efficacy seen in mice was due to an increase in the amount of drug being delivered to tumor cells. However, total DXR levels were similar in tumors for either targeted or non-targeted liposomes (81). Despite similar total drug levels in tumor, tumor distribution was markedly different between the two formulations. Using colloidal

gold-labeled liposomes, non-targeted liposomes were found to be associated more with the stroma of the tumors, while targeted liposomes were inside tumor cells. This led to the conclusion that the improved therapeutic activity seen with targeted-liposomes was due to more DXR being delivered inside tumor cells.

Recently, a single-chain fragment of the variable region (scFv) targeted to the HER2/*neu* receptor has been developed. This scFv, named F5, was selected by phage display and is characterized by its high binding to the HER2/*neu* receptor and its ability to trigger receptor-mediated endocytosis (78, 83). Since internalization of the drug-package appears to be essential for increasing the therapeutic activity of targeted liposomal therapy, this will theoretically increase the drug payload delivered inside tumor cells (122). Treating tumor-bearing mice with liposomes targeted via F5 resulted in improved therapeutic activity in a HER2/*neu* overexpressing BT-474 xenograft breast cancer model ($> 10^6$ copies/cells) compared to non-targeted liposomes (83). As a result of the promising preclinical data, F5-targeted liposomes are scheduled to enter clinical trials (78, 151).

In our laboratory, we have developed a method to quantify bioavailable DXR by measuring the amount of DXR bound to DNA in the nucleus of cancer cells (140). This appears to be an appropriate technique for measuring bioavailable drug in tumor cells since a significant portion of free DXR will distribute to the nucleus (123, 124, 152). Quantitation of bioavailable drug in tumor cells for drug delivered via F5-targeted liposomes or non-targeted

liposomes will help determine if the increased in therapeutic activity seen with F5-targeted liposomes is due to an increase in the payload of bioavailable drug that reaches the interior of the target cancer cells.

Cell association and cytotoxicity were determined using anti-HER2/*neu* and non-targeted liposomes to ensure that the mAb bound to BT-474 ATCC cells and that the cells are sensitive to DXR. Levels of DXR in total tumor and tumor nuclei were determined in mice subcutaneously injected with the tumorigenic subclone, BT-474 M3C5. When tumor xenografts were established (200-300 mm^3), mice were injected i.v. with free DXR, Doxil®, or F5-targeted Doxil®. Total tumor DXR and nuclear levels of DXR were determined as a function of time post-injection.

3.3 Materials and Methods

3.3.1. Chemicals and reagents

Doxorubicin hydrochloride (DXR), hydrogenated soy phosphatidylcholine (HSPC), Doxil® (PEGylated liposomal DXR (PLD), also called Stealth® liposomal DXR and Caelyx®), anti-HER2/*neu* scFv (F5)-targeted liposomal doxorubicin, and methoxypolyethyleneglycol (M_r 2000)-distearoylphosphatidylethanolamine ($mPEG_{2000}$-DSPE) were provided by ALZA Corporation (Mountain View, CA). Cholesterol (CHOL) was from Avanti Polar Lipids (Alabaster, AL). Maleimide-derivatized PEG_{2000}-DSPE (Mal-PEG-DSPE) was custom synthesized by Nektar Therapeutics, Inc. (Huntsville, AL). DMEM, RPMI 1640 media, fetal bovine serum (FBS), and

penicillin/streptomycin/glutamine were from Invitrogen (Burlington, ON, Canada). Bio-Rad Protein Assay Reagent was purchased from Bio-Rad Laboratories (Mississauga, Ontario, Canada). 2-iminothiolane (Traut's Reagent) and 3-(4,5-dimethylthiazol-2-ly)-2,5-diphenyltetrazolium bromide (MTT) and insulin were obtained from Sigma Chemical Co. (St. Louis, MO). The humanized $IgG_{1\kappa}$ mAb, Anti-HER2/*neu* (Herceptin®), was purchased from Roche-Applied Sciences. Nuclepore polycarbonate membranes (pore sizes, 0.4, 0.2, 0.1, and 0.08 μm) were purchased from Northern Lipids (Vancouver, British Columbia, Canada). Sephadex G-50, Sepharose CL-4B and Aqueous Counting Scintillant (ACS) were purchased from Amersham Biosciences (Baie d'Urfe, Quebec, Canada). Dextrose United States Pharmacopeia (USP) (D5W), 5% w/v in water was from Baxter Corp. (Mississauga, ON). Chol-[1,2-^{3}H-(*N*)]hexadecyl ether ([^{3}H]CHE, 1.48-2.22 TBq/mmol) and ^{125}I-NaI (185 MBq) were from PerkinElmer Life Sciences (Woodbridge, ON). Estrogen tablets (0.72 mg) were from Innovative Research of America (Sarasota, Florida, Unites States of America). All other chemicals were of the highest grade possible.

3.3.2. Animals, cell line, and tumor implantation

Female NCr nude mice (4-5 weeks) were purchased from Taconic. Mice were housed under viral and antigen free conditions and had access to food and water *ad libitum*. All animal protocols were approved by the Health Sciences Animal Policy and Welfare Committee, University of Alberta, and animals were

treated in accordance with the Guide to the Care and Use of Experimental Animals set forth by the Canadian Council on Animal Care.

The BT-474 cell line used for cell association and cytotoxicity studies was obtained from ATCC. The cell line was maintained in Dulbecco's modified essential medium (DMEM) supplemented with 10% FBS, penicillin G (100 units/ml), streptomycin sulphate (100 μg/ml) and L-glutamine (0.292 mg/ml) in a humidified 37 °C incubator with a 5% CO_2 atmosphere. The BT-474 M3C5 human breast cancer cell line was obtained from ALZA Corporation. This cell line was used for all *in vivo* experiments since it was selected by *in vivo* passage for its increased tumorigenicity compared to the parent cell line. The cell line was maintained in RPMI 1640 supplemented with 10% FBS, L-glutamine (0.292 mg/mL), and insulin (0.01 mg/ml) at 37°C in a humidified incubator with a 5% CO_2 atmosphere (114). Cells were kept in the exponential phase of cell growth.

3.3.3. Preparation of liposomes

Doxil® and F5-targeted liposomes were used as obtained from ALZA Corporation. To remove any DXR that may have leaked from the liposomes during storage, liposome formulations were chromatographed on a Sephadex G-50 column equilibrated with pyrogen-free HEPES-buffered saline (HBS). Non-targeted liposomes for cell association experiments were composed of HSPC: CHOL:$mPEG_{2000}$-DSPE at a 2:1:0.1 molar ratio. Anti-HER2/*neu*-targeted liposomes for cell association and cytotoxicity experiments were composed of HSPC:CHOL:$mPEG_{2000}$-DSPE:Mal-PEG_{2000}-DSPE at a 2:1:0.08:0.02 molar ratio

(SIL[anti-HER2/*neu*]). [^{3}H]CHE was added to liposomes as a non-exchangeable, non-metabolized lipid tracer. For cytotoxicity experiments, DXR was remote-loaded into liposomes using the ammonium sulphate gradient method previously described (51). The resulting liposomes contained 0.2:1 (w/w) drug/phospholipid ratios, and the diameter of liposomes was consistently in the range of 100 ± 20 nm, as determined by dynamic laser light scattering (Brookhaven BI-90 particle sizer, Brookhaven Instruments, Holtsville, NY). DXR concentrations were determined in methanol extracts of DXR-loaded liposomes from the absorption of the drug at 480 nm compared to a standard curve; phospholipid concentrations were determined from the specific activity of [^{3}H]CHE on a Beckman LS-6800 scintillation counter.

3.3.4 Preparation of Immunoliposomes

Aliquots of the anti-HER2/*neu* mAb were labeled with ^{125}I using Iodobeads® purchased from Pierce Biotechnology Inc (Rockford, Illinois). Anti-HER2/*neu* was coupled to the terminus of Mal-PEG-DSPE in preformed liposomes using the coupling method previously described (80). A trace amount of ^{125}I-labeled antibody was added to the unlabeled antibody prior to thiolation; antibody (10 mg/ml) was thiolated with Traut's reagent at a ratio of Traut's:IgG of 20:1 (mol/mol) in degassed HBS (pH 8.0) for 1 h. Unreacted Traut's reagent was subsequently removed by chromatography of the thiolation mixture through a Sephadex G-50 column equilibrated with degassed HBS (pH 7.4). The individual thiolated antibody was immediately added to liposomes and coupled overnight at

room temperature with continuous stirring. Unconjugated antibody was removed by chromatography on a Sepharose CL-4B column in HBS (pH 7.4).

The concentration of antibody coupled to liposomes was determined from the specific activity of the radioactive tracer (^{125}I) and the amount of ^{125}I associated with the liposomes

3.3.5. *In vitro* immunoliposomes binding and uptake

Binding experiments were performed at both 37°C and 4°C (permissive and non-permissive for internalization, respectively) as previously described (84). Briefly, non-targeted liposomes (SL) or SIL[anti-HER2/*neu*], were prepared with 74 kBq of [^{3}H]CHE label per μmol of PL. Liposomes were incubated with 1 x 10^{6} BT-474 ATCC cells, harvested in the exponential growth phase, at various phospholipid concentrations for 1 h at either 37°C or 4°C. Cells were washed to remove unbound liposomes, and the amount of [^{3}H]CHE was determined by scintillation counting in a Beckman LS-6800 scintillation counter. Cell association (pmol PL/10^{6} cells) was calculated from the specific activity of the liposomes. Specific binding was determined by subtracting non-specific binding of SL from the total binding of SIL.

3.3.6. *In vitro* cytotoxicity studies

Cytotoxicity of free DXR, free anti-HER2/*neu*, non-targeted liposomes (DXR-SL) or targeted liposomes (DXR-SIL[anti-HER2/*neu*]) was determined in the BT-474 ATCC cell line using the MTT dye reduction assay (153). Briefly, 4.0

x 10^5 cells/well were plated in 96-well plates and left to adhere overnight. The next day, cells were washed and incubated at 37°C for 1 h with the different DXR formulations in non-supplemented media. The cells were then washed and incubated for an additional 95 h before cell viability was assessed. Results are expressed as IC_{50}, which was obtained graphically using Graphpad Prism version 4.0 (GraphPad Software, Inc., San Diego CA).

3.3.7. *In vivo* tumor bioavailability experiments

NCr nude mice were subcutaneously (s.c.) implanted with a 60 day slow-release estrogen tablet (0.72 mg) in their right rear flank. The next day, 23 x 10^6 BT-474 M3C5 cells were implanted s.c. in the shoulder of the mice. When tumors reached a predetermined size (200-300 mm^3), the mice were given intravenous (i.v.) injections via the tail vein (200 μL) with 9 mg/kg of DXR either as free DXR, Doxil®, or F5-targeted liposomes. Control mice were injected with 200 μL sterile saline. Mice (3 per time point) were euthanized, and tumors were excised at various time points up to 7 d after injection. Total DXR in BT-474 M3C5 tumors was determined via an acidified isopropanol extraction method (140). Nuclear DXR was determined by isolating tumor cell nuclei from total tumor homogenates by differential centrifugation through a 1.3 M sucrose gradient at 1000 x g for 10 min and DXR was then extracted as previously described (140). The percent bioavailability of DXR in tumor tissue was determined from the AUC of nuclear drug relative to the AUC of drug in whole tumors over the time course of the experiment.

3.3.8. Statistics

The pharmacokinetic parameters, tumor $AUC_{0\text{-}24\ h}$ (free DXR) or tumor $AUC_{0\text{-}7d}$ (liposomal DXR), maximum drug concentration (C_{max}), and time to maximum concentration (T_{max}) were calculated for total and nuclear DXR using WinNonlin 4.1 software (Pharsight Corporation, Mountain View, CA). Statistical differences between groups were determined by analysis of variance (ANOVA) with a Tukey-Kramer post-test using GraphPad InStat Version 3.0 (GraphPad Software, Inc., San Diego, CA).

3.4 Results and Discussion

The HER2/*neu* receptor is overexpressed on many breast cancer cells and is a slowly internalizing receptor (154). We performed cell association experiments to determine if liposomes that are targeted with the commercially available antibody, anti-HER2/*neu* (Herceptin®), would bind to cells that overexpress HER2/*neu* to a greater extent than non-targeted liposome.

Cell association of SIL[anti-HER2/*neu*] and SL at both 4 °C and 37 °C was compared (Fig. 3.1). SIL[anti-HER2/*neu*] bound to BT-474 ATCC cells to a greater extent than SL at both 4 °C and 37 °C ($P<0.001$), but no difference was observed in cell binding of SIL[anti-HER2/*neu*] at 4 °C compared to 37 °C. These results are consistent with previous results from Kirpotin *et al*, where liposomes targeted with a Fab' fragment made from a humanized recombinant mAb against HER2/*neu* also showed no difference in the levels of targeted liposomes associated with BT-474 cells after a 2 h incubation at either 4 °C and 37 °C (80).

Upon further investigation these investigators concluded that ≥90% of the liposomes were internalized at 37 °C. That suggests that HER2/*neu* is slow to recycle back to the cell surface.

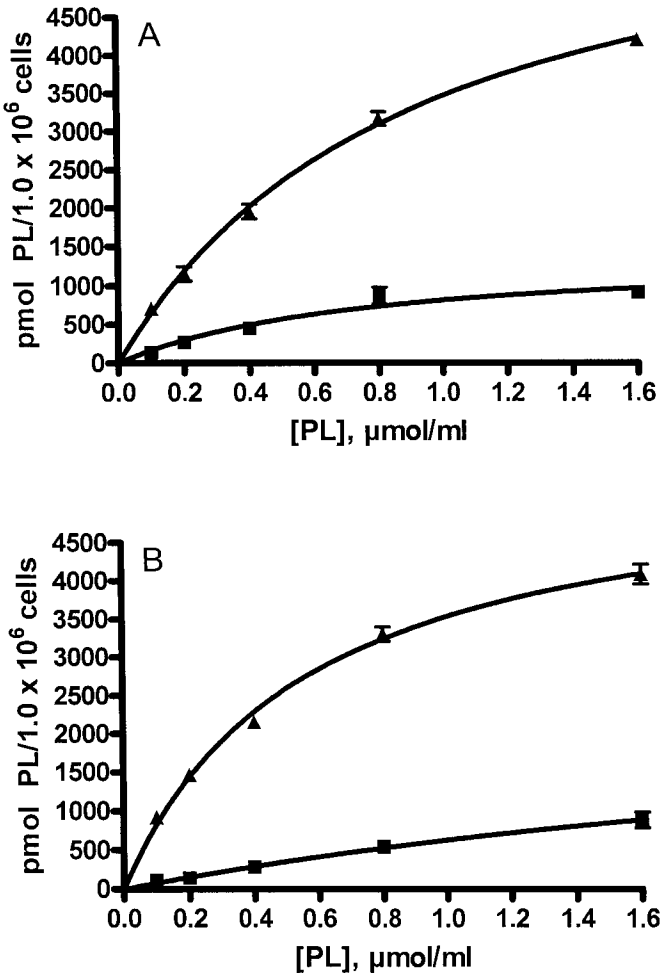

Figure 3.1. Cell association of liposomes with BT-474 ATCC cells as a function of lipid concentration and temperature. (▲) SIL[anti-HER2/neu], 70.4 µg mAb/µmol PL; (■) SL. Liposomes were labeled with [3H]CHE and were composed of either HSPC:CHOL:mPEG:Mal-PEG (2:1:0.08:0.02) for immunoliposomes or HSPC:CHOL:mPEG (2:1:0.1) for non-targeted liposomes. Liposomes were incubated with 1.0 x 106 BT-474 ATCC cells for 1 h in FACS tubes, after which the cells were washed with cold PBS to remove the unbound liposomes. Data are expressed as pmoles PL/1.0 x 106 cells. Each point is an average of 3 replicates ± S.D. (A), 4 °C; (B), 37 °C.

The *in vitro* cytotoxicity results for DXR-SL, DXR-SIL[anti-HER2/*neu*], free DXR and free anti-HER2/*neu* are presented in Figure 3.2. The IC_{50} against the BT-474 ATCC cell line for free DXR, SIL[anti-HER2/*neu*] and SL were 13.8, 65.4 and 793 μg/ml, respectively. The free antibody had no cytotoxicity, which was expected in an *in vitro* setting since it has been shown that the free antibody requires the presence of cytokines to exert cytotoxic effects (155). It was expected that the targeted liposomal formulation would be more cytotoxic than the non-targeted liposomal formulation *in vitro* since the liposome composition is one with very slow rates of drug leakage. Since drug has to be released from liposomes to have an effect, non-targeted liposomes will have very little cytotoxicity during the 1 h drug incubation period. In contrast, the targeted liposomes will bind to the target cells and the subsequent internalization of the liposome drug package by the cells will allow a large drug payload to be delivered internally into the cells. Intracellular release of this large payload from the lysosomal apparatus over the subsequent 96 h incubation time will lead to increased levels of cytotoxicity relative to non-targeted liposomes.

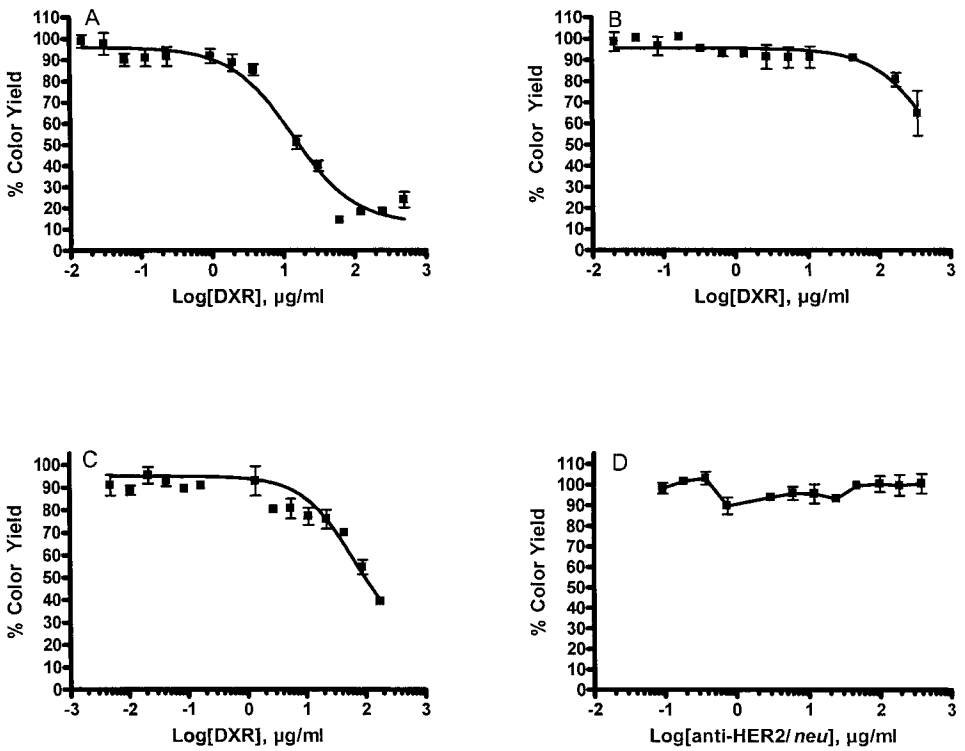

Figure 3.2. Cytotoxicity of various DXR-containing formulations against BT-474 ATCC cells. BT-474 ATCC cells (4.0 x 10^4 cells/well) were plated in 96-well plates and permitted to adhere overnight. The following day cells were incubated for 1 h in DMEM without fetal bovine serum (FBS) with increasing concentrations of **(A),** free DXR; **(B)**, DXR-SL; **(C)**, DXR-SIL[anti-HER2/*neu*], 74 µg Ab/ µmol PL; and **(D)**, free anti-HER2/*neu*, at antibody concentrations comparable to amount of coupled antibody. Cells were then washed 3 x with DMEM, and incubated with fresh medium containing FBS for a further 95 h, and a MTT assay was performed.

Figure 3.3A and 3.3B show levels of total tumor DXR and DXR levels in nuclei after mice were injected with either 9 mg/kg F5-Doxil® or Doxil®, respectively. Mice receiving F5-Doxil® had significantly higher accumulations of total DXR (1.8-fold higher) in tumors over 7 d than mice receiving Doxil® ($p < 0.01$). Total tumor DXR levels for both formulations appeared to reach C_{max} 24 h after injection. Nuclear levels of DXR reached C_{max} 24 h after injection with Doxil® but seem to be sustained over 168 h after injection with F5-Doxil®, although inter-animal variability makes this difficult to estimate. The percent of bioavailable DXR in tumors of mice that received Doxil® was 46%, which is similar to results obtained recently in a murine 4T1 breast cancer model (Chapter 2), although total and nuclear tumor uptake into this model was considerably lower than in the 4T1 model (140).

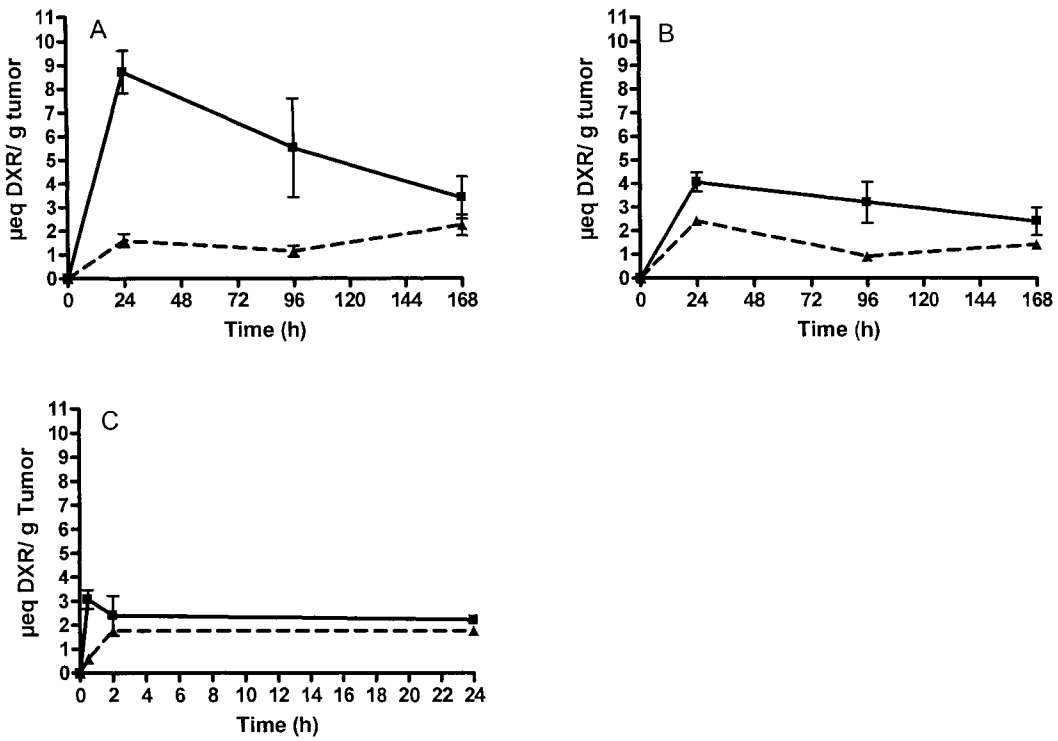

Figure 3.3. DXR concentrations in BT-474 M3C5 tumors in mice receiving F5-Doxil®, Doxil®, or free DXR. Female NCr nude mice were subcutaneoulsy implanted with BT-474 mammary carcinoma and were injected with F5-Doxil®, Doxil®, or free DXR at a DXR dose of 9 mg/kg when tumor volumes reached 200-300 mm^3. Total (solid line) and nuclear (dashed line) DXR levels were determined following acidified isopropanol extraction. Data represent mean ± SD of triplicate aliquots from 3 mice per time point. **(A),** F5-Doxil®; **(B),** Doxil®; **(C),** free DXR.

Nuclear accumulation of DXR in mice administered F5-Doxil®, appeared to be relatively constant over the 7 d that it was followed. Previously, our laboratory has shown that liposomes, when internalized *in vitro* by tumor cells, are delivered to the endocytotic pathway. Intracellular release of DXR and nuclear accumulation is a slow process (71), taking several days. Therefore, it is not surprising that tumor nuclear accumulation occurred up to 7 d after injection. As expected, total tumor DXR levels were higher than nuclear levels of DXR when F5-targeted liposomes were administered to mice ($p < 0.001$). In this experiment, only 26% of the drug delivered to tumors with the F5-Doxil® formulation was bioavailable.

The amount of total tumor and nuclear accumulation of free DXR was measured up to 24 h after injection (Figure 3.3C). Total tumor C_{max} was reached 30 min after injection of 9 mg/kg free DXR. In this animal model of breast cancer the C_{max} levels for free DXR and Doxil® were not significantly different ($p>0.1$). In the 4T1 model (Chapter 2) the C_{max} of total DXR in tumors was 4-fold higher for 9 mg/kg of Doxil® compared to a similar dose of free DXR(140). In addition, there was significantly less total tumor accumulation and nuclear accumulation of DXR over 7 d in the BT-474 tumors compared to the 4T1 tumors. In the 4T1 model, total tumor C_{max} for Doxil® was ~4 times higher than C_{max} for free DXR, and maximum tumor concentrations for Doxil® were 7-fold lower in the BT474 model than in the 4T1 model at the same DXR dose. One important difference between the two models is the extent of vascularization of the tumor. The 4T1

model is a well vascularized, whereas the BT-474 appears to be poorly vascularized – this may account for the poor uptake of DXR into the BT-474 tumor.

In previous experiments in BT-474 tumor bearing mice, by Nielson *et al.*, 3 weekly i.v. injections of 5 mg/kg of F5-Doxil® resulted in significantly improved tumor regression after 3 doses over mice receiving Doxil® (p=0.001) (83). In the current study, there was no statistical difference in tumor volumes (p> 0.1) between Doxil® and F5-Doxil® at 7 d post-injection after a single injection of each, and there was no statistical difference in bioavailable amounts of drug in the tumors (p> 0.1). Hence, the measurement of the amount of bioavailable drug in BT-474 tumors should be extended in this model to include multiple injections. Further experiments should also include combining measurements of bioavailable drug levels in tumors with apoptotic assays. With multiple injections of a targeted liposomal formulation not only may the amount of bioavailable drug in tumors be different than after injections with an non-targeted formulation, but targeting liposomes might alter the intracellular trafficking of the drug. This could result in an increase in cytotoxic effects by mechanisms that take place in sites other than the nucleus (i.e., mitochondria).

The ability to accurately quantitate bioavailable DXR in tumors and its relation to therapeutic activity will be a valuable tool in attempts to optimize liposomal formulations of anticancer drugs. Currently our lab and others are working on targeted triggered release liposomes (102, 156, 157). Triggered

release liposomes are designed to release their contents in response to an external stimulus, such as a temperature or pH change. pH-sensitive liposomes, for example, are formed from the non-bilayer phospholipid dioleoylphosphatidylethanolamine, which is stabilized in the bilayer state with PEG covalently attached to a lipid anchor via a pH-sensitive linker. The pH-sensitive liposomes are targeted to cells via an antibody or ligand against an internalizing receptor and once the liposomes are internalized into the lysosomal apparatus of the target cells, the enzyme rich, acidic environment will cleave the pH-sensitive linker and the liposomes will destabilize, releasing their drug. Triggered release formulations, such as pH-sensitive liposomes, should help to overcome the problem of slow release of entrapped drugs from liposomes after their receptor-mediated internalization and lead to enhanced therapeutic activity.

In summary, methods for quantitating the amount of bioavailable drug delivered to tumor cells or other target cell populations will aid in the development of improved liposomal formulations. It has been over 10 years since the last liposomal formulation was approved for clinical use, and the preclinical development of new improved liposomal formulations has been extensive. The ability to correlate therapeutic efficacy with a concrete measurement of cytotoxic drug in tumors may further help liposomal formulations be candidates for future clinical applications.

Table 3.1. Comparison of tumor pharmacokinetics of liposomal formulations of DXR. Tumor levels of total DXR and nuclear DXR were determined in mice bearing subcutaneously implanted BT-474 M3C5 mammary tumors, following administration of 9 mg/kg DXR as free DXR, Doxil® or F5-Doxil®. Area under the time versus concentration curves are AUC_{0-7d} for liposomal DXR formulations and $AUC_{0-24\,h}$ for free DXR. All parameters were determined using WinNonLin software.

Formulation	Doxil®		F5-Doxil®		Free DXR	
	Total	Nuclear	Total	Nuclear	Total	Nuclear
AUC (μeq h/g tumor)	512	234	938	241	55	41
% Bioavailable	46%		26%		74%	
C_{max} (μeq DXR/g tumor)	4.1	2.4	8.7	2.2	3.1	1.8
T_{max} (hr)	24	24	24	168	0.5	24
$t_{1/2}$ (hr)	189	ND	106	ND	75	ND
MRT (hr)	80	ND	73	ND	12	ND
Clearance (g/hr/kg)	7.7	ND	6.1	ND	30.3	ND

ND = no value determinable by the PK program
AUC = area under the curve, C_{max} = maximum drug concentration, MRT = mean residence time, $t_{1/2}$ = half-life, T_{max} = time to maximum drug concentration, μeq = μequivalents

CHAPTER 4[†]

Liposomes targeted via two different antibodies: Assay, B-cell binding and cytotoxicity

Laginha, K., Mumbengegwi, D., and Allen T. M. Biochim. Biophys. Acta, *1711*: 25-32, 2005

[†] All experimental work completed in this Chapter was performed by K. Laginha, except that D. Mumbengegwi helped with one of the binding studies.

4.1. Abstract

The selective toxicity of anticancer drugs can be improved with the use of antibody-targeted liposomes. We hypothesize that liposomes targeted via antibodies against two or more receptor populations will increase the apparent receptor density on the target cells, resulting in improved therapeutic effects. A fluorescent assay was developed, using the fluorophores Alexa Fluor® 350 and 532 to label monoclonal antibodies (mAb), and used to quantitate two different mAb populations coupled to the same liposome surface to within ± 10% of the values obtained with radiolabeled antibody (^{125}I) tracers. The binding and uptake of targeted liposomes by B lymphoma (Namalwa) cells was examined for either individual populations of anti-CD19-targeted or anti-CD20-targeted liposomes, mixed populations (1:1) of anti-CD19-targeted liposomes plus anti-CD20-targeted liposomes, and dual-targeted liposomes, i.e., equal amount of both anti-CD19 and anti-CD20 on the same liposomes. At similar antibody densities, binding and uptake of the dual-targeted liposomes was greater than that of either individually targeted liposomes alone, and showed additivity. At the same total lipid and antibody densities, 1:1 mixtures of individually targeted liposomes gave similar results to dual-targeted liposomes. Cytotoxicity was also additive, with DXR-loaded dual-targeted liposomes having approximately double the cytotoxicity of 1:1 mixtures of individually targeted liposomes.

4.2. Introduction

The lack of selectivity of anticancer drugs such as doxorubicin (DXR) leads to dose-limiting toxicities in vivo. Liposomal drug delivery systems have improved the selective toxicity of DXR by altering the pharmacokinetics and biodistribution of the drug. Associating drugs with liposomes enhances their localization to solid tumours through a passive targeting mechanism, which takes advantage of the enhanced vascular permeability and impaired lymphatic drainage in growing tumors; this phenomenon has been termed the enhanced permeability and retention (EPR) effect (35, 125). Several liposomal anticancer formulations have received clinical approval and many more are currently in clinical trials (158).

Currently, there is considerable interest in the use of ligand-targeted therapeutics, e.g., immunoliposomes, to increase the selectivity toxicity of anticancer drugs (59, 159). Immunoliposomes have monoclonal antibodies or antibody fragments coupled to their surface, which causes the liposomes to bind selectively to antigens or receptors that are either uniquely expressed or over-expressed on cancer cells, leading to increased drug delivery to the target cells (65, 73, 84, 135, 160-162). Cell surface antigen density has been shown to be an important factor in the efficacy of immunoliposomal therapy (135). The higher the antigen density, the greater the therapeutic effect of anti-HER2-targeted liposomal DXR (135). Since, in a clinical setting, it is not possible to alter antigen densities, we hypothesized that the antigen density can be artificially increased by

targeting to two or more antigen populations on target cells. This increase in the apparent antigen density will, we hypothesize, result in the delivery of more drug to the target cells, resulting in increased therapeutic effects. We further hypothesize that immunoliposomal drugs, targeted with two or more populations of antibodies on the liposomal surface, may be useful in delivering drug to a higher percentage of cells in tumor cell populations that have a heterogeneous expression of cell surface antigens. As well, activation of two or more cell surface antigens may lead to synergistic cytotoxic responses by engaging two or more mechanisms of cell kill. We have begun to test these hypotheses in the human B-cell lymphoma cell line, Namalwa, which expresses numerous cell surface antigens, such as CD19, CD20 and CD22.

In this paper, we have devised a fluorescent assay to quantitate two or more antibodies coupled to liposomal surfaces. This was necessary since it was difficult to find two or more non-overlapping radioactive tracers that could be easily and economically used for quantitation of multiple antibodies. In addition, the use of fluorescent tracers is safer than using radioactivity. Two different fluorophores with non-overlapping spectra, Alexa Fluor® 350 and Alexa Fluor® 532 were coupled to anti-CD19 and anti-CD20, respectively, to be used as tracers to quantitate anti-CD19 and/or anti-CD20 coupled to immunoliposomes. Subsequently, the binding and uptake of the various immunoliposomal populations was studied using the Namalwa cell line, and the cytotoxicity of DXR-loaded immunoliposomes was examined in the same cell line.

4.3. Methods and materials

4.3.1. Materials

Hydrogenated soy phosphatidylcholine (HSPC), and, methoxy poly(ethylene glycol) (M_r 2000) covalently linked to distearoylphosphatidylethanoloamine ($mPEG_{2000}$-DSPE) were generous gifts of ALZA Pharmaceuticals, Inc. (Mountain View, CA). Cholesterol (CHOL) was purchased from Avanti Polar Lipids (Alabaster, AL). Maleimide-derivatized PEG_{2000}-DSPE (Mal-PEG-DSPE) was custom synthesized by Nektar Therapeutics, Inc. (Huntsville, AL). Chol-[1,2-^{3}H-(*N*)]hexadecyl ether ([^{3}H]CHE, 1.48-2.22 TBq/mmol), and ^{125}I-NaI (185 MBq) were purchased from PerkinElmer Life Sciences (Woodbridge, Ontario, Canada). Bio-Rad Protein Assay Reagent was purchased from Bio-Rad Laboratories (Mississauga, Ontario, Canada). Alexa Fluor® 350 carboxylic acid succinimidyl ester and Alexa Fluor® 532 carboxylic acid succinimidyl ester were purchased from Molecular Probes (Eugene, OR). 2-iminothiolane (Traut's Reagent), polyclonal sheep IgG, and 3-(4,5-dimethyltiazol-2-ly)-2,5-diphenyltetrazolium bromide (MTT) were obtained from Sigma Chemical Co. (St. Louis, MO). Anti-CD20 (Rituxan) was purchased from University of Alberta Hospital Pharmacy (Edmonton, Alberta, Canada). Nuclepore polycarbonate membranes (pore sizes, 0.4, 0.2, 0.1, and 0.08 μm) were purchased from Northern Lipids (Vancouver, British Columbia, Canada). Sephadex G-50, Sepharose CL-4B and Aqueous Counting Scintillant (ACS) were purchased from Amersham Biosciences (Baie d'Urfe, Quebec, Canada). RPMI 1640, penicillin-streptomycin, and fetal bovine

serum were obtained from Invitrogen (Burlington, Ontario, Canada). All other chemicals were of the highest grade possible.

4.3.2. Antibodies and cell line

The murine IgG_{2a} monoclonal anti-CD19 antibody (mAb) was produced from the FMC63 murine hybridoma (from Dr. H. Zola, Children's Health Research Institute, Adelaide, Australia) and purified as previously described (94). A chimeric IgG1 monoclonal antibody, Rituxan, was used for anti-CD20. The human Burkitt's lymphoma cell line Namalwa (ATCC CRL 1432) was cultured in suspension in RPMI 1640 supplemented with 10% (v/v) fetal bovine serum, penicillin G (100 units/ml), streptomycin sulphate (100 μg/ml) and L-glutamine (0.292 mg/ml) in a humidified 37 °C incubator with a 5% CO_2 atmosphere. Cell surface expression of CD19 and CD20 by Namalwa cells was determined, as previously described, using single-color flow cytometry (122). Briefly, the Namalwa cells (1×10^6) were stained with primary mAb (anti-CD19 or anti-CD20) followed by a secondary anti-mouse-FITC IgG. Cell-associated fluorescence was analyzed on a Becton Dickinson FACScan using Lysis II software (Becton Dickinson, San Jose, CA) (122)

4.3.3. Preparation of liposomes

Non-targeted PEGylated (Stealth®) liposomes (SL) for binding studies, or to be loaded with DXR for cytotoxicity studies, were composed of HSPC:CHOL:PEG-DSPE at a molar ratio of 2:1:0.10. PEGylated (Stealth)

immunoliposomes (SIL) were composed of HSPC:CHOL:PEG-DSPE:Mal-PEG-DSPE at a molar ratio of 2:1:0.08:0.02. The non-exchangeable, non-metabolized lipid tracer [^{3}H]CHE was added as a tracer to quantitate phospholipids. A lipid mixture of chloroform stocks was prepared and dried to form a thin film using a rotovaporator; then placed in a vacuum overnight. The lipid films were hydrated at a concentration of 10-30 mM phospholipid (PL) in HEPES-buffered saline (HBS, 25mM HEPES, 140 mM NaCl, pH 7.4). Hydrated liposomes were extruded sequentially at 65 °C through a series of polycarbonate filters with pore sizes ranging from 0.4 μm down to 0.08 μm. Liposome diameters were determined to be 100± 20 nm using a Brookhaven BI-90 particle sizer (Brookhaven Instruments, Holtsville, NY). Alternatively DXR was loaded into liposomes using an ammonium sulphate gradient (51).

4.3.4. Preparation and assay of immunoliposomes

Aliquots of antibodies were labeled with either Alexa Fluor® 350 carboxylic acid succinimidyl ester or Alexa Fluor® 532 carboxylic acid succinimidyl ester according to the manufacturers' instructions. Other aliquots were labeled with ^{125}I using Iodobeads purchased from Pierce Biotechnology Inc (Rockford, Illinois). Sheep IgG (used as an inexpensive antibody for developing methods), anti-CD19 (internalizing mAb) or anti-CD20 (non-internalizing mAb) were coupled to the terminus of Mal-PEG-DSPE using the coupling method previously described (80). Trace amounts of antibodies, labeled with either of the Alexa Fluor® dyes or with ^{125}I, were added to the unlabeled antibodies prior to thiolation. Antibodies (10

mg/ml) were thiolated with Traut's reagent at a ratio of Traut's:IgG of 20:1 (mol/mol) in degassed HBS (pH 8.0) for 1 h; unreacted Traut's reagent was removed by chromatography on a Sephadex G-50 column with degassed HBS (pH 7.4). Individual thiolated antibodies or a 1:1 mixture of thiolated antibodies were immediately added to liposomes at an antibody:phospholipid molar ratio of 1000:1 and incubated overnight at room temperature with continuous stirring. Unconjugated antibody was removed by chromatography on a Sepharose CL-4B column in HBS (pH 7.4).

The concentrations of individual antibodies, labeled with ^{125}I, were determined from the specific activity of the radioactive tracer, following coupling to liposomes. Concentrations of individual antibodies, or mixtures of antibodies, labeled with either of the Alexa Fluor® tracers, were determined from their fluorescence yields compared to a standard curve. Non-labeled liposomes, at a comparable lipid concentration, were added to the standards to control for liposome light scattering in samples.

In order to determine if measurement artifacts might occur due to overlaps in their fluorescent spectra, fluorescence resonance energy transfer between antibodies labeled with Alexa Fluor® 350 (λ_{ex}: 346 nm, λ_{em}: 442 nm) and Alexa Fluor® 532 (λ_{ex}: 530 nm, λ_{em}: 554 nm) was determined. Standard curves were prepared with sheep IgG (10 mg/ml) labeled with either Alexa Fluor® 350 or Alexa Fluor® 532 or combinations of the two fluors. There were no statistical differences between the standard curves, indicating a lack of interference between

the two fluors. Because fluorescence quenching depends on of the distance (R^6) between the two fluors, the possibility of fluorescence self-quenching between fluor-labeled sheep IgG was examined as a function of antibody density. Fluorescence emissions were measured on a SLM-AMINCO 8100 Series 2 Spectrometer (Spectronic Instruments Inc., Rochester NY) at densities of 50, 100, and 150 μg sheep IgG/μmol PL before and after the addition of 10 % (v/v) Triton X-100 to solublize the liposomes. The results indicated no self-quenching of either fluor in this density range.

4.3.5. In vitro immunoliposomes binding and uptake

Binding experiments were performed at both 37°C and 4°C (permissive and non-permissive for internalization, respectively) as previously described (84). Briefly, non-targeted liposomes (SL) or targeted liposomes (SIL[anti-CD19], SIL[anti-CD20], SIL[anti-CD19] + SIL[anti-CD20], or SIL[anti-CD19 + anti-CD20]) were prepared with 74 kBq of [^{3}H]CHE label per μmol of PL. Liposomes were incubated with 1 x 10^6 Namalwa cells in the exponential growth phase at different phospholipid concentrations for 1 h at either 37°C or 4°C. Cells were then washed to remove unbound liposomes, and the amount of [^{3}H]CHE was determined by scintillation counting in a Beckman LS-6800 scintillation counter. Cell association (pmol PL/10^6 cells) was calculated from the specific activity of the liposomes. Specific binding was determined by subtracting non-specific binding of SL from the total binding of SIL.

4.3.6. In vitro cytotoxicity studies

Cytotoxicity of DXR-loaded liposomes, either non-targeted (DXR-SL) or targeted (DXR-SIL[anti-CD19], DXR-SIL[anti-CD20], DXR-SIL[anti-CD19] + DXR-SIL[anti-CD20] or DXR-SIL[anti-CD19 + anti-CD20]), was determined for Namalwa cells using the MTT dye reduction assay (153). Briefly, 5.0 x 10^5 cells/well were plated in 96-well plates and incubated at 37°C for 1 h with DXR-loaded liposome formulations. The cells were then washed and incubated for an additional 48 h before cell viability was assessed. Results are expressed as IC_{50}, which was obtained graphically using Graphpad Prism version 3.0 (GraphPad Software, Inc., San Diego CA).

4.3.7. Statistical analysis

Statistical comparisons were performed using analysis of the variance (ANOVA) with a Tukey-Kramer post-test with Graph Pad Instat Version 3.01 for Windows 95/NT (GraphPad Software, Inc., San Diego CA).

4.4. Results

Alexa Fluor® 350 and Alexa Fluor® 532 have non-overlapping excitation and emission spectra and do not undergo fluorescence resonance energy transfer (i.e., distance-dependent interaction between the electronic excited states of two dye molecules, in which excitation is transferred from a donor molecule to an acceptor molecule without the emission of a photon) (163). Standard curves, prepared with sheep IgG labeled with either fluor alone, or with 1:1 mixtures of sheep IgG labeled with either fluor, gave curves that were not statistically different

($p > 0.1$), confirming that no fluorescence interference occurred between these dye pairs. Nor did either of the Alexa Fluor® dyes self-quench (i.e., fluorescence emission from one molecule absorbed by an adjacent molecule of the same fluor) when labeled antibodies were coupled to liposomes within the range of antibody densities normally employed. Fluorescence emission signals of coupled antibodies were measured before and after the addition of the detergent Triton X-100, which solubilized the liposomes and dispersed the label. Antibody densities from 50-150 μg Ab / μmol PL resulted in fluorescence signals that were the same before and after the addition of Triton X-100 ($p > 0.1$), confirming that self-quenching was not a problem in this density range.

4.4.1. Fluorescence assay for quantifying coupled antibodies

Levels of sheep IgG coupled to liposomes were determined with sheep IgG that was labeled with Alexa Fluor® 350, Alexa Fluor® 532, or ^{125}I. The results were very similar (73.3 ± 1.2, 73.0 ± 2.6 or 66.3 ± 1.2 μg Ab/μmol PL, respectively). As well, anti-CD20 and anti-CD19 were labelled with Alexa Fluor 350 and Alexa Fluor 532, respectively, and both populations of antibodies were coupled to liposomes at a 1:1 ratio in the presence of a trace amount of ^{125}I-labeled anti-CD20. The results showed that equal amounts of each antibody bound to the liposomes; the values for anti-CD20 and anti-CD19 from fluorescent analysis were 48.5 ± 6.5 and 51.5 ± 6.6 μg Ab/μmol PL, respectively. This is comparable to the value for anti-CD20 of 45.9 ± 2.2 μg Ab / μmol PL obtained in the same liposomes using a radiolabeled marker.

4.4.2. Binding and uptake of immunoliposomes

The [^{3}H]-CHE counts associated with Namalwa cells at 4°C measure binding of antibody-targeted liposomes to cell surface antigens, and at 37°C the counts measure a combination of binding and receptor-mediated internalization of SIL[anti-CD19]. SIL[anti-CD20] are not internalized (122), so the counts for this antibody, measure surface binding at both temperatures. Binding and uptake of SIL[anti-CD19], SIL[anti-CD20], SIL[anti-CD19] + SIL[anti-CD20], or SIL[anti-CD19 + anti-CD20] were compared. Several factors need to be considered in designing these experiments; these include the concentration of lipid in each liposome population, the antibody density for each liposome population, the total liposome concentration and the total antibody concentration (Fig. 4.1).

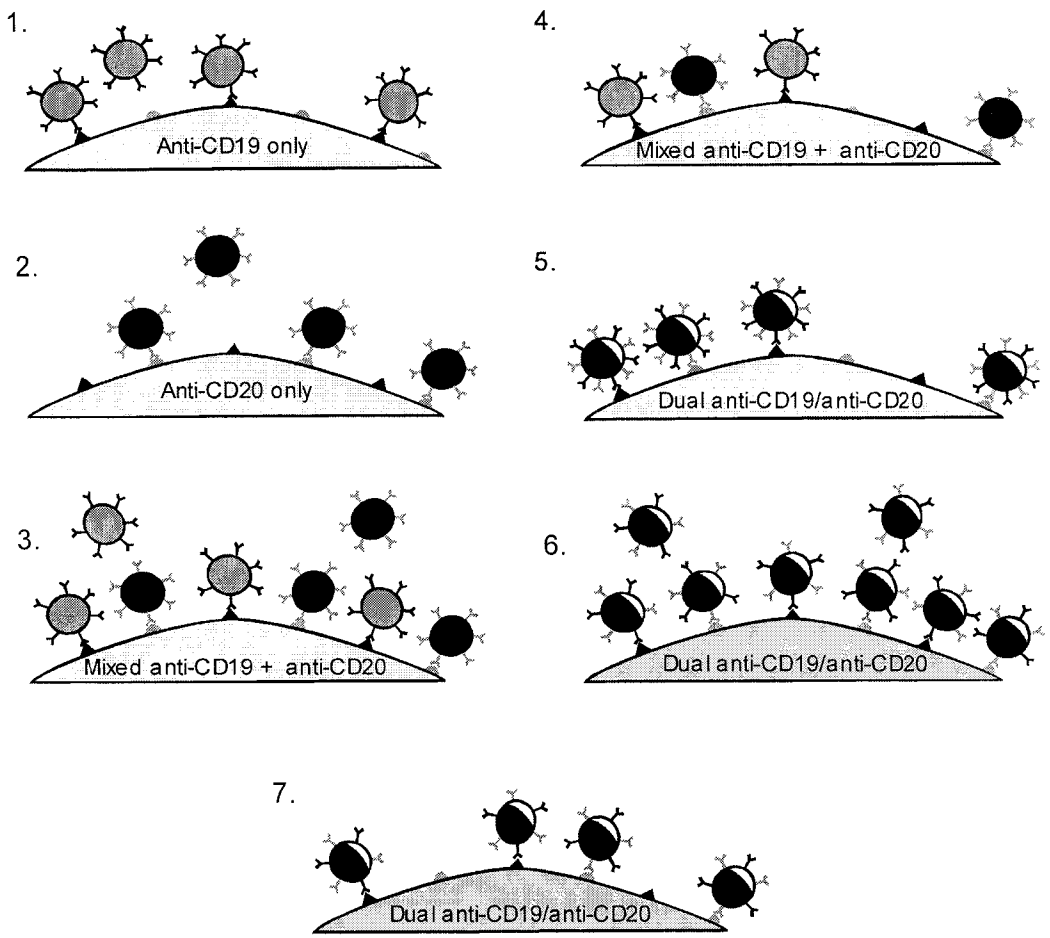

Figure 4.1. Single-targeted immunoliposomes, dual-targeted immunoliposomes and combination of single-targeted immunoliposomes binding to Namalwa cells. 1. SIL[anti-CD19]. **2.** SIL[anti-CD20] **3.** 50:50 mixtures of SIL[anti-CD19] and SIL[anti-CD20]. In the example, the individual antibody concentrations are the same as in 1 and 2, but the liposome concentration is double that in either 1 or 2. **4.** 50:50 mixtures of SIL[anti-CD19] and SIL[anti-CD20], with the same antibody concentration, antibody density and liposome concentration as in 1 and 2. **5.** SIL[anti-CD19 + anti-CD20], in which the individual antibody concentrations and the total liposome concentration are the same as in 1 and 2, but the antibody density is double that in either 1 or 2. **6.** SIL[anti-CD19 + anti-CD20] at the same total antibody concentration and antibody density for the individual antibodies as in 1 and 2, but the total lipid concentration is double that of either 1 or 2. 7. Dual-targeted liposomes, with the same antibody concentration, antibody density and liposome concentration as in 1 and 2.

Specific cellular association was determined by subtracting the non-specific absorption of SL from the binding/uptake of SIL. Binding experiments at 4°C showed no significant difference between SIL[anti-CD19] and SIL[anti-CD20] (Fig. 4.2A). At 37°C, SIL[anti-CD19] showed higher binding and uptake than SIL[anti-CD20] (Fig 4.2B); this is most likely due to receptor-mediated endocytosis and recycling of theCD19 antigen back to the cell surface where it can participate in further binding and internalization (84). At both 4°C and 37°C, mixtures of two separate populations of liposomes showed an additive effect (Fig. 4.1-4). Dual-targeted immunoliposomes with anti-CD19 and anti-CD20 densities between 32-44 μg Ab/μmol PL each (total antibody density of approximately double the individual populations, as in Fig. 4.1-5), were subadditive (Fig. 4.2A,B). Another set of binding and uptake experiments was performed using SIL[anti-CD19 + anti-CD20] having total antibody and liposome concentrations that were equivalent to those that would occur when individuals populations of SIL[anti-CD19] and SIL[anti-CD20] were combined (Fig. 4.1-7). In these experiments there was no statistical differences between binding and uptake of SIL[anti-CD19] + SIL[anti-CD20] *versus* that of SIL[anti-CD19 + anti-CD20] (Fig. 4.3).

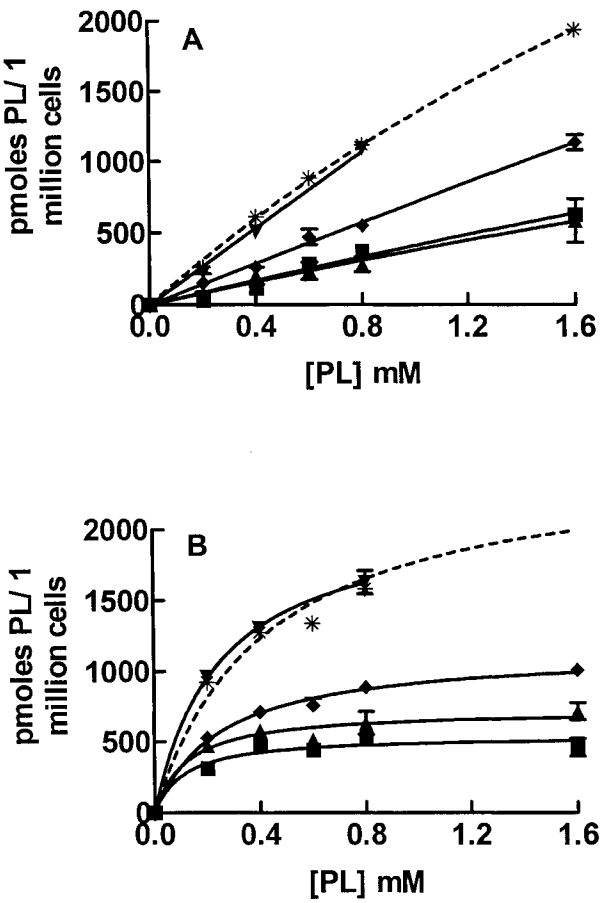

Figure 4.2. Specific cell association of immunoliposomes with Namalwa cells as a function of lipid concentration and temperature. (A) 4°C; (B) 37°C. (▲) SIL[anti-CD19], 41 μg/μmol PL; (■) SIL[anti-CD20], 45 μg/μmol PL; (▼) 50:50 mixtures of SIL[anti-CD19] + SIL[anti-CD20]; (♦) SIL[anti-CD19 + anti-CD20], 44 μg anti-CD19/μmol PL and 32 μg anti-CD20/μmol PL (total antibody density of approximately double that of the individual immunoliposome populations as in Fig. 4.1-5), compared at the same total liposome concentrations; (*) represents the theoretical line for additive effects at the same total liposome concentration (Fig. 4.1-4). Liposomes were labeled with [3H]CHE and were composed of HSPC:CHOL:mPEG-DSPE:Mal-PEG-DSPE (2:1:0.06:0.02). They were incubated with 1 x 106 Namalwa cells for 1 h, after which the cells were washed with cold PBS to remove the unbound liposomes. Data are expressed as pmoles PL/106 cells. Each point is an average of 3 replicates ± S.D from one representative experiment.

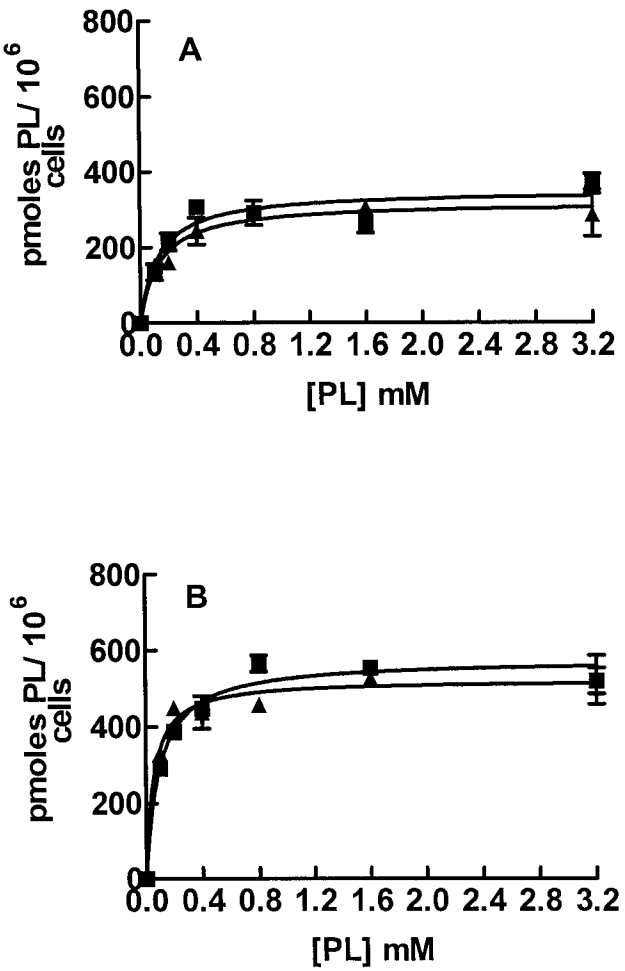

Figure 4.3. Specific cell association of immunoliposomes with Namalwa cells as a function of lipid concentration and temperature. (A) 4°C; (B) 37°C. (■) SIL[anti-CD19] + SIL[anti-CD20], 61 μg anti-CD19/μmol PL and 48 μg anti-CD20/μmol PL; (▲) SIL[anti-CD19+ anti-CD20], 38 μg anti-CD19/μmol PL and 30 μg anti-CD20/μmol PL (Fig. 4.1-7). The experimental protocol was as in Fig. 4.2 caption.

4.4.3. In vitro cytotoxicity

The *in vitro* IC_{50} values for DXR-SL, DXR-SIL[anti-CD19], DXR-SIL[anti-CD20], DXR-SIL[anti-CD19] + DXR-SIL[anti-CD20], and DXR-SIL[anti-CD19 + anti-CD20] are presented in Table 4.1. All DXR-loaded targeted immunoliposomes were significantly more cytotoxic to Namalwa cells than DXR-SL, for a 1 h incubation time. DXR-SIL[anti-CD19 + anti-CD20] had IC_{50}s that were approximately half those of the individual liposome populations.

Table 4.1. Cytotoxicity of liposomal doxorubicin formulations against Namalwa cells. Namalwa cells (5 x 10^4 cells/well) were plated in 96-well plates and incubated with increasing concentrations of liposomal DXR, and various targeted-liposomal formulations for 1 h. Cells were then washed 3 times with PBS and incubated with fresh medium for a further 47 h, and a MTT assay was performed. Antibody concentrations of anti-CD19 and anti-CD20 on liposomes were as follows: DXR-SIL[anti-CD19], 60-65 mg mAb/mmol PL; DXR-SIL[anti-CD20], 39-51 mg mAb/mmol PL; DXR-SIL[anti-CD19], 56 mg mAb/mmol PL + DXR-SIL[anti-CD20], 55 mg mAb/mmol PL; DXR-SIL[anti-CD19 + anti-CD20], 25-30 mg anti-CD19/mmol PL and 24-26 mg anti-CD20 /mmol PL (Fig. 4.1-7).

Formulation	**IC_{50}, 1hr** (μM DXR)
DXR-SL	30.5
DXR-SIL[anti-CD19]	5.2, 3.0
DXR-SIL[anti-CD20]	1.9, 5.5
DXR-SIL[[anti-CD19] + [anti-CD20]	2.3
DXR-SIL[anti-CD19 + anti-CD20]	2.0, 2.0

4.5. Discussion

In this paper, we developed a fluorescence assay to quantify different populations of antibodies coupled to the same population of liposomes. The ability to assess antibody densities on liposomes by fluorescence has advantages over radioactive labels and it also allows one to distinguish and quantify two or more antibodies on the liposomal surface. The fluorescence labels, Alexa Fluor® 350 (λ_{ex}: 346 nm, λ_{em}: 442 nm) and Alexa Fluor® 532 (λ_{ex}: 530 nm, λ_{em}: 554 nm), were carefully chosen to have non-overlapping fluorescence spectra. As well, their spectra do not overlap with the excitation and emission wavelengths of the drug DXR (λ_{ex}: 470 nm, λ_{em}: 590 nm), which was used in cytotoxicity studies

The ability to quantitate two different antibodies coupled to the same liposomes enabled us to test the hypothesis that dual-targeting of liposomes would increase the binding, uptake and cytotoxicity of immunoliposomes compared to single-targeted immunoliposomes due to an increased apparent receptor density. Binding and uptake experiments showed that when dual-coupled liposomes (SIL[anti-CD19 + anti-CD20]) were targeted at the same total antibody and lipid concentrations as two individual sets of single-targeted immunoliposomes, either (SIL[anti-CD19] or SIL[anti-CD20]), an additive response was obtained, which was similar in magnitude to that obtained with a 1:1 mixture of SIL[anti-CD19] + SIL[anti-CD20]. The total antibody concentration of anti-CD19 and anti-CD20 on dual-targeted liposomes was, in this instance, designed to be equivalent to that on a single antibody-targeted immunoliposome. In other words, the density of each

antibody was half that of the antibody density on individual sets of single antibody-targeted immunoliposomes (Fig. 4.1-7 vs. 4.1-1 or 4.1-2).

When we investigated dual-targeted immunoliposomes with antibody densities for anti-CD19 and anti-CD20 that were the same as that on single antibody-targeted immunoliposomes (i.e., double the antibody density on individual populations of single-targeted liposomes, as in Fig. 4.1-5), an additive response was expected. However, we obtained sub-additive binding and uptake. At high antibody densities, there may be steric hindrance of binding. These experiments show the importance of considering the antibody and liposome concentrations when interpreting the experimental results.

In vitro cytotoxicity studies revealed that DXR-SIL[anti-CD19] or DXR-SIL[anti-CD20] have similar cytotoxic profiles after a 1 h incubation. However, the cytotoxicities for each are likely due to different mechanisms of action. The cytotoxicity of DXR-SIL[anti-CD20], directed against a non-internalizing antigen, is most likely due to DXR being released from liposomes bound to the cell surface and uptake of the free drug into the target cell. In vivo, drug released from these liposomes would be redistributed away from the target cells, but in cell culture, the drug will be rapidly taken up into the cells. CD19 is an internalizing receptor, by contrast, and the cytotoxicity of DXR-SIL[anti-CD19] is most likely attributable to receptor-mediated endocytosis of the liposomes followed by slow breakdown of the liposomes in the lysosomal apparatus and subsequent intracellular trafficking of the released drug. In vivo, we have demonstrated this mechanism leads to

improved therapeutic effects over those seen for a non-internalizing antibody, but in vitro the cytotoxicity is equivalent (122). Dual-targeted liposomes were slightly more cytotoxic in vitro than single-targeted liposomes.

Recently, the therapeutic effects of liposomal vincristine (VCR) or DXR, targeted with either anti-CD19 or anti-CD20 or 1:1 mixtures of each, were investigated in severe combined immunodefficient (SCID) mice injected with Namalwa cells (73). Results showed that 1:1 mixtures of two separate populations of liposomes loaded with DXR, i.e., DXR-SIL[anti-CD19] and DXR-SIL[anti-CD20], had no enhanced therapeutic effect over DXR-SIL[anti-CD19] on its own. However, 1:1 mixtures of VCR-SIL[anti-CD19] and VCR-SIL[αCD20] had a higher cure rate in mice then either set of targeted immunoliposomes alone. In these experiments, the therapeutic effect of neither DXR-SIL[anti-CD19 + anti-CD20] or VCR-SIL[anti-CD19 + anti-CD20] was examined, due to difficulties in measuring the concentrations of each antibody population in dual-targeted liposomes.

With the development of a fluorescent assay to quantitate two or more populations of antibodies on liposomes, further experiments can now be carried out. It is now possible to determine whether having two separate populations of antibodies coupled to a single population of liposomes is more advantageous than (or equivalent to) mixtures of two separate populations of liposomes, each coupled to a different antibody. This will enable us to test the hypothesis that the interaction of two different antibodies on the same liposome with two different

antigen sites in close proximity on the same cell may lead to synergistic cytotoxicity, by simultaneously engaging two or more additive or synergistic mechanisms of cell kill. In an in vivo setting, dual-targeted liposomes may also behave in a manner similar to bispecific antibodies with one antibody binding to target cells while unattached antibodies recruit effector cells or molecules that can effectively kill the tumor cells. Steric hindrance is also likely to be less of a factor for dual-targeted liposomes in vivo as the greater apparent receptor density may increase association of liposomes with cells through increased avidity in a non-static environment. In an in vivo setting, there may be added benefits of targeting two antigens by the same liposome that are impossible to predict with in vitro studies.

Survival studies comparing the therapeutic efficacy of dual-targeted immunoliposomes to single-targeted liposomes or mixtures of single-targeted liposomes are warranted. As well, survival studies, similar to those performed previously (73), could be performed with dual-targeted immunoliposomes loaded with different cytotoxic drugs. If the advantages of dual-targeted liposomes over single-targeted liposomes are slight, then consideration also has to be given to issues surrounding the manufacturing and regulatory approval of one versus the other. From the manufacturing point of view, the preparation of dual-targeted liposomes is no more complex than manufacturing single-targeted liposomes. From the therapeutic perspective, one gains the possibility of synergistic interactions with the appropriate choice of dual-targeted liposomes, but one loses

the simplicity of being able to mix and match a combination of various (approved) populations of single-targeted liposomes to suit individual patient disease profiles (93). Further experiments will be necessary to determine if there are substantial advantages of one approach over the other.

CHAPTER 5

Summarizing discussion

The aim of the research described in this thesis was to develop and evaluate methodologies that may lead to improvements in the design and formulation of liposomal drugs. Three areas were explored: 1) Development of a method to quantitate the amount of total and bioavailable DXR from liposomal DXR in murine breast cancer tumors and correlation of the results with therapeutic activity of liposomal DXR against murine breast cancer. 2) Use of the methodology developed in 1) to compare the amount of total and bioavailable DXR from non-targeted and anti-HER2/*neu*-targeted liposomal DXR in xenograft models of HER2/*neu* overexpressing breast cancer. 3) Development and evaluation of methodologies to increase the apparent antigen density of target cells by attaching different antibodies to individual liposomes. As part of this latter project, methods for measuring the levels of more than one type of antibody attached to the same liposome were also developed.

In the liposome field, it is widely appreciated that direct measurement of the amount of biologically active drug at the site of drug action would be an asset in assisting with the design of improved liposomal drug therapies. For conventional chemotherapy, the issue of bioavailability is less problematic since the drug does not have to escape from a carrier to be bioavailable. Since drug carriers alter the pharmacokinetics and biodistribution of their entrapped drugs, they are considered by the FDA to be new drugs. During the clinical development process for new drugs, the FDA requires that pharmacokinetics and bioavailability be evaluated,

and an assay that can directly measure drug bioavailability would be advantageous.

In Chapter 2 and 2A we examined the difference in levels of bioavailable DXR in tumors when tumor-bearing mice were treated with either the clinically approved liposomal DXR formulation, Doxil®, a leaky liposomal formulation of DXR composed of DOPC:CHOL:mPEG-DSPE, or free DXR. It is intuitive that altering the rate of drug release from liposomes might have an effect on therapeutic activity, depending on the properties of the encapsulated drug. Doxil® has a very slow rate of drug leakage *in vivo* with a $t_{1/2}$ of 315 h. When DXR-loaded liposomes extravasate into the tumor interstitial space, cytotoxic effects of DXR are determined by the amount of drug that is released from the carrier. We found that with a leakier liposomal formulation, less total drug and less bioavailable drug was in the tumors compared to Doxil®. This resulted in only a slight delay in tumor growth compared to free DXR, whereas Doxil® substantially delayed tumor growth compared to free DXR in the 4T1 murine mammary carcinoma model. The amount of biologically active DXR delivered by the leaky liposomal formulation was sub-optimal.

When Doxil® was administered to mice at a dose of 9 mg /kg there was 45-fold higher nuclear levels of drug in tumors compared to tumors from mice that received the same dose of free DXR. With such a large increase in DXR in the nucleus of tumor cells, you would expect to achieve close to curative therapy in animals that received Doxil®. In the tumor growth delay experiments from

Chapter 2A, mice that received 9 mg/kg of Doxil® did exhibit the greatest degree of tumor growth delay, but the degree of increase in therapeutic effect was less than might be expected from the 45-fold increase in nuclear DXR. Therefore, other factors in addition to levels of nuclear DXR must play a role in the therapeutic results.

In our experiments, perhaps not surprisingly, the therapeutic effect was also correlated with *total* drug delivered to tumors. From the data it is possible to calculate the amount of liposomal (non-released) drug plus released (non-nuclear) drug from the data for total drug and nuclear drug. For example, if you take the $AUC_{0\text{-}7d}$ results obtained for nuclear levels of DXR in tumors after liposomal drug delivery in Table 2.1 and subtract that amount from total drug delivered to tumors, you get an amount of drug that is representative of drug remaining in the liposomes plus drug that is released from the liposomes but not in the nucleus of tumor cells. These values are presented in Table 5.1. Since DXR has cytotoxic actions in subcellular organelles other than the nucleus, it is important to consider these values in evaluating therapeutic activity. In Table 5.1, values obtained for total tumor drug minus nuclear drug would also give us the same rank order of tumor growth delay that we get when comparing the different nuclear levels of drug for the 9 mg/kg dosages of Doxil®, DOPC-PLD and free DXR. It would be interesting to see if this insight could extend to the model presented in Chapter 3.

Table 5.1. Comparison between liposomal formulations of total liposomal DXR and released, non-nuclear DXR. Nuclear levels of DXR calculated from the area under the time concentration versus concentration curves ($AUC_{0\text{-}7\ d}$) in 4T1 tumors from Table 2.1 were subtracted from total tumor DXR $AUC_{0\text{-}7\ d}$ levels. This is representative of liposomal drug in tumors and bioavailable drug that is not in the nucleus of tumor cells over the 7 d or 24 h time course of the experiment.

Formulation	AUC (μeq·h/g·tumor)		
	Total DXR	Nuclear DXR	Total – nuclear DXR
Free DXR, 9 mg/kg	45.8	43.3	2.5
Doxil®, 9 mg/kg	3988	1970	2018
Doxil®, 16 mg/kg	5918	2444	3474
DOPC-PLD, 9 mg/kg	641	172	469

In future studies, it may also be beneficial to combine measurements of bioavailable drug in tumors with apoptotic assays. One of the main mechanisms of action of chemotherapeutic drugs is by inducing apoptosis. Quantitating levels bioavailable drug in tumors and correlating this with measurements of apoptosis, e.g. caspase levels, may provide additional insights into designing drug delivery formulations with appropriate release rates and drug dosing regimens. For example, in the studies presented in Table 2.1 and Table 5.1, when 16 mg/kg of Doxil® was administered to mice, total tumor DXR and nuclear DXR where higher than in mice that were administered 9 mg/kg of Doxil®. According to the therapeutic study done in Chapter 2A, administering 16 mg/kg of Doxil® to 4T1 tumor-bearing mice did not result in the greatest tumor growth delay. Indeed, the mice in this group had to be euthanized due to severe toxic side-effects. If the extent of apoptosis was quantified in these experiments, we may have seen no increase in cytotoxic effects in tumors between the two different DXR dosages, even though substantially more drug was in the tumors when a higher dose of Doxil® was administered to mice.

Clearly overdosing with chemotherapy agents and drug delivery systems for these agents must be avoided, in order to avoid dose-limiting toxicities. In contrast, if the dose of drug is too low, there may be no therapeutic effects. The combination of apoptosis and bioavailability assays may give more insight into optimal dosing regimens.

In Chapter 3, when F5-Doxil® was administered to mice bearing the BT-474 xenograft breast cancer model, there was a 2.5-fold increase in total tumor DXR, but similar nuclear levels of DXR in tumors (Table 5.2) compared to mice that received 9 mg/kg of Doxil®. This model is less sensitive to DXR than the 4T1 murine breast cancer model and administration of a single dose of DXR did not lead to statistical difference in tumor volumes over the the 7 d time course of the experiment. The F5 scFv targeting moiety was selected for its ability to trigger a high rate of receptor-mediated endocytosis. Hence the intracellular distribution of DXR will be different for the targeted and non-targeted liposomal formulations. For non-targeted formulations, release of drug in the vicinity of tumor cells or tumor-associated cells, such as endothelial cells or macrophages will lead to rapid, non-selective, DXR uptake and rapid trafficking to cellular nuclei. For targeted formulations, the drug package is internalized into the lysosomal pathway and release of the drug from liposomes sequestered in endosomes or lysosomes must occur before the drug can traffic to other intracellular organelles that are the site of drug action. There is evidence that the process of release of DXR from endosomes or lysosomes is a slow process (71), taking several days. Hence, it is not surprising that nuclear uptake of DXR from targeted liposomes is not higher than for non-targeted liposomes over the 7d time course of this experiment. A therapeutic study in the BT-474 model using a single dose of either the targeted or the non-targeted formulation would tells us if the 2.5-fold increase in total drug in the tumor would result in increased anti-tumor activity.

Therefore, the value presented in Table 5.2 for F5-Doxil®, which includes liposomal drug plus free drug that is not in the nucleus of tumor cells may have a greater impact on therapeutic activity if it represents actual drug within tumor cells, opposed to drug from Doxil® that is most likely in the interstitial space of tumors. In addition, further studies involving measuring the amount of total drug and bioavailable drug in tumors after treatment with the two different liposomal DXR formulations are warranted because another group has shown that F5-Doxil® in multiple dosages is more therapeutically effective than Doxil® in this breast cancer model (83). Quantifying total drug delivered to tumors, drug that is in the nucleus of tumor cells, therapeutic activity and tumor distribution of the liposomes may give additional insight into the therapeutic activity of F5-Doxil® in HER2/*neu* overexpressing breast cancer models.

Table 5.2. Comparison between liposomal formulations of total liposomal DXR and released, non-nuclear, DXR. Nuclear levels of DXR, calculated from the area under the time concentration versus concentration curves ($AUC_{0\text{-}7\ d}$) in BT-474 M3C5 tumors from Table 3.1 were subtracted from total tumor DXR $AUC_{0\text{-}7\ d}$ levels. This is representative of liposomal drug in tumors and bioavailable drug that is not in the nucleus of tumor cells over the 7 d or 24 h time course of the experiment.

Formulation	AUC (μeq·h/g·tumor)		
	Total DXR	Nuclear DXR	Total - nuclear DXR
Free DXR, 9 mg/kg	55	41	14
Doxil®, 9 mg/kg	512	234	278
F5-Doxil®, 9 mg/kg	938	241	697

Doxorubicin had ideal properties for the development of an assay for bioavailable drug in tumors. Its innate fluorescent properties made measurement of drug levels simple (164). Further its strong binding to DNA resulted in our being able to use tumor cell nuclei as a sink for determining bioavailable drug. Hence, the bioavailability assay can easily be used by other researchers. Although this assay was a good indicator for the therapeutic activity in the studies we presented, further refinement is needed for a more accurate assessment of bioavailable drug that includes both drug in the nucleus, and drug in other intracellular organelles. Even through isolated nuclei result in a purer preparation than other intracellular organelles, never-the-less, contamination of the nuclear preparation with other organelles such as mitochondria, lysosomes, and plasma membrane still occurred. We made the reasonable assumption that most or all of the DXR would eventually end up in the nuclei, where strong DNA binding would create a sink for the drug, but we recognized that DXR has cytotoxic actions in other organelles. Other researchers have shown that only about 65-74% of free DXR exposed to cells will traffic to the nucleus (152). Our measurements of total minus nuclear drug may provide a measurement for drug that has affects in other intracellular organelles.

In addition, DXR may accumulate in some of the cancer cells beyond levels that are necessary for triggering apoptosis or for other types of cytotoxicity, or the drug may accumulate in other types of cells such as tumor macrophages. This may also account for therapeutic effects being not as great as the increase in

nuclear levels of drug would suggest. This is also related to the focal accumulation of liposomal drugs in tumors, compared to the more uniform exposure of tumor cells to free drug. The distribution of liposomal drugs is non-uniform, with cells in some parts of the tumor appearing to be exposed to high levels of drug, but other cells appearing to receiving little or no drug (37, 165, 166). Even though the total nuclear levels of drug are 45-fold, this is averaged over tumor cells that receive little or no drug and cells that receive excess drug. Tumor cells that are not exposed to apoptotic levels of drug will continue to contribute to the increase in tumor volume.

In discussing our results it is also helpful to consider concepts of exponential growth and log-kill kinetics (167). It has been shown, in Chinese hamster ovary cells, that greater than 60% of free DXR is intercalated into DNA within 20 min of drug exposure in an *in vitro* setting, but cytotoxicity levels continued in an exponential fashion well after maximum intracellular levels were reached (168). Malignant cells undergo exponential growth, where the number of cells double over a fixed unit of time. Chemotherapeutic drugs kill malignant cells in a log fashion, in that treatment will reduce the number of exponentially growing malignant cells by a log amount. This concept of log-kill kinetics is why most chemotherapy treatments are given in repeated cycles. The more times malignant cells are exposed to cytotoxic drugs, the greater the decrease in cell number, hopefully leading to total cancer remission. This concept can be extended to the studies presented in Chapter 2 of this thesis. We had substantially more total and

bioavailable drug in 4T1 tumors when 9 mg/kg of Doxil® was administered to tumor-bearing mice compared to 9 mg/kg of free DXR, which led to a substantial delay in tumor growth for the liposomal drug. We may not have seen cures in these mice because, with a single dose, the degree of log cell kill was low, resulting in only a delay of exponential cell growth. This combined with focal distribution of the drugs may explain why the tumor growth delay was not related to the fold-increased in nuclear levels of DXR. Measurements of total tumor and bioavailable drug in this study and the study presented in Chapter 3 with the BT-474 xenograft breast cancer model would be interesting to compare with those for mice received multiple doses of the different treatments.

Recently, a method has been devised using micellar electrokinetic capillary chromatography with laser-induced fluorescence detection to measure the amount of DXR in single nuclei without contamination of the sample with other organelles (152). Although our method can be used to obtain a first approximation of the relationship between therapeutic activity and total tumor and bioavailable drug in tumors, a more accurate measurement may be useful when trying to develop a liposomal formulation for clinical trials. This assay could also be extended to examine the amount of DXR in other intracellular organelles in tumor cells since DXR has cytotoxic effects in organelles other than the nucleus. Measurements of nucleic drug and drug in different intracellular organelles would give a more accurate assessment of bioavailable drug in tumors.

In Chapter 4, we reported a method for increasing the apparent antigen density on target cells and developed an assay that could accurately quantitate the amount of two different antibodies coupled to the surface of liposomes. *In vitro* results showed that liposomes targeted with both anti-CD19 and anti-CD20 had additive cell binding to the Namalwa cell line. Although this work was never continued *in vivo*, it would be interesting to see the results from such an experiment. In an *in vivo* environment, not only could more bioavailable drug be delivered to cancerous B-cells, but cell binding of the two different antibodies coupled to the same liposome may result in synergistic cell signaling effects, leading to greater cell kill.

From a clinical perspective, coupling antibodies to drug-loaded liposomes is a promising strategy to increase the therapeutic activity of mAb therapy alone. Doxil® has been shown to have increased anti-tumor effects and/or decreased side-effects compared to free DXR in several solid tumors due to its ability to passively target these tumors via the EPR effect. Coupling antibodies to the surface of liposomal anticancer drugs may selectively target the liposomes to cancer cells and promote their internalization, resulting in an even larger drug payload being delivered to the cells. The therapeutic benefit has been clearly demonstrated in mice using a combination treatment with separate populations of anti-CD19 liposomal VCR and anti-CD20 targeted liposomal VCR in an animal model of B-cell lymphoma. Further studies should be designed in various animal models of cancer in order to examine combinations of different antibody-targeted liposomes,

containing the same or different drugs, or even liposomes targeted with two different antibodies present on the same liposomal membrane (73). With the success of single antibody-targeted liposomes in various cancer models, the development of the fluorescence assay to quantitate two different antibodies on the surface of liposomes lends itself well to future studies examining the effects of combinations of targeted liposomes or dual-targeted liposomes in different cancer models.

From a commercial aspect, it would be relatively simple to produce targeted-liposomes on a large scale. A method devised in the Allen laboratory called post-insertion, lends itself well to this type of application (93, 94). This method utilizes antibodies that are coupled to PEG-DSPE micelles which can transfer in a time- and temperature-dependent manner into the bilayer of preformed drug-loaded liposomes. This method is currently being optimized in the large-scale production of F5-Doxil® (78). With the therapeutic benefits of targeted liposomes having been demonstrated in animal models of B-cell lymphoma and HER2/*neu* breast cancer, and with the approval of free mAbs for treatment of these diseases (Rituxan® and Herceptin®, respectively), clinical testing of targeted-liposomes may be a realistic goal. Combination therapy is been a mainstay in cancer chemotherapy for over 20 years and since many cancers overexpress more than one cell surface receptor, e.g. B-cell lymphoma and CD19, CD20, CD22, combinations of different drug-loaded liposomes targeted with the same or different antibodies or even two antibodies on the same liposome may be a

possibility (169). With the ability to easily couple antibodies to preformed drug-loaded liposomes personalized treatment depending on the receptor expression on the specific cancer may be a future goal (93).

In summary, a potentially useful assay was developed to quantitate the amount of bioavailable drug in tumor cells after liposomal DXR delivery. We were able to show in the 4T1 mammary carcinoma model that measurement of the amount of total and bioavailable drug was a good approximation of therapeutic activity. Bioavailability studies were also done in the BT-474 breast cancer model, although therapeutic activity in this model was beyond the scope of this thesis. In addition to the bioavailability assay, we developed an assay that can accurately quantitate the amount of two different antibodies coupled to the surface of liposomes. This assay, will be useful in further studies investigating the therapeutic benefit of targeting liposomes with two different antibodies, and, since it relies on a fluorescence assay, will likely be safer than the radioisotope assays that are commonly used. We feel that both assays developed in this thesis work will aid future research in the liposome field.

References

1. Allen, T. M., Hansen, C. B., and Lopes de Menezes, D. E. Pharmacokinetics of long circulating liposomes. Adv. Drug Del. Rev., *16:* 267-284, 1995.
2. Berry, G., Billingham, M., Alderman, E., Richardson, P., Torti, F., Lum, B., Patek, A., and Martin, F. J. The use of cardiac biopsy to demonstrate reduced cardiotoxicity in AIDS Kaposi's sarcoma patients treated with pegylated liposomal doxorubicin. Ann. Oncol., *9:* 711-716, 1998.
3. Allen, T. M. and Hansen, C. B. Pharmacokinetics of Stealth versus conventional liposomes: effect of dose. Biochim. Biophys. Acta, *1068:* 133-141, 1991.
4. Safra, T., Muggia, F., Jeffers, S., Tsao-Wei, D. D., Groshen, S., Lyass, O., Henderson, R., Berry, G., and Gabizon, A. Pegylated liposomal doxorubicin (Doxil): reduced clinical cardiotoxicity in patients reaching or exceeding cumulative doses of 500 mg/m2. Ann. Oncol., *11:* 1029-1033, 2000.
5. Gabizon, A. Pegylated liposomal doxorubicin: metamorphosis of an old drug into a new form of chemotherapy. Cancer Invest., *19:* 424-436, 2001.
6. Northfelt, D. W., Martin, F. J., Working, P., Volberding, P. A., Russell, J., Newman, M., Amantea, M. A., and Kaplan, L. D. Doxorubicin encapsulated in liposomes containing surface-bound polyethylene glycol:

pharmacokinetics, tumour localization, and safety in patients with AIDS-related Kaposi's sarcoma. J. Clin. Pharmacol., *36:* 55-63, 1996.

7. Harasym, T. O., Cullis, P. R., and Balley, M. B. Intratumor distribution of doxorubicin following i.v. administration of drug encapsulated in egg phosphaticdylcholine/cholesterol liposomes. Cancer Chemother. Pharmacol., *40:* 309-317, 1997.

8. Lim, H. J., Masin, D., Madden, T. D., and Bally, M. B. Influence of drug release characteristics on the therapeutic activity of liposomal mitoxantrone. J. Pharmacol. Exp. Therap., *281:* 566-573, 1997.

9. Hong, R.-L., Huang, C.-J., Tseng, Y.-L., Pang, V. F., Chen, S.-T., Liu, J.-J., and Chang, F.-H. Direct comparison of liposomal doxorubicn with or without polyethylene glycol coating in C-26 tumor-bearing mice: Is surface coating with polyethylene glycol beneficial? Clin. Cancer Res., *5:* 3645-3652, 1999.

10. Waterhouse, D. N., Tardi, P. G., Mayer, L. D., and Bally, M. B. A comparison of liposomal formulations of doxorubicin with drug administered in free form. Drug Safety, *24:* 903-920, 2001.

11. Gabizon, A., Shmeeda, H., and Barenholz, Y. Pharmacokinetics of pegylated liposomal doxorubicin: review of animal and human studies. Clin. Pharmacokinet., *42:* 419-436, 2003.

12. Charrois, G. J. R. and Allen, T. M. Rate of biodistribution of STEALTH® liposomes to tumor and skin: influence of liposome diameter and

implications for toxicity and therapeutic activity. Biochim. Biophys. Acta, *1609:* 102-108, 2003.

13. Charrois, G. J. R. and Allen, T. M. Drug release rate influences the pharmacokinetics, biodistribution, therapeutic activity, and toxicity of pegylated liposomal doxorubicin formulations in murine breast cancer. Biochim. Biophys. Acta, *1663:* 167-177, 2004.

14. Canadian Cancer Statistics. Toronto, ON: National Cancer Institute of Canada, 2005.

15. Pegram, M. D., Pienkowski, T., Northfelt, D. W., Eiermann, W., Patel, R., Fumoleau, P., Quan, E., Crown, J., Toppmeyer, D., Smylie, M., Riva, A., Blitz, S., Press, M. F., Reese, D., Lindsay, M. A., and Slamon, D. J. Results of two open-label, multicenter phase II studies of docetaxel, platinum salts, and trastuzumab in HER2-positive advanced breast cancer. J. Natl. Cancer Inst., *96:* 759-769, 2004.

16. Slamon, D. J., Leyland-Jones, B., Shak, S., Fuchs, H., Paton, V., Bajamonde, A., Fleming, T., Eiermann, W., Wolter, J., Pegram, M., Baselga, J., and Norton, L. Use of chemotherapy plus a monoclonal antibody against HER2 for metastatic breast cancer that overexpresses HER2. N. Engl. J. Med., *344:* 783-792, 2001.

17. Vogel, C. L., Cobleigh, M. A., Tripathy, D., Gutheil, J. C., Harris, L. N., Fehrenbacher, L., Slamon, D. J., Murphy, M., Novotny, W. F., Burchmore, M., Shak, S., Stewart, S. J., and Press, M. Efficacy and safety of

trastuzumab as a single agent in first-line treatment of HER2-overexpressing metastatic breast cancer. J. Clin. Oncol., *20:* 719-726, 2002.

18. Buzdar, A. U., Ibrahim, N. K., Francis, D., Booser, D. J., Thomas, E. S., Theriault, R. L., Pusztai, L., Green, M. C., Arun, B. K., Giordano, S. H., Cristofanilli, M., Frye, D. K., Smith, T. L., Hunt, K. K., Singletary, S. E., Sahin, A. A., Ewer, M. S., Buchholz, T. A., Berry, D., and Hortobagyi, G. N. Significantly higher pathologic complete remission rate after neoadjuvant therapy with trastuzumab, paclitaxel, and epirubicin chemotherapy: results of a randomized trial in human epidermal growth factor receptor 2-positive operable breast cancer. J. Clin. Oncol., *23:* 3676-3685, 2005.

19. O'Brien, M. E., N., W., Inbar, M., Rosso, R., Grischke, E., Santoro, A., Catane, R., Kieback, D. G., Tomczak, P., Ackland, S. P., Orlandi, F., Mellars, L., Alland, L., Tendler, C., and Group, C. B. C. S. Reduced cardiotoxicity and comparable efficacy in a Phase III trial of pegylated liposomal doxorubicin HCl (CAELYX/Doxil) versus conventional doxorubicin for first-line treatment of metastatic breast cancer. Ann. Oncol., *15:* 440-449, 2004.

20. Siu, L. L. and Moore, M. J. Pharmacology and Anticancer Drugs. *In:* The Basic Science of Oncology, 4th edition, pp. 322-348. New York, NY: McGraw Hill, 2005.

21. Gewirtz, D. A. A critical evaluation of the mechanisms of action proposed for the antitumor effects of the anthracycline antibiotics adriamycin and daunorubicin. Biochem. Pharmacol., *57:* 727-741, 1999.

22. Bangham, A. D., Standish, M. M., and Watkins, J. C. Diffusion of univalent ions across the lamellae of swollen phospholipids. J. Mol. Biol., *13:* 238-252, 1965.

23. Sessa, G. and Weissmann, G. Phospholipid spherules (liposomes) as a model for biological membranes. J. Lipid Res., *9:* 310-318, 1968.

24. Olson, F., Hunt, C. A., Szoka, F. C., Vail, W. J., and Papahadjopoulos, D. Preparation of liposomes of defined size distribution by extrusion through polycarbonate membranes. Biochim. Biophys. Acta, *557:* 9-23, 1979.

25. Gregoriadis, G. and Ryman, B. E. Liposomes as carriers of enzymes or drugs: a new approach to the treatment of storage diseases. Biochem. J., *124:* 58P, 1971.

26. Kobayashi, T., Tsukagoshi, S., and Sakurai, Y. Enhancement of the cancer chemotherapeutic effect of cytosine arabinoside entrapped in liposomes on mouse leukemia L-1210. Gann., *66:* 719-720, 1975.

27. Allen, T. M. and Stuart, D. Liposome pharmacokinetics: classical, sterically stabilized, cationic liposomes and immunoliposomes. *In:* A. S. Janoff (ed.), Liposomes: Rational Design, pp. 63-97. New York, NY: Marcel Dekker, Inc., 1998.

28. Batist, G., Ramakrishnan, G., Rao, C. S., Chandrasekharan, A., Gutheil, J., Guthrie, T., Shah, P., Khojasteh, A., Nair, M. K., Hoelzer, K., Tkaczuk, K., Park, Y. C., and Lee, L. W. Reduced cardiotoxicity and preserved antitumor efficacy of liposome-encapsulated doxorubicin and cyclophosphamide compared with conventional doxorubicin and cyclophosphamide in a randomized, multicenter trial of metastatic breast cancer. J. Clin. Oncol., *19:* 1444-1454, 2001.

29. Mayer, L. D., Dougherty, G., Harasym, T. O., and Bally, M. B. The role of tumor-associated macorphages in the delivery of liposomal doxourbicin to solid murine fibrosarcoma tumors. J. Pharmacol. Exp. Ther., *280:* 1406-1414, 1997.

30. Allen, T. M., Hansen, C., and Rutledge, J. Liposomes with prolonged circulation times: factors affecting uptake by reticuloendothelial and other tissues. Biochim. Biophys. Acta, *981:* 27-35, 1989.

31. Klibanov, A. L., Maruyama, K., Torchilin, V. P., and Huang, L. Amphipathic polyethyleneglycols effectively prolong the circulation time of liposomes. FEBS Lett., *268:* 235-237, 1990.

32. Allen, T. M., Hansen, C. B., Martin, F., Redemann, C., and Yau-Young, A. Liposomes containing synthetic lipid derivatives of poly(ethylene glycol) show prolonged circulation half-lives in vivo. Biochim. Biophys. Acta, *1066:* 29-36, 1991.

33. Torchilin, V. P., Omelyanenko, V. G., Papisov, M. I., Bogdanov, A. A., Trubetskoy, V. S., Herron, J. N., and Gentry, C. A. Poly(ethylene glycol) on the liposome surface: on the mechanism of polymer coated liposome longevity. Biochim. Biophy. Acta, *1195:* 11-20, 1994.

34. Torchilin, V. P. and Papisov, M. I. Why do polyethylene glycol-coated liposomes circulate so long? molecular mechanism of liposome steric protection with polyethylene glycol: role of polymer chain flexiblity. J. liposome Res., *4:* 725-739, 1994.

35. Maeda, H., Wu, J., Sawa, T., Matsumura, Y., and Hori, K. Tumor vascular permeability and the EPR effect in macromolecular therapeutics: a review. J. Control. Release, *65:* 271-284, 2000.

36. Yuan, F., Dellian, M., Fukumura, D., Leunig, M., Berk, D. A., Torchilin, V. P., and Jain, R. K. Vascular permeability in a human tumor xenograft: molecular size dependence and cutoff size. Cancer Res., *55:* 3752-3756, 1995.

37. Yuan, F., Leunig, M., Huang, S. K., Berk, D. A., Papahadjopoulos, D., and Jain, R. K. Microvascular permeability and interstitial penetration of sterically stabilized (Stealth) liposomes in a human tumor xenograft. Cancer Res., *54:* 3352-3356, 1994.

38. Stohrerm, M., Boucher, Y., Stangassinger, M., and Jain, R. K. Oncotic pressure in solid tumors is elevated. Cancer Res., *60:* 4251-4255, 2000.

39. Rivera, E. Liposomal anthracyclines in metastatic breast cancer: clinical update. The Oncologist, *8, Suppl 2:* 3–9, 2003.

40. Ranson, M. R., Carmichael, J., O'Byrne, K., Stewart, S., Smith, D., and Howell, A. Treatment of advanced breast cancer with sterically stabilized liposomal doxorubicin: results of a multicenter phase II trial. J. Clin. Oncol., *15:* 3185-3191, 1997.

41. Northfelt, D. W., Dezube, B. J., Thommes, J. A., Miller, B. J., Fischl, M. A., Friedman-Kien, A., Kaplan, L. D., Du Mond, C., Mamelak, R. D., and Henry, D. H. Pegylated-liposomal doxorubicin versus doxorubicin, bleomycin, and vincristine in the treatment of AIDS-related Kaposi's sarcoma: results of a ramdomized phase III clinical trial. J. Clin. Oncol., *17:* 2445-2451, 1998.

42. Gordon, A. N., Fleagle, J. T., Guthrie, D., Parkin, D. E., Gore, M. E., and Lacave, A. J. Recurrent epithelial ovarian carcinoma: a randomized phase III study of pegylated liposomal doxourbicin versus topotecan. J. Clin. Oncol., *19:* 3312-3322, 2001.

43. Muggia, F. and Hamilton, A. Phase III data on Caelyx in ovarian cancer. Eur. J. Cancer, *37:* S15-S18, 2001.

44. Woodle, M. C. and Papahadjopoulos, D. Liposome preparation and size characterization. Meth. Enzymol., *171:* 193-217, 1989.

45. Batzri, S. and Korn, E. D. Single bilayer liposomes prepared without sonication. Biochim. Biophys. Acta, *16:* 1015-1019, 1973.

46. Szoka, F. and Papahadjopoulos, D. Procedure for preparation of liposomes with large internal aqueous space and high capture by reverse-phase evaporation. Proc. Natl. Acad. Sci. USA, *75:* 4194-4198, 1978.

47. Allen, T. M. Stealth liposomes as a drug sustained release system for 1-ß-D-arabinosylfuranosylcytosine (cytosine arabinoside). *In:* D. Lasic and F. Martin (eds.), Stealth Liposomes, pp. 187-196. Boca Raton, FL: CRC Press, Inc., 1995.

48. Bandak, S., Goren, D., Horowitz, A., Tzemach, D., and Gabizon, A. Pharmacological studies of cisplatin encapsulated in long-circulating liposomes in mouse tumor models. Anticancer Drugs, *10:* 911-920, 1999.

49. Mayer, L. D., Madden, T. D., Bally, M. B., and Cullis, P. R. pH gradient-mediated drug entrapment in liposomes. *In:* G. Gregoriadis (ed.), Liposome technology: Entrapment of drugs and other materials., 2 edition, Vol. 2, pp. 27-44. Boca Raton, FL.: CRC Press, Inc., 1993.

50. Haran, G., Cohen, R., Bar, L. K., and Barenholz, Y. Transmembrane ammonium sulfate gradients in liposomes produce efficient and stable entrapment of amphipathic weak bases. Biochim. Biophys. Acta, *1151:* 201-215, 1993.

51. Bolotin, E. M., Cohen, R., Bar, L. K., Emanuel, S. N., Lasic, D. D., and Barenholz, Y. Ammonium sulphate gradients for efficient and stable remote loading of amphipathic weak bases into liposomes and ligandosomes. J. Liposome Res., *4:* 455-479, 1994.

52. Chiu, G. N., Abraham, S. A., Ickenstein, L. M., Ng, R., Karlsson, G., Edwards, K., Wasan, E. K., and Bally, M. B. Encapsulation of doxorubicin into thermosensitive liposomes via complexation with the transition metal manganese. J. Control. Release, *104:* 271-288, 2005.

53. Mayer, L. D., Bally, M. B., and Cullis, P. R. Uptake of adriamycin into large unilamellar vesicles in response to a pH gradient. Biochim. Biophys. Acta, *857:* 123-126, 1986.

54. Xingong, L., Hirsh, D. J., Cabral-Lilly, D., Zirkel, A., Gruner, S. M., Janoff, A. S., and Perkins, W. R. Doxorubicin physical state in solution and inside liposomes loaded via a pH gradient. Biochim. Biophys. Acta, *1415:* 23-40, 1998.

55. Cheung, B. C. L., Sun, T. H. T., Leenhouts, J. M., and Cullis, P. R. Loading of doxorubicin into liposomes by forming Mn^{2+}-drug complexes. Biochim. Biophys. Acta, *1414:* 205-216, 1998.

56. Fenske, D. B., Wong, K. F., Maurer, E., Maurer, N., Leenhouts, J. M., Boman, N., Amankwa, L., and Cullis, P. R. Ionophore-mediated uptake of ciprofloxacin and vincristine into large unilamellar vesicles exhibiting transmembrane ion gradients. Biochim. Biophys. Acta, *1414:* 188-204, 1998.

57. Zhigaltsev, I. V., Maurer, N., Akhong, Q. F., Leone, R., Leng, E., Wang, J., Semple, S. C., and Cullis, P. R. Liposome-encapsulated vincristine,

vinblastine and vinorelbine: a comparative study of drug loading and retention. J. Control. Release, *104:* 103-111, 2005.

58. Semple, S. C., Leone, R., Wang, J., Leng, E. C., Klimuk, S. K., Eisenhardt, M. L., Yuan, Z. N., Edwards, K., Maurer, N., Hope, M. J., Cullis, P. R., and Ahkong, Q. F. Optimization and characterization of a sphingomyelin/cholesterol liposome formulation of vinorelbine with promising antitumor activity. J. Pharm. Sci., *94:* 1024-1038, 2005.

59. Allen, T. M. Ligand-targeted therapeutics in anticancer therapy. Nat. Rev. Cancer, *2:* 750-763, 2002.

60. Kohler, G. and Milstein, C. Continuous cultures of fused cells secreting antibody of predetermined specificity. Nature (London), *256:* 495-497, 1975.

61. Reichert, J. M., Rosensweig, C. J., Faden, L. B., and Dewitz, M. C. Monoclonal antibody successes in the clinic. Nat. Biotechnol., *23:* 1073-1078, 2005.

62. Ichikawa, K., Hikita, T., Maeda, N., Yonezawa, S., Takeuchi, Y., Asai, T., Namba, Y., and Oku, N. Antiangiogenic photodynamic therapy (PDT) by using long-circulating liposomes modified with peptide specific to angiogenic vessels. Biochim. Biophys. Acta, *1669:* 69-74, 2005.

63. Xiong, X. B., Huang, Y., Lu, W. L., Zhang, X., Zhang, H., Nagai, T., and Zhang, Q. Intracellular delivery of doxorubicin with RGD-modified

sterically stabilized liposomes for an improved antitumor efficacy: in vitro and in vivo. J. Pharm. Sci., *94:* 1782-1793, 2005.

64. Pastorino, F., Brignole, C., Marimpietri, D., Cilli, M., Gambini, C., Ribatti, D., Longhi, R., Allen, T. M., Corti, A., and Ponzoni, M. Vascular damage and anti-angiogenic effects of tumor vessel-targeted liposomal chemotherapy. Cancer Res., *63:* 7400-7409, 2003.

65. Goren, D., Horowitz, A. T., Tzemack, D., Tarshish, M., Zalipsky, S., and Gabizon, A. Nuclear delivery of doxorubicin via folate-targeted liposomes with bypass of nultidrug-resistance efflux pump. Clin. Cancer Res., *6:* 1949-1957, 2000.

66. Derycke, A. S., Kamuhabwa, A., Gijsens, A., Roskams, T., De Vos, D., Kasran, A., Huwyler, J., Missiaen, L., and de Witte, P. A. Transferrin-conjugated liposome targeting of photosensitizer AlPcS4 to rat bladder carcinoma cells. J. Natl. Cancer Inst., *96:* 1620-1630, 2004.

67. Eliaz, R. E., Nir, S., and Szoka, F. C., Jr. Interactions of hyaluronan-targeted liposomes with cultured cells: modeling of binding and endocytosis. Methods Enzymol., *387:* 16-33, 2004.

68. Yanagie, H., Tomita, T., Kobayashi, H., Fujii, Y., Takahashi, T., Hasumi, K., Nariuchi, H., and Sekiguchi, M. Application of boronated anti-CEA immunoliposome to tumour cell growth inhibition in in vitro boron neutron capture therapy model. Br. J. Cancer, *63:* 522-526, 1991.

69. Mamot, C., Drummond, D. C., Greiser, U., Hong, K., Kirpotin, D. B., Marks, J. D., and Park, J. W. Epidermal growth factor receptor (EGFR)-targeted immunoliposomes mediate specific and efficient drug delivery to EGFR- and EGFRvIII-overexpressing tumor cells. Cancer Res., *63:* 3154-3161, 2003.

70. Park, J. W., Carter, P., Kotts, C., Shalaby, R., Giltinan, D., Wirth, C., Asgari, H., Wood, W. I., Papahadjopoulos, D., and Benz, C. Development of anti-HER-2 immunoliposomes for breast cancer therapy. Proc. Am. Soc. Clin. Oncol., *12:* 118, 1993.

71. Lopes de Menezes, D. E., Kirchmeier, M. J., Gagne, J.-F., Pilarski, L. M., and Allen, T. M. Cellular trafficking and cytotoxicity of anti-CD19-targeted liposomal doxorubicin in B lymphoma cells. J. Liposome Res., *9:* 199-228, 1999.

72. Pastorino, F., Brignole, C., Marimpietri, D., Pagnan, G., Morando, A., Ribatti, D., Semple, S. C., Gambini, C., Allen, T. M., and Ponzoni, M. Targeted delivery and antitumour effects of c-myc antisense oligodeoxynucleotides in human melanoma cells mediated by anti-GD2-immunoliposomes. Clin. Cancer Res., *9:* 4595-4605, 2003.

73. Sapra, P. and Allen, T. M. Improved outcome when B-cell lymphoma is treated with combinations of immunoliposomal anticancer drugs targeted to both the CD19 and CD20 epitopes. Clin. Cancer Res., *10:* 2530-2537, 2004.

74. de Kruif, J., Storm, G., van Bloois, L., and Logtenberg, T. Biosynthetically lipid-modified human sc Fv fragments from phage display libraries as targeting molecules for immunoliposomes. FEBS Lett., *399:* 232-236, 1996.

75. Moase, E., Qi, W., Ishida, T., Gabos, Z., Longenecker, B. M., Zimmermann, G. L., Ding, L., Krantz, M., and Allen, T. M. Anti-MUC-1 immunoliposomal doxorubicin in the treatment of murine models of metastatic breast cancer. Biochim. Biophys. Acta, *1510:* 43-55, 2001.

76. Mercadal, M., Domingo, J. C., Petriz, J., Garcia, J., and de Madariaga, M. A. Preparation of immunoliposomes bearing poly(ethylene glycol)-coupled monoclonal antibody linked via a cleavable disulfide bond for ex vivo applications. Biochim. Biophys. Acta, *1509:* 299-310, 2000.

77. Lukyanov, A. N., Elbayoumi, T. A., Chakilam, A. R., and Torchilin, V. P. Tumor-targeted liposomes: doxorubicin-loaded long-circulating liposomes modified with anti-cancer antibody. J. Control. Release, *100:* 135-144, 2004.

78. Nellis, D. F., Ekstrom, D. L., Kirpotin, D. B., Zhu, J., Andersson, R., Broadt, T. L., Ouellette, T. F., Perkins, S. C., Roach, J. M., Drummond, D. C., Hong, K., Marks, J. D., Park, J. W., and Giardina, S. L. Preclinical manufacture of an anti-HER2 scFv-PEG-DSPE, liposome-inserting conjugate. 1. Gram-scale production and purification. Biotechnol. Prog., *21:* 205-220, 2005.

79. Park, J. W., Hong, K., Carter, P., Asgari, H., Guo, L. Y., Keller, G. A., Wirth, C., Shalaby, R., Kotts, C., Wood, W. I., Papahadjopoulos, D., and Benz, C. C. Development of anti-p185^{HER2} immunoliposomes for cancer therapy. Proc. Natl. Acad. Sci. USA, *92:* 1327-1331, 1995.

80. Kirpotin, D., Park, J. W., Hong, K., Zalipsky, S., Li, W.-L., Carter, P., Benz, C. C., and Papahadjopoulos, D. Sterically stabilized anti-HER2 immunoliposomes: design and targeting to human breast cancer cells *in vitro*. Biochemistry, *36:* 66-75, 1997.

81. Park, J. W., Kirpotin, D. B., Hong, K., Shalaby, R., Shao, Y., Nielsen, U. B., Marks, J. D., Papahadjopoulos, D., and Benz, C. C. Tumor targeting using anti-HER2 immunoliposomes. J. Control. Release, *74:* 95-113, 2001.

82. Nielsen, U. B. and Marks, J. D. Internalizing antibodies and targeted cancer therapy: direct selection from phage display libraries. Pharmaceutical Science and Technology Today, *3:* 282-291, 2000.

83. Nielsen, U. B., Kirpotin, D. B., Pickering, E. M., Hong, K., Park, J. W., Shalaby, M. R., Shao, Y., Benz, C. C., and Marks, J. D. Therapeutic efficacy of anti-ErbB2 immunoliposomes targeted by a phage antibody selected for cellular endocytosis. Biochim. Biophys. Acta, *1591:* 109-118, 2002.

84. Lopes de Menezes, D. E., Pilarski, L. M., and Allen, T. M. In vitro and in vivo targeting of immunoliposomal doxorubicin to human B-cell lymphoma. Cancer Res., *58:* 3320-3330, 1998.

85. Sapra, P., Moase, E. H., Ma, J., and Allen, T. M. Improved therapeutic responses in a xenograft model of human B-lymphoma (Namalwa) for liposomal vincristine versus liposomal doxorubicin targeted via anti-CD19 IgG2a or Fab' fragments. Clin. Cancer Res., *10:* 1100-1111, 2004.

86. Sarris, A. H., Hagemeister, F., Romaguera, J., Rodriguez, M. A., McLaughlin, P., Tsimberidou, A. M., Medeiros, L. J., Samuels, B., Pate, O., Oholendt, M., Kantarjian, H., Burge, C., and Cabanillas, F. Liposomal vincristine in relapsed non-Hodgkin's lymphomas: early results of an ongoing phase II trial. Ann. Oncol., *11:* 69-72, 2000.

87. Sapra, P., Tyagi, P., and Allen, T. M. Ligand-targeted liposomes for cancer treatment. Curr. Drug Deliv., *2:* 369-381, 2005.

88. Klibanov, A. L., Maruyama, K., Beckerleg, A. M., Torchilin, V. P., and Huang, L. Activity of amphipathic poly(ethyleneglycol) 5000 to prolong the circulation time of liposomes depends on the liposome size and is unfavorable for immunoliposome binding to target. Biochim. Biophys. Acta, *1062:* 142-148, 1991.

89. Blume, G., Cevc, G., Crommelin, M. D., Bakker-Woudenberg, L. A., Kluft, C., and Storm, G. Specific targeting with poly(ethylene glycol)-modified liposomes: coupling of homing devices to the ends of the polymeric chains combines effective target binding with long circulation times. Biochim. Biophys. Acta, *1149:* 180-184, 1993.

90. Allen, T. M., Brandeis, E., Hansen, C. B., Kao, G. Y., and Zalipsky, S. A new strategy for attachment of antibodies to sterically stabilized liposomes resulting in efficient targeting to cancer cells. Biochim. Biophys. Acta, *1237:* 99-108, 1995.

91. Maruyama, K., Takizawa, T., Yuda, T., Kennel, S. J., Huang, L., and Iwatsuru, M. Targetability of novel immunoliposomes modified with amphipathic poly(ethylene glycol)s conjugated at their distal terminals to monoclonal antibodies. Biochim. Biophys. Acta, *1234:* 74-80, 1995.

92. Zalipsky, S. Synthesis of end-group functionalized polyethylene glycol-lipid conjugates for preparation of polymer-grafted liposomes. Bioconjugate Chem., *4:* 296-299, 1993.

93. Ishida, T., Iden, D. L., and Allen, T. M. A combinatorial approach to producing sterically stabilized (Stealth) immunoliposomal drugs. FEBS Lett., *460:* 129-133, 1999.

94. Iden, D. L. and Allen, T. M. In vitro and in vivo comparison of immunoliposomes made by conventional coupling techniques with those made by a new post-insertion technique. Biochim. Biophys. Acta, *1513:* 207-216, 2001.

95. Harrington, K. J., Lewanski, C. R., Northcote, A. D., Whittaker, J., Wellbank, H., Vile, R. G., Peters, A. M., and Stewart, J. S. Phase I-II study of pegylated liposomal cisplatin (SPI-077) in patients with inoperable head and neck cancer. Ann. Oncol., *12:* 493-496, 2001.

96. Cabanes, A., K.E., B., Gokhale, P. C., Treat, J. A., and Rahman, A. Comparative in vivo studies with paclitaxel and liposome-encapsulated paclitaxel. Int. J. Oncol., *12:* 1035-1040, 1998.

97. Allen, T. M. A study of phospholipid interactions between high-density lipoproteins and small unilamellar vesicles. Biochim. Biophys. Acta, *640:* 385-397, 1981.

98. Lim, H. J., Masin, D., Mcintosh, N. L., Madden, T. D., and Balley, M. B. Role of drug release and liposome-mediated drug delivery in governing the therapeutic activity of liposomal mitoxatrone used to treat human A431 and LS180 solid tumors. J. Pharm. Exp. Ther., *292:* 337-345, 2000.

99. Adlakha-Hutcheon, G., Bally, M. B., Shew, C. R., and Madden, T. D. Controlled destabilization of a liposomal drug delivery system enhances mitoxantrone antitumor activity. Nat. Biotechnol., *17:* 775-779, 1999.

100. Needham, D., Anyarambhatla, G., Kong, G., and Dewhirst, M. W. A new tempertature-sensitive liposome for use with mild hyperthermia: characterization and testing in a human tumour xenograft model. Cancer Res., *60:* 1197-1201, 2000.

101. Needham, D. and Dewhirst, M. W. The development and testing of a new temperature-sensitive drug delivery system for the treatment of solid tumors. Adv. Drug Deliv. Rev., *53:* 285-305, 2001.

102. Ishida, T., Kirchmeier, M. J., Moase, E. H., Zalipsky, S., and Allen, T. M. Targeted delivery and triggered release of liposomal doxorubicin enhances

cytotoxicity against human B lymphoma cells. Biochim. Biophys. Acta, *1515:* 144-158, 2001.

103. Simoes, S., Moreira, J. N., Fonseca, C., Duzgunes, N., and de Lima, M. C. On the formulation of pH-sensitive liposomes with long circulation times. Adv. Drug Deliv. Rev., *56:* 947-965, 2004.

104. Slepushkin, V., Simoes, S., de Lima, M. C., and Duzgunes, N. Sterically stabilized ph-sensitive liposomes. Methods Enzymol., *387:* 134-147, 2004.

105. Roux, E., Passirani, C., Scheffold, S., Benoit, J. P., and Leroux, J. C. Serum-stable and long-circulating, PEGylated, pH-sensitive liposomes. J. Control. Release, *94:* 447-451, 2004.

106. Chu, C. J., Dijkstra, J., Lai, M. Z., Hong, K., and Szoka, F. C. Efficiency of cytoplasmic delivery by pH-sensitive liposomes to cells in culture. Pharm. Res., *7:* 824-834, 1990.

107. Guo, X. and Szoka, F. C. J. Chemical approaches to triggerable lipid vesicles for drug and gene delivery. Acc. Chem. Res., *36:* 335-341, 2003.

108. Kong, G., Braun, R. D., and Dewhirst, M. W. Characterization of the effect of hyperthermia on nanoparticle extravasation from tumor vasculature. Cancer Res., *61:* 3027-3032, 2001.

109. Shargel, L. and Yu, A. B. C. Bioavailability and Bioequivalence. *In:* Applied Biopharmaceutics and Pharmacokinetics, 4th edition, pp. 247-279. New York, NY: McGraw Hill, 1999.

110. Northfelt, D. W., Martin, F. J., Kaplan, L. D., Russell, J., Andersen, M., Lang, J., and Volberding, P. A. Pharmacokinetics, tumour localization and safety of Doxil (liposomal doxorubicin) in AIDS patients with Kaposi's sarcoma (Meeting abstract). Proc. Am. Soc. Clin. Oncol., *12:* A8, 1993.

111. Barabas, K., Sizensky, J. A., and Faulk, W. P. Transferrin conjugates of adriamycin are cytotoxic without intercalating nuclear DNA. J. Biol. Chem., *267:* 9437-9442, 1992.

112. Morjani, H., Millot, J. M., Belhoussine, R., Sebille, S., and Manfait, M. Anthracycline subcellular distribution in human leukemic cells by microspectrofluorometry: factors contributing to drug-induced cell death and reversal of multidrug resistance. Leukemia, *11:* 1170-1179, 1997.

113. Miller, F. R., Medina, D., and Heppner, G. H. Preferential growth of mammary tumours in intact mammary fatpads. Cancer Res., *41:* 3863-3867, 1981.

114. Aslakson, C. J. and Miller, F. R. Selective events in the metastatic process defined by analysis of the sequential dissemination of subpopulations of a mouse mammary tumor. Cancer Res., *52:* 1399-1405, 1992.

115. Lasfargues, E. Y., Coutinho, W. G., and Redfield, E. S. Isolation of two human tumor epithelial cell lines from solid breast carcinomas. J. Natl. Cancer Inst., *61:* 967-978, 1978.

116. Mass, R. D., Press, M. F., Anderson, S., Cobleigh, M. A., Vogel, C. L., Dybdal, N., Leiberman, G., and Slamon, D. J. Evaluation of Clinical

Outcomes According to HER2 Detection by Fluorescence In Situ Hybridization in Women with Metastatic Breast Cancer Treated with Trastuzumab. Clin. Breast Cancer, *6:* 240-246, 2005.

117. Cobleigh, M. A., Vogel, C. L., Tripathy, D., Robert, N. J., Scholl, S., Fehrenbacher, L., Wolter, J. M., Paton, V., Shak, S., Lieberman, G., and Slamon, D. J. Multinational study of the efficacy and safety of humanized anti-HER2 monoclonal antibody in women who have HER2-overexpressing metastatic breast cancer that has progressed after chemotherapy for metastatic disease. J. Clin. Oncol., *17:* 2639-2648, 1999.

118. Press, O. W., Appelbaum, F., Ledbetter, J. A., Martin, P. J., Zarling, J., Kidd, P., and Thomas, E. D. Monoclonal antibody IF5 (anti-CD20) serotherapy of human B cell lymphomas. Blood, *69:* 584-591, 1987.

119. Press, O. W., Farr, A. G., Borroz, K. I., Andersen, S. K., and Martin, P. J. Endocytosis and degradation of monoclonal antibodies targeting human B-cell malignancies. Cancer Res., *49:* 4906-4912, 1989.

120. Vangeepuram, N., Ong, G. L., and Mattes, M. J. Processing of antibodies bound to B-cell lymphomas and lymphoblastoid cell lines. Cancer, *80:* 2425-2430, 1997.

121. Linenberger, M. L., Maloney, D. G., and Bernstein, I. D. Antibody-directed therapies for hematological malignancies. Trends Mol. Med., *8:* 69-76, 2002.

122. Sapra, P. and Allen, T. M. Internalizing antibodies are necessary for improved therapeutic efficacy of antibody-targeted liposomal drugs. Cancer Res., *62:* 7190-7194, 2002.

123. Marafino, B. J., Jr., Giri, S. N., and Siegel, D. M. Pharmacokinetics, covalent binding and subcellular distribution of [3H]doxorubicin after intravenous administration in the mouse. J. Pharmacol. Exp. Ther., *216:* 55-61, 1981.

124. Terasaki, T., Iga, T., Sugiyama, Y., Sawada, Y., and Hanano, M. Nuclear binding as a determinant of tissue distribution of adriamycin, daunomycin, adriamycinol, daunorubicinol and actinomycin D. J. Pharmacobiodyn., *7:* 269-277, 1984.

125. Maeda, H., Sawa, T., and Konno, T. Mechanism of tumor-targeted delivery of macromolecular drugs, including the EPR effect in solid tumor and clinical overview of the prototype polymeric drug SMANCS. J. Control. Release, *74:* 47-61, 2001.

126. Ishida, O., Maruyama, K., Sasaki, K., and Iwatsuru, M. Size-dependent extravastion and interstial localization of polyethyleneglycol liposomes in solid tumor-bearing mice. Int. J. Pharm., *190:* 49-56, 1999.

127. Kirchmeier, M. J., Ishida, T., Chevrette, J., and Allen, T. M. Correlations between the rate of intracellular release of endocytosed liposomal doxorubicin and cytotoxicity as determined by a new assay. J. Liposome Res., *11:* 15-29, 2001.

128. Wu, N. Z., Braun, R. D., Gaber, M. H., Lin, G. M., Ong, E. T., Shan, S., Papahadjopoulos, D., and Dewhirst, M. W. Simultaneous measurement of liposome extravasation and content release in tumors. Microcirculation, *4:* 83-101, 1997.

129. Eliaz, R. E., Nir, S., Marty, C., and Szoka, F. C., Jr. Determination and modeling of kinetics of cancer cell killing by doxorubicin and doxorubicin encapsulated in targeted liposomes. Cancer Res., *64:* 711-718, 2004.

130. Szewczyk, A. and Wojtczak, L. Mitochondria as a pharmacological target. Pharmacol. Rev., *54:* 101-127, 2002.

131. Kluza, J., Marchetti, P., Gallego, M. A., Lancel, S., Fournier, C., Loyens, A., Beauvillain, J. C., and Bailly, C. Mitochondrial proliferation during apoptosis induced by anticancer agents: effects of doxorubicin and mitoxantrone on cancer and cardiac cells. Oncogene, *23:* 7018-7030, 2004.

132. Vaage, J., Donovan, D., Uster, P., and Working, P. Tumour uptake of doxorubicin in polyethylene glycol-coated liposomes and therapeutic effect against a xenografted human pancreatic carcinoma. Br. J. Cancer, *75:* 482-486, 1997.

133. Allen, T. M., Mumbengegwi, D. R., and Charrois, G. J. Anti-CD19-targeted liposomal doxorubicin improves the therapeutic efficacy in murine B-cell lymphoma and ameliorates the toxicity of liposomes with varying drug release rates. Clin. Cancer Res., *11:* 3567-3573, 2005.

134. Gabizon, A., Catane, R., Uziely, B., Kaufman, B., Safra, T., Cohen, R., Martin, F., Huang, A., and Barenholz, Y. Prolonged circulation time and enhanced accumulation in malignant exudates of doxorubicin encapsulated in polyethylene-glycol coated liposomes. Cancer Res., *54:* 987-992, 1994.

135. Park, J. W., Hong, K., Kirpotin, D. B., Colbern, G., Shalaby, R., Baselga, J., Shao, Y., Nielsen, U. B., Marks, J. D., Moore, D., Papahadjopoulos, D., and Benz, C. C. Anti-HER2 immunoliposomes: Enhanced efficacy attributable to targeted delivery. Clin. Cancer Res., *8:* 1172-1181, 2002.

136. Zalipsky, S., Qazen, M., Walker, J. A. I., Mullah, N., Quinn, Y. P., and Huang, S. K. New detachable poly(ethylene glycol) conjugates: cystein-cleavable lipopolymers regenerating natural phospholipid, diacy phosphatidylethanolamine. Bioconjugate Chem., *10:* 703-707, 1999.

137. Kim, E. S., Lu, C., Khuri, F. R., Tonda, M., Glisson, B. S., Liu, D., Jung, M., Hong, W. K., and Herbst, R. S. A phase II study of STEALTH cisplatin (SPI-77) in patients with advanced non-small cell lung cancer. Lung Cancer, *34:* 427-432, 2001.

138. Zamboni, W. C., Gervais, A. C., Egorin, M. J., Schellens, J. H., Zuhowski, E. G., Pluim, D., Joseph, E., Hamburger, D. R., Working, P. K., Colbern, G., Tonda, M. E., Potter, D. M., and Eiseman, J. L. Systemic and tumor disposition of platinum after administration of cisplatin or STEALTH liposomal-cisplatin formulations (SPI-077 and SPI-077 B103) in a

preclinical tumor model of melanoma. Cancer Chemother. Pharmacol., *53:* 329-336, 2004.

139. Viglianti, B. L., Abraham, S. A., Michelich, C. R., Yarmolenko, P. S., MacFall, J. R., Bally, M. B., and Dewhirst, M. W. In vivo monitoring of tissue pharmacokinetics of liposome/drug using MRI: illustration of targeted delivery. Magn. Reson. Med., *51:* 1153-1162, 2004.

140. Laginha, K., Verwoert, S., Charrois, G. J. R., and Allen, T. M. Determination of doxorubicin levels In whole tumor and tumor nuclei in murine breast cancer tumors. Clin. Cancer. Res., *11:* 6944-6949, 2005.

141. Eckardt, J. R., Campbell, E., Burries, H. A., Weiss, G. R., Rodriguez, G. I., Fields, S. M., Thurman, A. M., Peacock, N. W., Cobb, P., Rothenberg, M. L., Ross, M. E., and Von Hoff, D. D. A Phase II trial of DaunoXome, liposome encapsulated daunorubicin, in patients with metastatic adenocarcinoma of the colon. Am. J. Clin. Oncol. Cancer Clin. Trials, *17:* 498-501, 1994.

142. Forssen, E. A. The design and development of DaunoXome^{R} for solid tumor targeting in vivo. Adv. Drug Del. Rev., *24:* 133-150, 1997.

143. Mross, K., Niemann, B., Massing, U., Drevs, J., Unger, C., Bhamra, R., and Swenson, C. E. Pharmacokinetics of liposomal doxorubicin (TLC-D99; Myocet) in patients with solid tumors: an open-label, single-dose study. Cancer Chemother. Pharmacol., *54:* 514-524, 2004.

144. Yeo, W., Chan, K. K., Mukwaya, G., Ross, M., Leung, W. T., Ho, S., Chan, A. T., and Johnson, P. J. Phase II studies with DaunoXome in patients with nonresectable hepatocellular carcinoma: clinical and pharmacokinetic outcomes. Cancer Chemother. Pharmacol., *44:* 124-130, 1999.

145. Swenson, C. E., Bolcsak, L. E., Batist, G., Guthrie, T. H., Jr., Tkaczuk, K. H., Boxenbaum, H., Welles, L., Chow, S. C., Bhamra, R., and Chaikin, P. Pharmacokinetics of doxorubicin administered i.v. as Myocet (TLC D-99; liposome-encapsulated doxorubicin citrate) compared with conventional doxorubicin when given in combination with cyclophosphamide in patients with metastatic breast cancer. Anticancer Drugs, *14:* 239-246, 2003.

146. Perkins, S. L., Lones, M. A., Davenport, V., and Cairo, M. S. B-Cell non-Hodgkin's lymphoma in children and adolescents: surface antigen expression and clinical implications for future targeted bioimmune therapy: a children's cancer group report. Clin. Adv. Hematol. Oncol., *1:* 314-317, 2003.

147. Lopez-Guerrero, J. A., Llombart-Cussac, A., Noguera, R., Navarro, S., Pellin, A., Almenar, S., Vazquez-Alvadalejo, C., and Llombart-Bosch, A. HER2 amplification in recurrent breast cancer following breast-conserving therapy correlates with distant metastasis and poor survival. Int. J. Cancer, *118:* 1743-1749, 2005.

148. Dybdal, N., Leiberman, G., Anderson, S., McCune, B., Bajamonde, A., Cohen, R. L., Mass, R. D., Sanders, C., and Press, M. F. Determination of HER2 gene amplification by fluorescence in situ hybridization and concordance with the clinical trials immunohistochemical assay in women with metastatic breast cancer evaluated for treatment with trastuzumab. Breast Cancer Res. Treat., *93:* 3-11, 2005.

149. Romond, E. H., Perez, E. A., Bryant, J., Suman, V. J., Geyer, C. E., Jr., Davidson, N. E., Tan-Chiu, E., Martino, S., Paik, S., Kaufman, P. A., Swain, S. M., Pisansky, T. M., Fehrenbacher, L., Kutteh, L. A., Vogel, V. G., Visscher, D. W., Yothers, G., Jenkins, R. B., Brown, A. M., Dakhil, S. R., Mamounas, E. P., Lingle, W. L., Klein, P. M., Ingle, J. N., and Wolmark, N. Trastuzumab plus adjuvant chemotherapy for operable HER2-positive breast cancer. N. Engl. J. Med., *353:* 1673-1684, 2005.

150. Park, J. W., Hong, K., Kirpotin, D. B., Meyer, O., Papahadjopoulos, D., and Benz, C. C. Anti-HER2 immunoliposomes for targeted therapy of human tumors. Cancer Lett., *118:* 153-160, 1997.

151. Nellis, D. F., Giardina, S. L., Janini, G. M., Shenoy, S. R., Marks, J. D., Tsai, R., Drummond, D. C., Hong, K., Park, J. W., Ouellette, T. F., Perkins, S. C., and Kirpotin, D. B. Preclinical manufacture of anti-HER2 liposome-inserting, scFv-PEG-lipid conjugate. 2. Conjugate micelle identity, purity, stability, and potency analysis. Biotechnol. Prog., *21:* 221-232, 2005.

152. Xiong, G., Chen, Y., and Arriaga, E. A. Measuring the doxorubicin content of single nuclei by micellar electrokinetic capillary chromatography with laser-induced fluorescence detection. Anal. Chem., *77:* 3488-3493, 2005.

153. Mosmann, T. Rapid colorimetric assay for cellular growth and survival: application to proliferation and cytotoxicity assays. J. Immunol. Methods, *65:* 55-63, 1983.

154. Hendriks, B. S., Opresko, L. K., Wiley, H. S., and Lauffenburger, D. Quantitative analysis of HER2-mediated effects on HER2 and epidermal growth factor receptor endocytosis: distribution of homo- and heterodimers depends on relative HER2 levels. J. Biol. Chem., *278:* 23343-23351, 2003.

155. Warburton, C., Dragowska, W. H., Gelmon, K., Chia, S., Yan, H., Masin, D., Denyssevych, T., Wallis, A. E., and Bally, M. B. Treatment of HER-2/neu overexpressing breast cancer xenograft models with trastuzumab (Herceptin) and gefitinib (ZD1839): drug combination effects on tumor growth, HER-2/neu and epidermal growth factor receptor expression, and viable hypoxic cell fraction. Clin. Cancer Res., *10:* 2512-2524, 2004.

156. Turk, M. J., Reddy, J. A., Chmielewski, J. A., and Low, P. S. Characterization of a novel pH-sensitive peptide that enhances drug release from folate-targeted liposomes at endosomal pHs. Biochim. Biophys. Acta, *1559:* 56-68, 2002.

157. Fonseca, C., Moreira, J. N., Ciudad, C. J., Pedroso de Lima, M. C., and Simoes, S. Targeting of sterically stabilised pH-sensitive liposomes to human T-leukaemia cells. Eur. J. Pharm. Biopharm., *59:* 359-366, 2005.

158. Allen, T. M. and Cullis, P. R. Drug delivery systems: entering the mainstream. Science, *303:* 1818-1822, 2004.

159. Sapra, P. and Allen, T. M. Ligand-targeted liposomal anticancer drugs. Prog. Lipid Res., *42:* 439-462, 2003.

160. Vingerhoeds, M. H., Steerenberg, P. A., Hendriks, J. J. G. W., Kekker, L. C., van Hoesel, Q. G. C. M., Crommelin, D. J. A., and Storm, G. Immunoliposome-mediated targeting of doxorubicin to human ovarian carcinoma in vitro and in vivo. Br. J. Cancer, *74:* 1023-1029, 1996.

161. Maruyama, K., Takahashi, N., Tagawa, T., Nagaike, K., and Iwatsuru, M. Immunoliposomes bearing polyethyleneglycol-coupled Fab' fragment show prolonged circulation time and high extravasation into targeted solid tumors *in vivo*. FEBS Lett., *413:* 177-180, 1997.

162. Moreira, J. N., Hansen, C. B., Gaspar, R., and Allen, T. M. A growth factor antagonist as a targeting agent for sterically stabilized liposomes in human small cell lung cancer. Biochim. Biophys. Acta, *1514:* 303-317, 2001.

163. Haugland, R. Handbook of Fluorescent Probes and Research Products, 9 edition. Eugene, OR: Molecular Probes, 2003.

164. Formelli, F., Pollini, C., Casazza, A. M., di Marco, A., and Mariani, A. Fluorescence assays and pharmacokinetic studies of 4'-deoxydoxorubicin and doxorubicin in organs of mice bearing solid tumors. Cancer Chemother. Pharmacol., *5:* 139-144, 1981.

165. Jain, R. K. Vascular and interstitial barriers to delivery of therapeutic agents in tumors. Cancer Metastasis Rev., *9:* 253-266, 1990.

166. Zu, N. Z., Da, D., Rudoll, T. L., Needham, D., Whorton, A. R., and Dewhirst, M. W. Increased microvascular permeability contributes to preferential accumulation of Stealth liposomes in tumor tissue. Cancer Res., *53:* 3765-3770, 1993.

167. Norton, L. Theoretical concepts and the emerging role of taxanes in adjuvant therapy. Oncologist, *6 Suppl 3:* 30-35, 2001.

168. Bates, D. A., Fung, H., and Mackillop, W. J. Adriamycin uptake, intracellular binding and cytotoxicity in Chinese hamster ovary cells. Cancer Lett., *28:* 213-221, 1985.

169. Case, D. C., Jr. Combination chemotherapy of advanced, diffuse, non-Hodgkin's lymphoma: results with cyclo-phosphamide, adriamycin, vincristine, prednisone, and bleomycin (CHOP-Bleo). J. Maine Med. Assoc., *70:* 348-350, 352, 368, 1979.